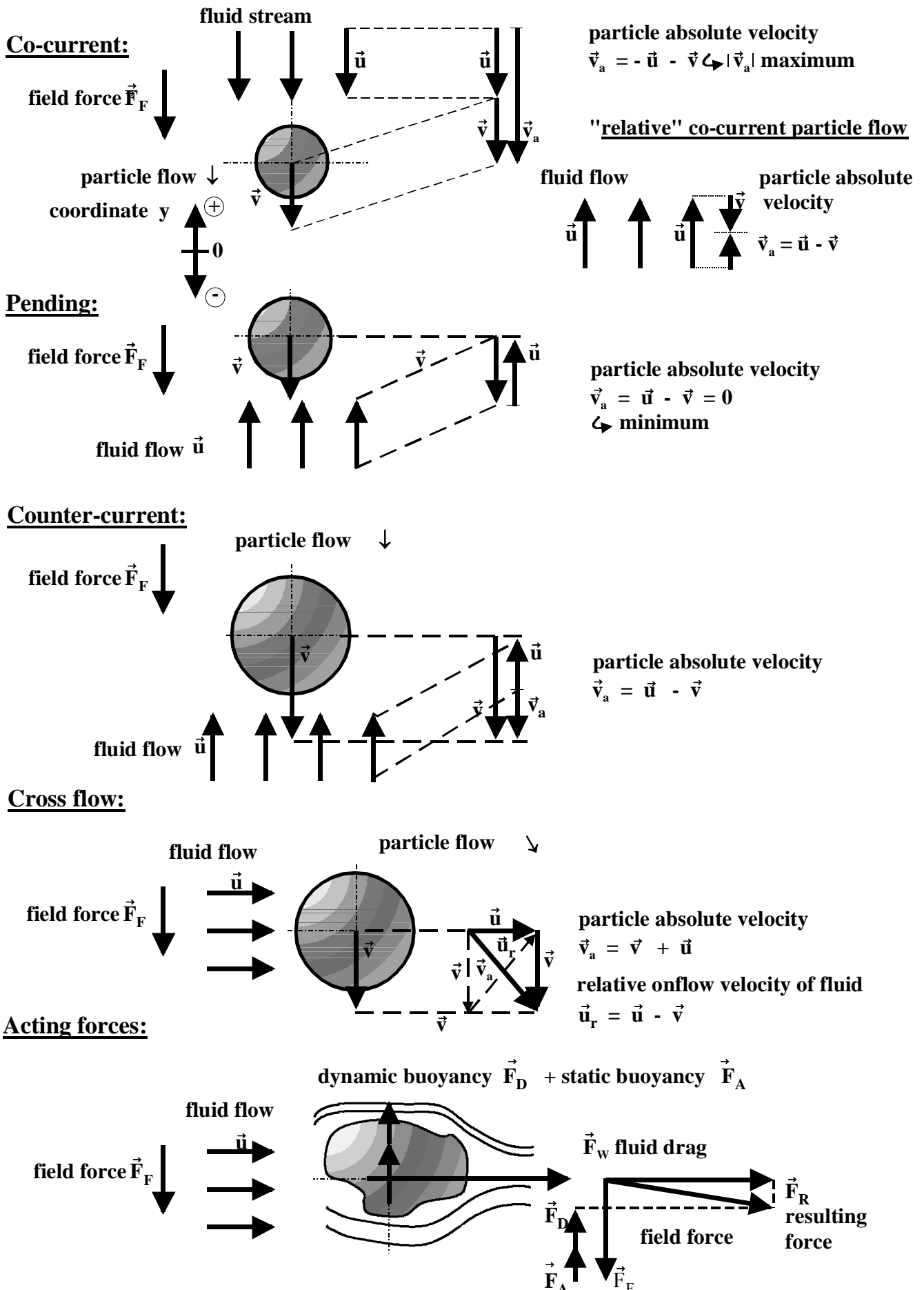


4. Particle separation in a fluid flow
 - 4.1 Single particle flow in a fluid and flow-around pattern
 - 4.1.1 Stationary particle sedimentation
 - 4.1.2 Uniformly accelerated particle sedimentation
 - 4.1.3 Swarm confinement of particles clusters
 - 4.1.4 Fluid flow through particle beds
 - 4.2 Micro- and macroturbulence
 - 4.3 Particle diffusion in a dispersion medium
 - 4.4 Dynamics of particle transport in turbulent fluids (turbulent particle dispersion or diffusion)
 - 4.5 Particle separation efficiency in a turbulent flow field
 - 4.5.1 Separation function of turbulent cross flow separation
 - 4.5.2 Separation function of counter-current separation
 - 4.5.3 Multistage cross-flow separation model
 - 4.5.3.1 Separation function, cut point and separation efficiency
 - 4.5.3.2 Utilization of separation stages
 - 4.5.3.3 Examples of zigzag air separator
 - 4.6 Machines and apparatuses of particle classification
 - 4.7 Apparatuses of dust collection

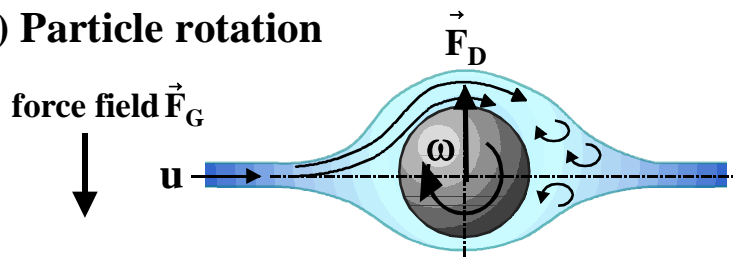
Particle Flow in a Fluid



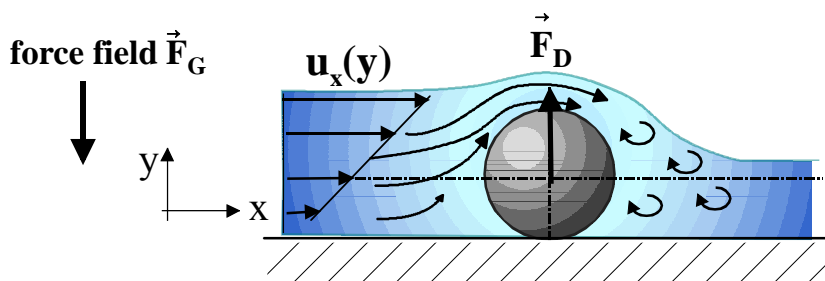
Flow-around of Smooth Spheres

1. Effect of dynamic buoyancy $F_D = c_D \cdot A_p \cdot \rho_f \cdot u^2/2$

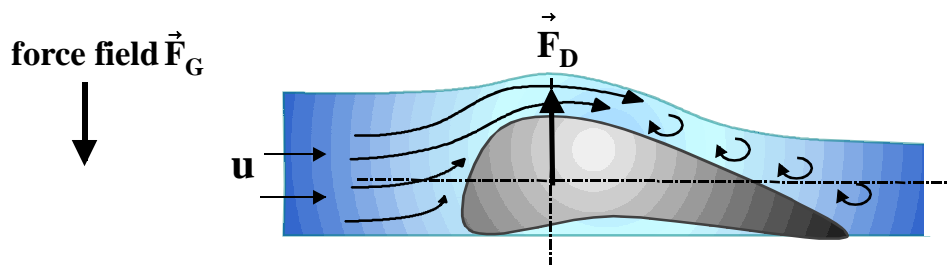
a) Particle rotation



b) Non-uniform onflow of symmetric sphere



c) Non-uniform onflow profile of asymmetric body

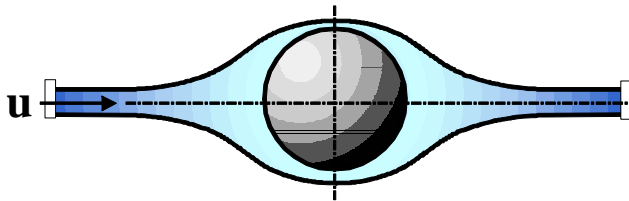


Flow-around Pattern of Smooth Spheres

2. Flow-around ranges

Prerequisites: uniform, laminar and stationary onflow of smooth sphere at rest

I) Viscous flow-around pattern, $Re < 0.25$, STOKES



$Re = u \cdot d \cdot \rho_f / \eta$ particle REYNOLDS number

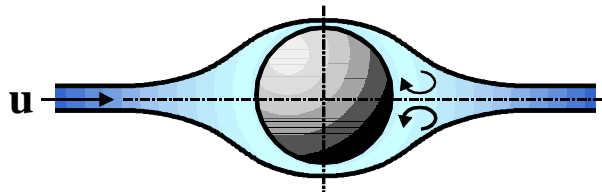
$c_w = \frac{24}{Re}$ drag coefficient

$F_w = c_w \cdot A_p \cdot \rho_f \cdot u^2 / 2$ drag force, generally

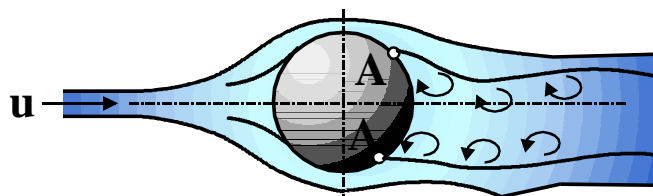
$F_{w,lam} = 3 \cdot \pi \cdot \eta \cdot d \cdot u$ drag force, laminar

II) Transition regime, $0.25 < Re < 10^3$

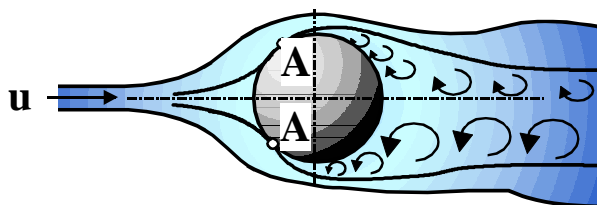
IIa) Laminar flowing eddies, $24 < Re < 130$



IIb) Eddy separation (separation point A), instationary eddy shedding, vortex street $130 < Re < 1000$



III) Square range of inertia, $10^3 < Re < 2 \cdot 10^5$, NEWTON

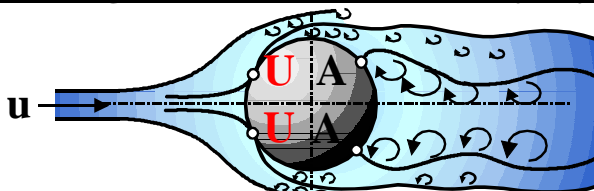


$c_w = 0.44$

for $Re < 2 \cdot 10^5$ $c_w = \frac{24}{Re} + \frac{4}{\sqrt{Re}} + 0.4$

or $c_w = \frac{24}{Re} + \sqrt{\frac{32}{Re}} + \frac{1}{3}$

IV) Range of turbulent boundary layer flow at onflow (transition point U):



$2 \cdot 10^5 < Re < 4 \cdot 10^5$

$c_w = 0.07$ to 0.3

To 4.1.1: Equivalent Falling Classes of Particles

- balance of the forces of buoyancy, weight and fluid resistance
- correlation between particle size d and the quasi-stationary settling velocity v_s in the field of gravity g :

$$v_s^2 = \frac{2}{c_w} \cdot \frac{\rho_s - \rho_f}{\rho_f} \cdot \frac{V_p}{A_p} \cdot g \quad (1)$$

A_p onflow cross-sectional area of the particle

c_w drag coefficient of the fluid flow pattern around the particle

V_p particle volume

ρ_f, ρ_s fluid and solid density

- for constant particle shape, “large” (i+1) and “lightweight” (L) particles settle just as fast as “small” (i) and “heavy” (S) particles.

$$v_s(d_{i+1}, \rho_{s,L}) = v_s(d_i, \rho_{s,S}) \quad (2)$$

- Depending on the particle flow-around patterns $v_s \propto d^\alpha$ and with

$$c_w \propto \text{Re}^{\frac{1-2\alpha}{3}} \quad (3)$$

$\text{Re} = v_s \cdot d \cdot \rho_f / \eta_f$ particle Reynolds number

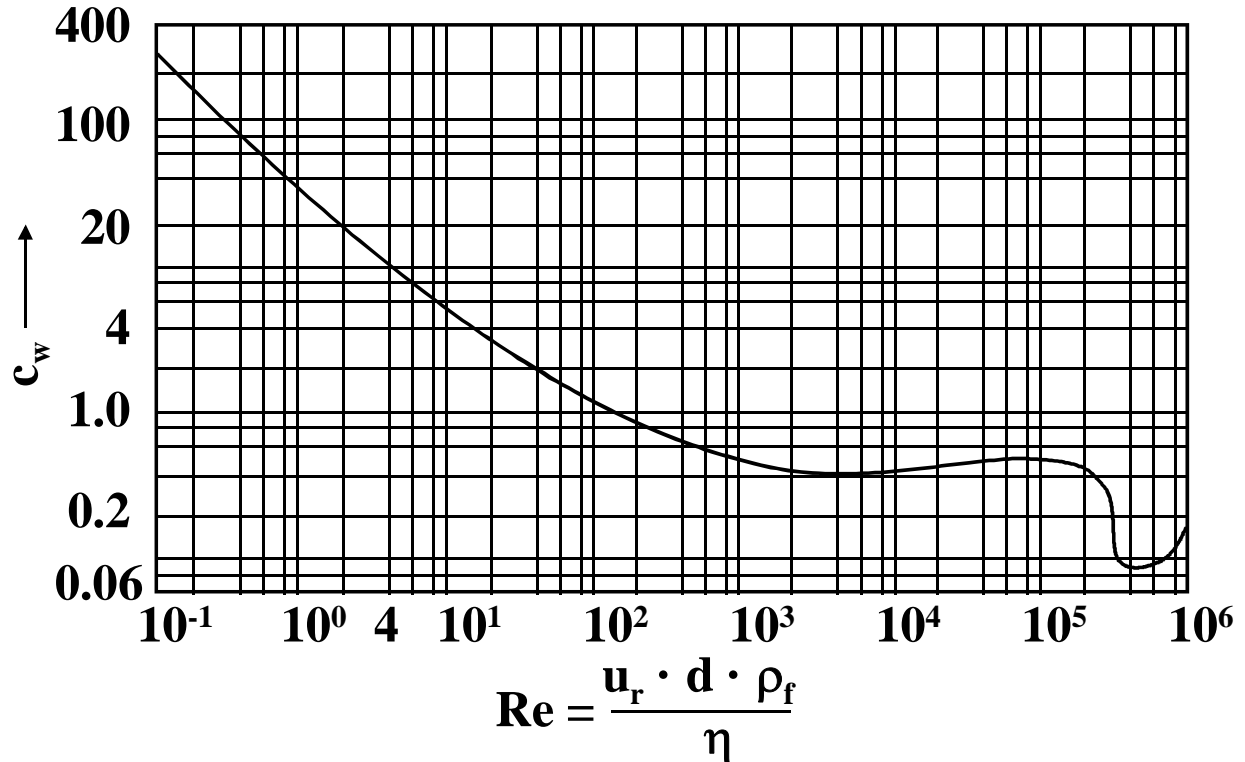
Equivalent-falling condition dependent on the particle flow-around pattern

Exponent α	$\frac{\alpha+1}{3 \cdot \alpha}$	Flow pattern	Reynolds number	Drag coefficient
2	1/2	laminar (Stokes)	$\text{Re} < 1$	$c_w \propto \text{Re}^{-1}$
$1/2 < \alpha < 2$	1/2 ... 1	transition	$1 < \text{Re} < 10^3$	$c_w \propto \text{Re}^{-1 \dots 0}$
1/2	1	turbulent (Newton)	$10^3 < \text{Re} < (2 - 4) \cdot 10^5$	$c_w \propto \text{Re}^0$

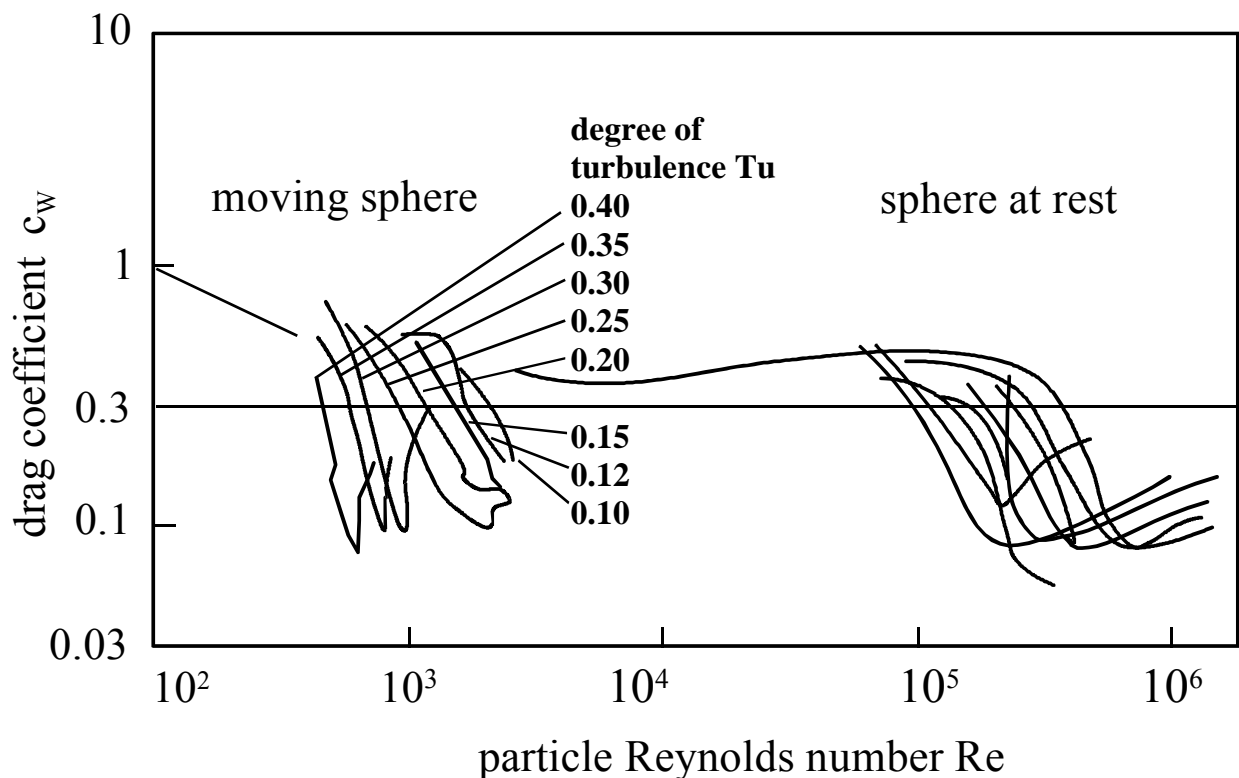
$$\frac{d_{i+1}}{d_i} = \left(\frac{\rho_{s,S} - \rho_f}{\rho_{s,L} - \rho_f} \right)^{\frac{\alpha+1}{3\alpha}} \quad \text{or} \quad \frac{v_s}{v_{sT}} = \left(\frac{d}{d_T} \right)^\alpha = \left(\frac{\rho_s - \rho_f}{\rho_{s,T} - \rho_f} \right)^{\frac{\alpha+1}{3}} \quad (4)$$

Flow-around Pattern of Smooth Spheres

3. Drag coefficient $c_w = f(\text{Re})$

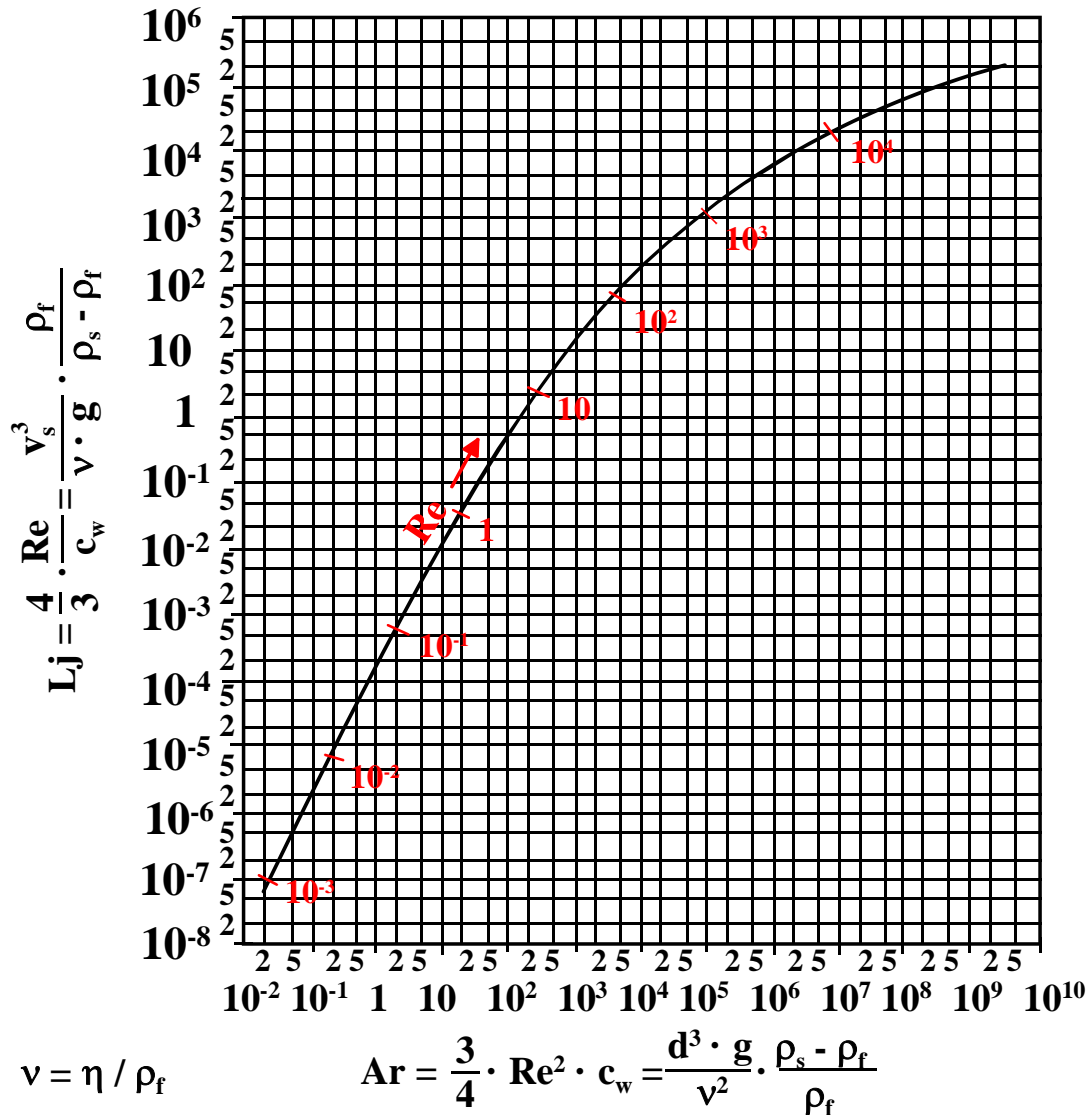


4. Influence of turbulence intensity of particle onflow on the drag coefficient c_w of moving spheres or spheres at rest



Flow-around of Single Particles

5. Ljascenko number $L_j = \Omega = f(Ar)$ of smooth spheres



6. Particle shape coefficient k_{ψ} of stationary settling velocity $v_{s,\psi} = k_{\psi} v_{s, sphere}$

body shape	equival. sphere diameter d_v	shape factor ψ_A	shape coefficients	
			$k_{\psi, St}$	$k_{\psi, N}$
sphere	d	1	1	1
cube	1,241 a	0,806	0,92	0,56
parallel epiped				
a x a x 2 a	1,563 a	0,767	0,90	0,52
a x 2 a x 2 a	1,970 a	0,761	0,89	0,51
a x 2 a x 3 a	2,253 a	0,725	0,88	0,48
a x a x 0,1a	0,576 a	0,435	0,70	0,30
a x a x 0,01a	0,267 a	0,110	0,19	0,15
cylinder				
h = 2 d	1,442 d	0,831	0,93	0,58
h = d	1,145 d	0,875	0,95	0,64
h = 0,5 d	0,909 d	0,826	0,93	0,58
h = 0,15 d	0,608 d	0,570	0,79	0,38
h = 0,01d	0,247 d	0,120	0,22	0,15



Dimensionless Groups and their Significance

Name	Symbol	Formula	Physical interpretation	Comments
Archimedes number	Ar	$\frac{g \cdot d^3 (\rho_p - \rho_f) \cdot \rho_f}{\eta^2}$	$\frac{\text{inertial force} \cdot \text{buoyancy force}}{(\text{viscous force})^2}$	Particle settling
Bingham number	Bm	$\frac{\tau_0 \cdot d}{\eta \cdot u}$	$\frac{\text{yield stress}}{\text{viscous force}}$	Flow of Bingham fluids = yield number
Bingham Reynolds number	Re _B	$\frac{d \cdot u \cdot \rho_f}{\eta}$	$\frac{\text{inertial force}}{\text{viscous force}}$	Flow of Bingham fluids (i.e. viscoplastics)
Blake number	B	$\frac{u \cdot \rho_f}{\eta \cdot (1 - \varepsilon) \cdot d}$	$\frac{\text{inertial force}}{\text{viscous force}}$	Flow through particle beds
Bond number	B _o	$\frac{(\rho_l - \rho_g) \cdot d^2 \cdot g}{\sigma_{lg}}$	$\frac{\text{gravitational force}}{\text{surface tension force}}$	Atomization = Eotvos number, Eo
Capillary number	Ca	$\frac{\eta \cdot u}{\sigma_{lg}}$	$\frac{\text{viscous force}}{\text{surface tension force}}$	Two-phase flow, free surface flow
Cauchy number	C	$\frac{\rho_f \cdot u^2}{\beta}$	$\frac{\text{inertial force}}{\text{compressibility force}}$	Compressible flow, hydraulic transients
Cavitation number	σ	$\frac{p - p_c}{\rho_l \cdot u^2 / 2}$	$\frac{\text{excess pressure above vapor pressure}}{\text{velocity head}}$	Cavitation
Centrifuge number	z	$\frac{a}{g} = \frac{R \cdot \omega^2}{g}$	$\frac{\text{centrifugal force}}{\text{gravity force}}$	Centrifugal fields, = Froude number
Dean number	De	$\frac{Re}{(D_c / D_R)^{1/2}}$	Reynolds number · $\frac{\text{inertial force}}{\text{centrifugal force}}$	Flow in curved channels
Deborah number	De	$t_{relax} \cdot \omega$	$\frac{\text{fluid relaxation time}}{\text{flow characteristic time}}$	Viscoelastic flow
Degree of turbulence	Tu	$\frac{\sqrt{u'^2}}{u}$	$\frac{\text{root mean squared of flow rate fluctuations}}{\text{fluid flow rate}}$	Turbulence intensity
Drag coefficient	c _w	$\frac{F_W}{A_p \cdot \rho_f \cdot u^2 / 2}$	$\frac{\text{fluid drag force}}{\text{projected area} \cdot \text{velocity head}}$	Flow-around objects, particle settling
Elasticity number	El	$\frac{t_{relax} \cdot \eta}{\rho_f \cdot u^2}$	$\frac{\text{elastic force}}{\text{inertial force}}$	Viscoelastic flow
Euler number	Eu	$\frac{\Delta p}{\rho_f \cdot u^2}$	$\frac{\text{frictional pressure loss}}{2 \cdot \text{velocity head}}$	Fluid friction in conduits
Fanning friction factor	f	$\frac{D_B \cdot \Delta p}{2 \cdot \rho_f \cdot u^2 \cdot d} = \frac{2 \cdot \tau_w}{\rho_f \cdot u^2}$	$\frac{\text{wall shear stress}}{\text{velocity head}}$	Fluid friction in conduits, Darcy friction factor = 4·f
Froude number	Fr	$\frac{u^2}{g \cdot R}$	$\frac{\text{inertial force}}{\text{gravity force}}$	Often defined as Fr = u / √(g · R)
Densometric Froude number	Fr'	$\frac{\rho_f \cdot u^2}{(\rho_p - \rho_f) \cdot g \cdot d}$	$\frac{\text{inertial force}}{\text{gravity force}}$	Fr' = $\frac{u}{\sqrt{(\rho_p - \rho_f) \cdot g \cdot d / \rho_f}}$



Figure 4.9

Hedstrom number	He	$\frac{d^2 \cdot \tau_0 \cdot \rho_f}{\eta^2}$	Bingham Reynolds number · Bingham number	Flow of Bingham fluids (viscoplastics)
Hodgson number	H	$\frac{V \cdot \omega \cdot \Delta p}{\dot{V} \cdot \bar{p}}$	$\frac{\text{time constant of system}}{\text{period of pulsation}}$	Pulsating gas flow
Ljaščenco Number	Lj	$\frac{v_s^3 \cdot \rho_f^2}{\eta \cdot g \cdot \rho_p - \rho_f}$	$\frac{(\text{inertial force})^2}{\text{viscous force} \cdot \text{fluid drag force}}$	Particle settling, $= \frac{4 \cdot \text{Re}}{3 \cdot c_w}$
Mach number	M	$\frac{u}{c_s}$	$\frac{\text{fluid velocity}}{\text{sonic velocity}}$	Flow of compressible fluids
Newton number	Ne	$\frac{F_w}{\rho_f \cdot A_p \cdot u^2}$	$\frac{\text{fluid drag force}}{\text{inertial force}}$	Flow-around of particles, = c_w fluid drag coefficient
Ohnesorge number	Z	$\frac{\eta}{(\rho_f \cdot d \cdot \sigma_{lg})^{1/2}}$	$\frac{\text{viscous force}}{(\text{inertial force} \cdot \text{surface tension force})^{1/2}}$	Atomization = $\frac{\text{Weber number}}{\text{Reynolds number}}$
Peclet number	Pe	$\frac{D_B \cdot u}{D}$	$\frac{\text{convective transport}}{\text{diffusive transport}}$	Heat, mass transfer, mixing, = Bodenstein number Bo
Pipeline parameter	Pn	$\frac{v \cdot u_o}{2 \cdot g \cdot H}$	$\frac{\text{maximum water - hammer pressure rise}}{2 \cdot \text{static pressure}}$	Water “hammer”
Power number	c_p	$\frac{P}{\rho_f \cdot n^3 \cdot D_A^5}$	$\frac{\text{impeller drag force}}{\text{inertial force}}$	Agitation
Prandtl velocity ratio	u^+	$\frac{u}{(\tau_w / \rho_f)^{1/2}}$	velocity normalized by friction velocity	Turbulent flow near a wall, friction velocity = $\sqrt{\tau_w / \rho_f}$
Reynolds number	Re	$\frac{d \cdot u \cdot \rho_f}{\eta}$	$\frac{\text{inertial force}}{\text{viscous force}}$	Fluid flow
Schmidt number	Sc	$\frac{D_t}{\nu}$	$\frac{\text{diffusive transport}}{\text{viscous friction}}$	Turbulent Schmidt number
Stokes number	St	$C_{u} \cdot \frac{d^2 \cdot u \cdot \rho_s}{18 \cdot \eta \cdot D}$	$\frac{\text{particle inertial force}}{\text{fluid drag force}}$	Particle impact in fluid flow against tool
Strouhal number	St	$\frac{f \cdot D_R}{u}$	vortex shedding frequency · characteristic flow time scale	Vortex shedding, von Karman vortex streets
Weber number	We	$\frac{\rho_f \cdot u^2 \cdot d}{\sigma_{lg}}$	$\frac{\text{inertial force}}{\text{surface tension force}}$	Bubble, drop formation

Nomenclature		SI Units
a	Acceleration	m/s ²
A _p	Projected particle area	m
c _s	Sonic velocity	m/s
d	Characteristic particle dimension (diameter)	µm
D _A	Diameter of agitator	m



Figure 4.10

D_B	Characteristic width of flow channel	m
D_R	Diameter of pipe or process chamber	m
D_c	Diameter of flow channel curvature	m
D	Diffusivity	m^2/s
D_t	Turbulent Diffusion coefficient	m^2/s
f'	Vortex shedding frequency	1/s
F_W	Drag force	N
g	Acceleration of gravity	m/s
H	Static head (height of isostatic pressure)	m
n	Rotational speed or number of revolutions	1/s
p	Pressure	Pa
p_v	Vapor pressure	Pa
\bar{p}	Average static pressure	Pa
Δp	Frictional pressure drop	Pa
P	Power	W
R	Radius of process chamber or apparatus	m
t_{relax}	Fluid relaxation time	s
u	Local fluid velocity	m/s
\bar{u}	Characteristic or average fluid velocity	m/s
v	Wave propagation speed	m/s
v_s	Particle settling velocity	m/s
V	Volume of process chamber	m^3
V_p	Particle volume	m^3
\bar{V}	Average volumetric flow rate	m^3/s
β	Bulk compression modulus	Pa
ε	Porosity, void fraction	m^3/m^3
η	(dynamic) fluid viscosity	$Pa \cdot s$
η_p	Infinite shear viscosity (Bingham fluid, $\dot{\gamma} \rightarrow \infty$)	$Pa \cdot s$
ν	Kinematic fluid viscosity	m^2/s
ρ_f	Fluid density	kg/m^3
ρ_g, ρ_l	Gas, liquid densities	kg/m^3
ρ_p	Particle or dispersed phase density	kg/m^3
σ_{lg}	Surface tension	N/m
τ_0	Yield shear stress of Bingham fluid	Pa
ω	Characteristic frequency or reciprocal time scale of flow	1/s

In: Perry, R.H., Green, D.W., Maloney, J.O., Perry's Chemical Engineers' Handbook (CD version), pp. 6-49, McGraw-Hill, New York (1999)



Figure 4.11

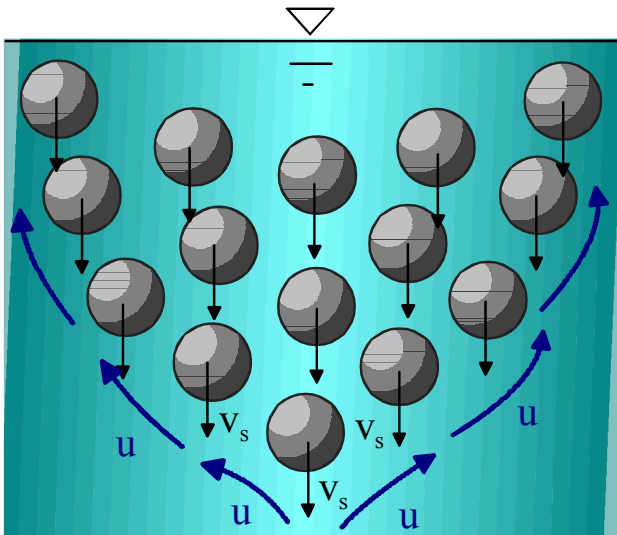
4.1.2 Survey about Models of Uniformly Accelerated Particle Sedimentation (TOMAS 2010)

Microprocess variables	Laminar Flow-around of Particles	Turbulent Flow-around of Particles
Reynolds number, c_W	$Re_{St} < 0.25 - 1, c_W = 24/Re_{St}$	$10^3 < Re_N < Re_c = 2 \cdot 10^5, c_W = 0.44$
Stationary Settling Velocity	$v_{s,St} = \frac{(\rho_s - \rho_f) \cdot d^2 \cdot g}{18\eta}$	$v_{s,N} = \sqrt{\frac{4 \cdot (\rho_s - \rho_f) \cdot d \cdot g}{3 \cdot c_W \cdot \rho_f}}$
Particle Size Range	$d_{St} \leq \sqrt[3]{\frac{18 \cdot \eta^2 \cdot Re_{St}}{\rho_f \cdot (\rho_s - \rho_f) \cdot g}}$	$d_N \geq \sqrt[3]{\frac{3 \cdot c_W \cdot \eta^2 \cdot Re_N^2}{4 \cdot \rho_f \cdot (\rho_s - \rho_f) \cdot g}}$
Differential Equation	$\frac{dv(t)}{dt} = g \cdot \left(1 - \frac{v}{v_s}\right)$	$\frac{dv(t)}{dt} = g \cdot \left(1 - \frac{v^2}{v_s^2}\right)$
Velocity-Time Law	$v(t) = v_s \cdot \left[1 - \exp\left(-\frac{t}{t_{63,vs}}\right)\right]$	$v(t) = v_s \cdot \tanh\left(\frac{t}{t_{76,vs}}\right)$
Characteristic Settling Time	$t_{63,vs} = \frac{v_s}{g} = \frac{(\rho_s - \rho_f) \cdot d^2}{18 \cdot \eta}$	$t_{76,vs} = \frac{v_s}{g} = \sqrt{\frac{4 \cdot (\rho_s - \rho_f) \cdot d}{3 \cdot c_W \cdot \rho_f \cdot g}}$
Characteristic Settling Velocities	$v(t = t_{63,vs}) = v_s \cdot [1 - \exp(-1)] = 0.63 \cdot v_s$ $v(t_{95} = 3 \cdot t_{63,vs}) = v_s \cdot [1 - \exp(-3)] = 0.95 \cdot v_s$	$v(t = t_{76}) = v_s \cdot \tanh(1) = 0.76 \cdot v_s$ $v(t_{96} = 2 \cdot t_{76,vs}) = v_s \cdot \tanh(2) = 0.964 \cdot v_s$
Differential Equation	$\frac{ds(t)}{dt} = v_s \cdot \left[1 - \exp\left(-\frac{t}{t_{63,vs}}\right)\right]$	$\frac{ds(t)}{dt} = v_s \cdot \tanh\left(\frac{t}{t_{76,vs}}\right)$
Distance-Time Law	$s(t) = v_s \cdot \left\{t - t_{63,vs} \cdot \left[1 - \exp\left(-\frac{t}{t_{63,vs}}\right)\right]\right\}$	$s(t) = v_s \cdot t_{76,vs} \cdot \ln\left \cosh\left(\frac{t}{t_{76,vs}}\right)\right $
Characteristic Acceleration Distances	$s(t = t_{63,vs}) = 0.37 \cdot v_s \cdot t_{63,vs} = 0.37 \cdot v_s^2 / g$ $s(t_{95} = 3 \cdot t_{63,vs}) = 2.05 \cdot v_s \cdot t_{63,vs} = 2.05 \cdot v_s^2 / g$	$s(t_{76}) = 0.433 \cdot v_s \cdot t_{76,vs} = 0.433 \cdot v_s^2 / g$ $s(t_{96}) = 1.33 \cdot v_s \cdot t_{76,vs} = 1.33 \cdot v_s^2 / g$

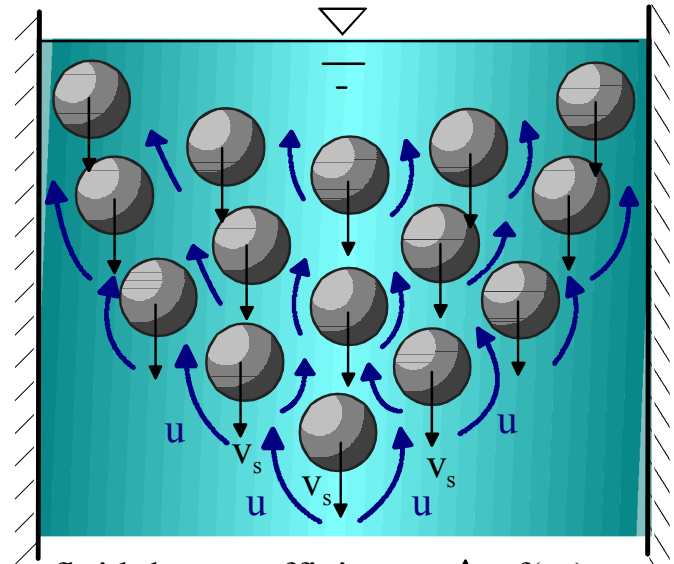
Flow-around of Particles - Swarm Confinement

7. Swarm confinement at sedimentation of particle cluster

- a) Free flow-around of particle swarm b) Confined flow field, permeation of particle swarm



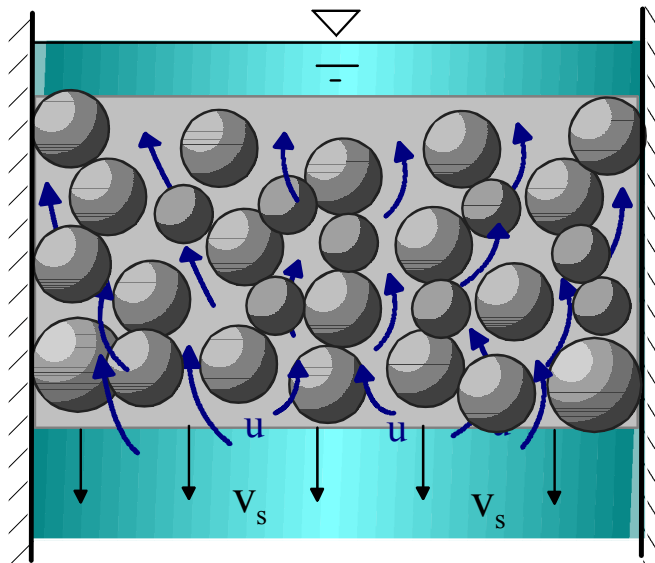
fluid drag coefficient $c_w \downarrow$
 settling velocity $v_s \uparrow$



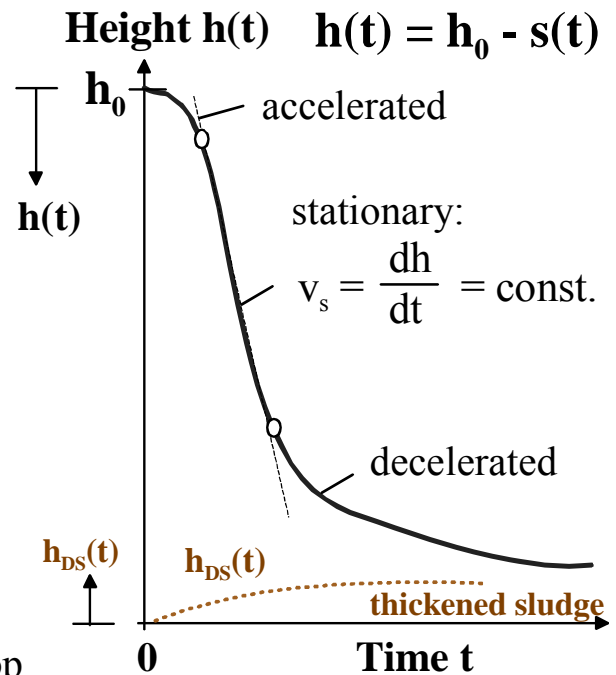
fluid drag coefficient $c_w \uparrow = f(\phi_s)$
 settling velocity $v_s \downarrow = f(\phi_s)$

8. Zone sedimentation of particle bed

Sedimentation and permeation (flow-through) of comparatively dense, agglomerated particle layers



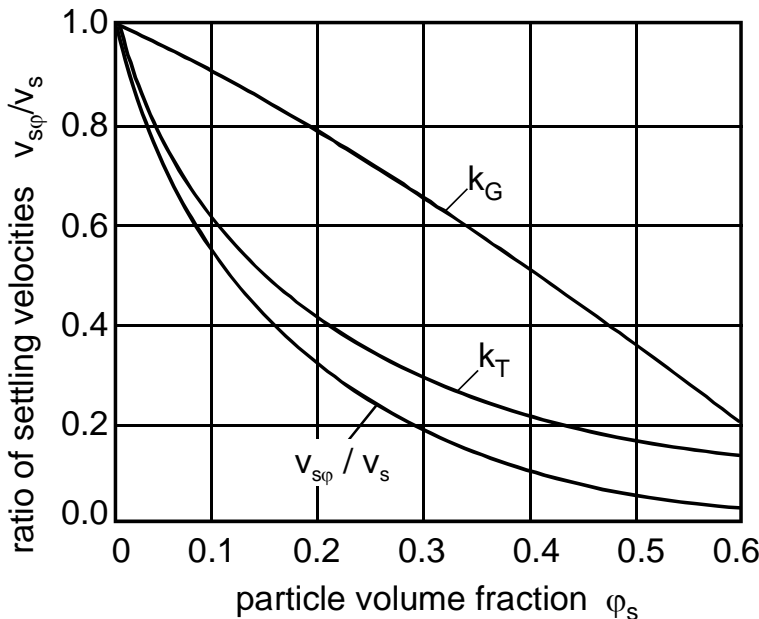
fluid drag force $F_w \rightarrow \Delta p$ pressure drop
 fluid drag coefficient $c_w \rightarrow Eu = \Delta p / (\rho_f u^2) = f(\phi_s, d_{pore})$ EULER number
 settling velocity $v_s = f(\phi_s) \neq f(d)$



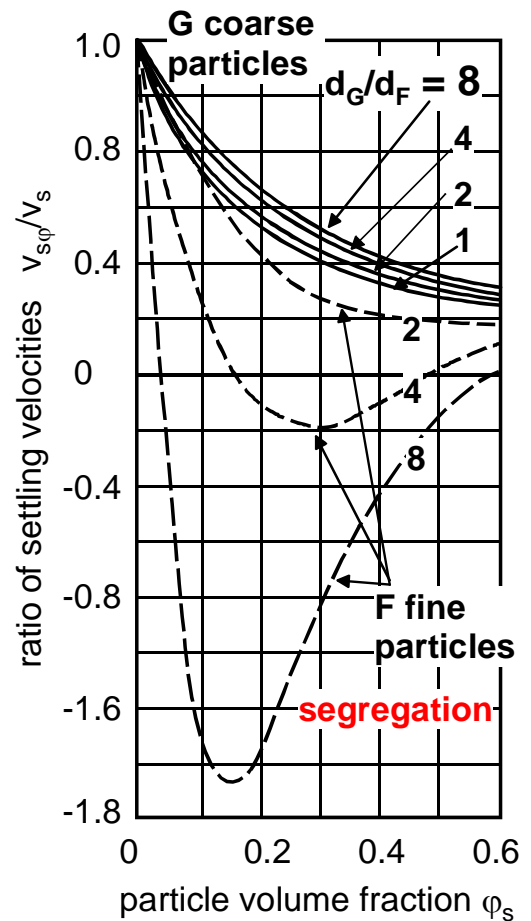
Flow-around of Particles - Swarm Confinement

9. Ratio of settling velocities of smooth spheres $\frac{v_{s\phi}}{v_s} = k_G \cdot k_T$

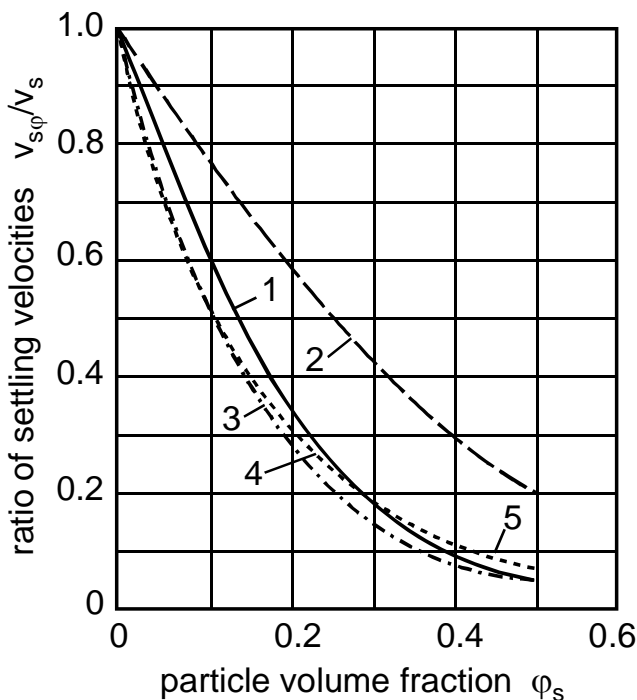
a) as function of particle volume fraction ϕ_s in a monodisperse suspension (k_G counter-current factor, k_T swarm turbulence factor) (acc. to Brauer and Thiele)



b) as function of particle volume fraction ϕ_s for 2 size fractions with $\phi_{s,G} = \phi_{s,F}$ and d_G/d_F as parameter (acc. to Brauer and Thiele)



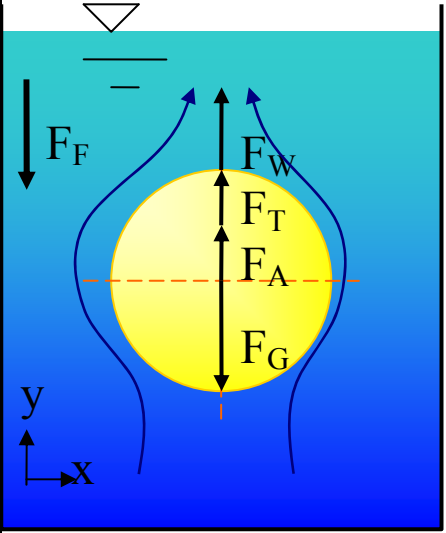
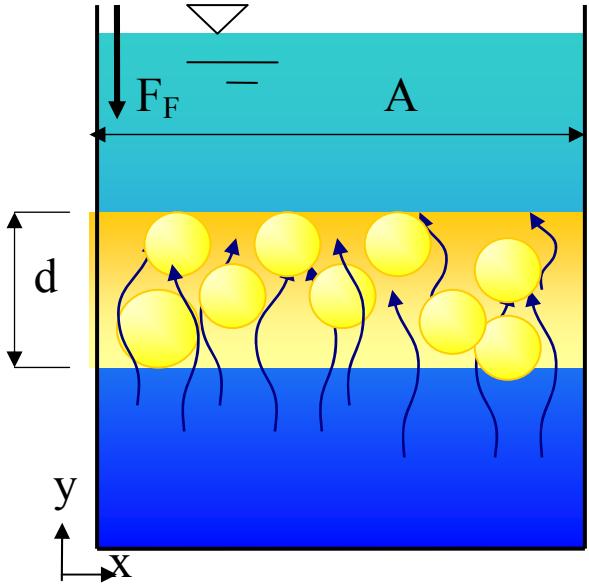
10. Comparison of various formulas to include swarm confinement in monodisperse suspensions



No.	Authors	flow-around range
1	RICHARDSON & Zaki	STOKES
2		NEWTON
3	STEINOUR	STOKES
4	BRAUER & Mitarb.	STOKES
5	fit curve of various experimental values	STOKES

Figure 4.14

Force Balance of Particle Sedimentation in a static Fluid at **uniform** (stationary) **Onflow** and (Statistically) Homogeneous **Flow-Around** and **Flow-Through**

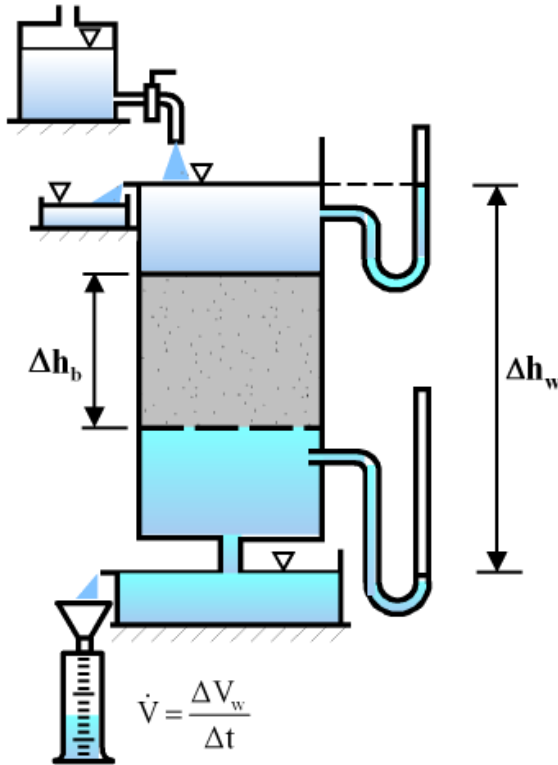
Forces	Microscopic Particle Flow-around	Macroscopic Particle Bed Flow-through
Particle model	Smooth sphere	Statistically homogeneous particle bed
Sink model	Single particle sedimentation	Zone sedimentation
		
Gravity	$F_G = \rho_s \cdot V_p \cdot g$	$\frac{F_G}{A} = \rho_{Tr} \cdot g \cdot dy$
Buoyancy	$F_A = \rho_f \cdot V_p \cdot g$	$\frac{F_A}{A} = \rho_f \cdot g \cdot dy$
Fluid drag	$F_W = c_w(\text{Re}(u_r)) \cdot \rho_f \cdot A_p \cdot \frac{u_r^2(t)}{2}$	$\Delta p = \frac{F_W}{A} = \text{Eu}(\text{Re}(u_r)) \cdot \rho_f \cdot \frac{u_r^2(t)}{2}$
Inertia	$F_T = \rho_s \cdot V_p \cdot \dot{v}(t)$	$\frac{F_T}{A} = \rho_{Tr} \cdot \dot{v}(t) \cdot dy$

Fluid Flow through Particle Beds

1. **Darcy's law** (development of water purification process, model: laminar permeation of groundwater through sand, $Re < 0,5 \dots 20$):

$$u \propto \text{grad } p \Rightarrow u = k \cdot \text{grad } p \quad \text{or} \quad (1)$$

$$\dot{V} = k \cdot A \cdot \text{grad } p \quad (2)$$



original Darcy (1856):

$$\text{grad } p = \frac{\Delta h_w}{\Delta h_b} \quad (3)$$

$$\dot{V} = k_f \cdot A \cdot \frac{\Delta h_w}{\Delta h_b} \quad (4a)$$

$$\text{or } u = k_f \cdot \frac{\Delta h_w}{\Delta h_b} \quad (4b)$$

k_f – permeability

2. **Permeability according to Carman and Kozeny:**

$$u = \frac{\varepsilon^3}{K_{CK} \cdot \eta \cdot A_{S,V}^2 \cdot (1 - \varepsilon)^2} \cdot \text{grad } p \quad (5)$$

$$k_f = \frac{\varepsilon^3 \cdot \rho_f \cdot g}{K_{CK} \cdot \eta \cdot A_{S,V}^2 \cdot (1 - \varepsilon)^2} = \frac{\varepsilon^3 \cdot \rho_f \cdot g \cdot d_{ST}^2}{36 K_{CK} \cdot \eta \cdot (1 - \varepsilon)^2} \quad (6)$$

3. **Reference values of permeability and flow behaviour (flow function ff):**

$k_f^{1)}$ in m/s	permeability	soil behaviour	$ff_c =$ σ_f / σ_c	flowability	$\approx d_{ST}^{2)}$ in μm
0 - 10^{-9}	practically impermeable (- 3.15 cm/a)	very binding	0 - 2	very cohesive	0 - 0,5
10^{-9} - 10^{-7}	very low (- 26 cm/month)	binding		cohesive	0.5 - 5
10^{-7} - 10^{-5}	low (- 86 cm/d)	low binding	2 - 4	cohesive	5 - 50
10^{-5} - 10^{-3} 10^{-3} - 1	medium (- 3.6 m/h) high	non binding	> 4	easy to free flowing	50 - 500 500 - 15 mm

¹⁾ according to Terzaghi / Peck

²⁾ $K_{CK} = 5$ (spheres), $\rho_f = 10^3 \text{ kg/m}^3$, $\eta = 10^{-3} \text{ Pa.s}$, $\varepsilon = 0.38$



Figure 4.17

Stressing and Flow of Wet Particle Dispersions

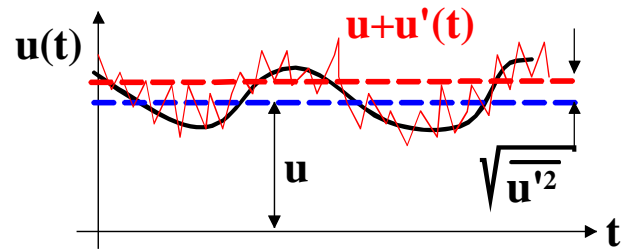
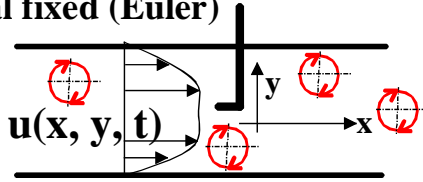
	particle in liquid dispersion (suspension) ← ↔		paste ← ↔	liquid in particle packing → ↔
	diluted	concentrated	liquid saturated	moist packing
suspension and particle flow pattern				
flow function				
cubical cell packing model				
particle separation	$\frac{a}{d} > 1$	$0 < \frac{a}{d} < 0.2$	$\frac{a}{d} = 0$ contact	$-0.01 < \frac{a}{d} < 0$ contact deformation
particle volume fraction	$\phi_s < 0.066$	$0.3 < \phi_s < \frac{\pi}{6}$	$\epsilon_{s,0} = \frac{\pi}{6}$ pore saturation $S = 1$	$\epsilon_s > \frac{\pi}{6}$ $S < 1$
particle friction	$\phi_i = 0$	$\phi_i = 0$	$\phi_i \geq 0$	$\phi_i > 30^\circ$

Figure 4.19

Turbulent Eddies in Fluids

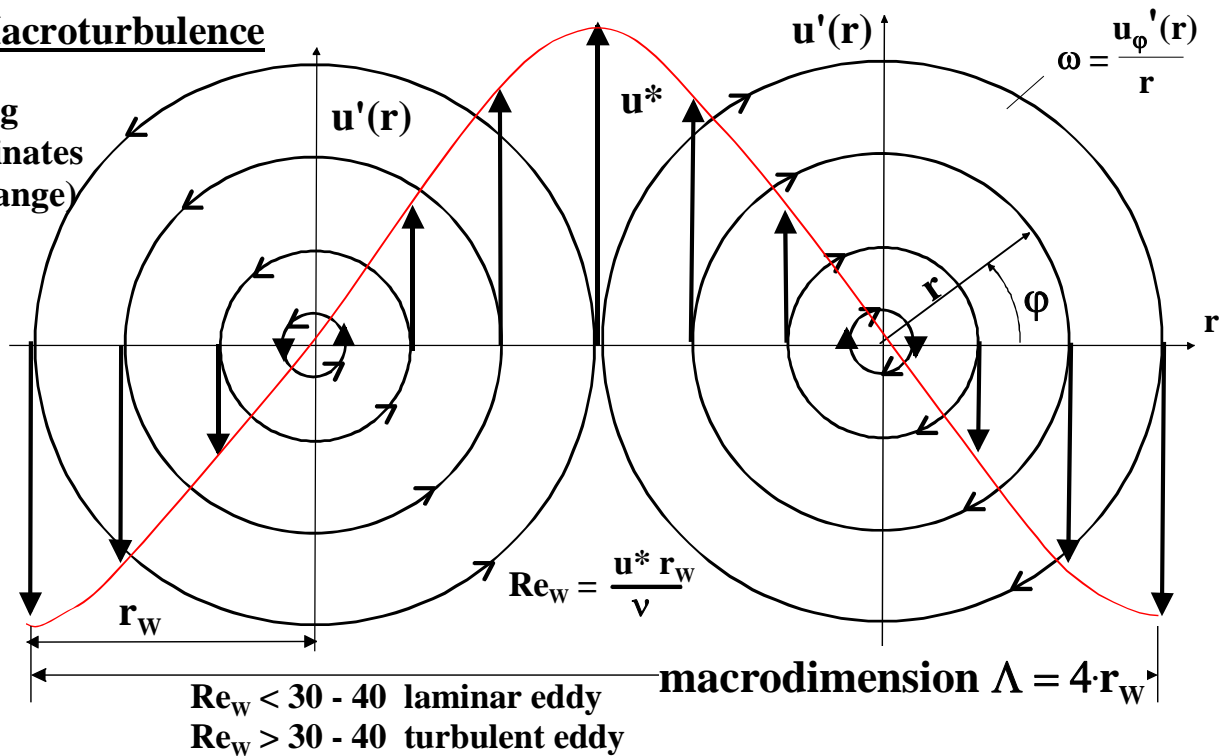
a) Turbulent flow rate fluctuations

local fixed (Euler)

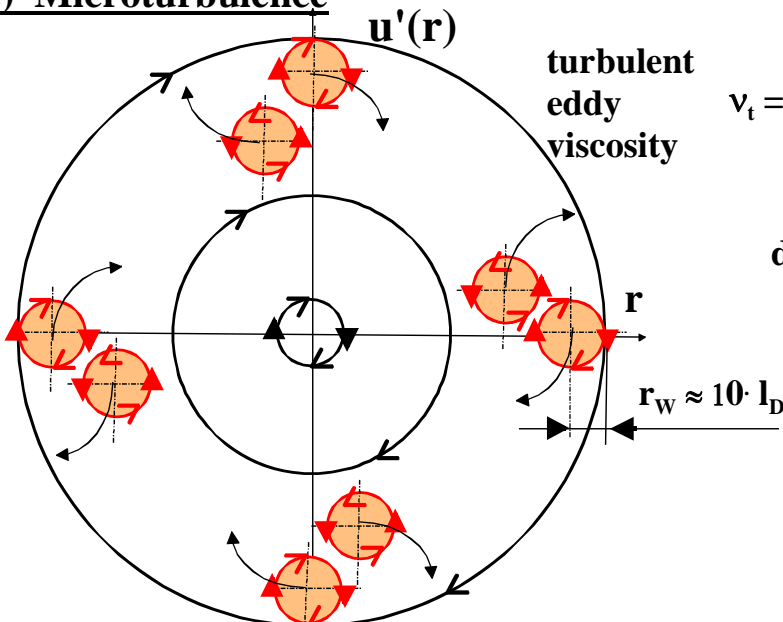


b) Macroturbulence

moving coordinates (Lagrange)



c) Microturbulence



turbulence intensity $Tu = \frac{\sqrt{u'^2}}{u}$

$\nu_t = 0.09 \frac{k^2}{\epsilon} = 0.09 \frac{(u_x'^2 + u_y'^2 + u_z'^2)^2}{dP_D/dm}$

dissipation rate $\epsilon = 1.65 \frac{(\overline{u'^2})^{3/2}}{\Lambda}$

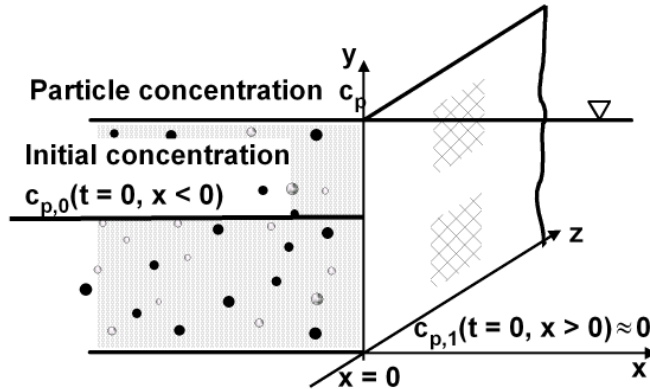
Kolmogorov dimension $l_D = \left(\frac{\nu^3}{\epsilon}\right)^{1/4}$

Thermokinetic Particle Diffusion in Dispersion Medium

Prerequisites:

External field forces = 0
 Fluid drag = 0
 Fluid flow rates $u_x = u_y = u_z = 0$
 One-dimensional model $\frac{\delta}{\delta y} = \frac{\delta}{\delta z} = 0$

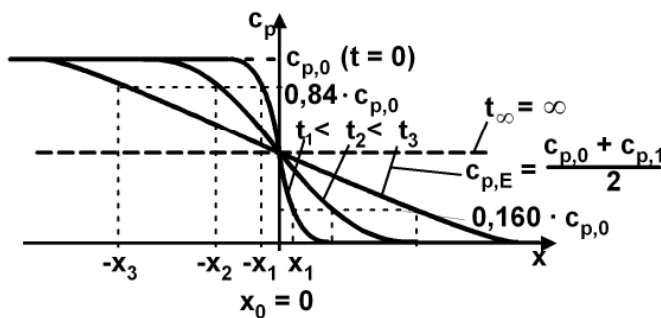
a) Vessel with separation membrane



Boundary and initial conditions:

for $t = 0, x < 0, c_p = c_{p,0}$
 for $t = 0, x > 0, c_p = c_{p,1} = 0$
 for $t = \infty, c_{p,E} = (c_{p,0} + c_{p,1}) / 2$

b) Time and spatial function of the particle concentration c_p



$$c_p(x, t) = c_{p,0} - (c_{p,0} - c_{p,1}) \cdot \phi(x, t) \quad (4)$$

$$\phi(x, t) = \frac{1}{\sqrt{2\pi}} \int_{-\infty}^x \exp\left(-\frac{x^2}{4D_p \cdot t}\right) dx$$

$$\phi(x < 0, t = 0) = 0$$

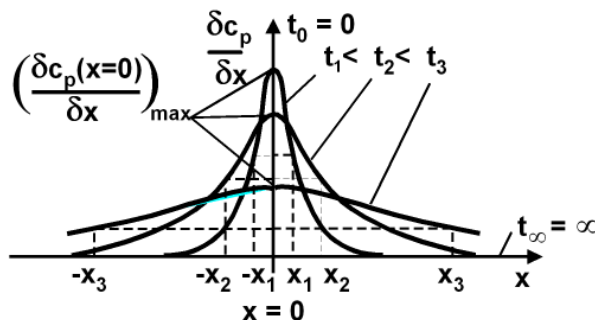
$$\phi(x = 0, t) = \phi(x, t = \infty) = 0,5$$

$$\phi(x = \infty, t) = 1$$

characteristic diffusion distance or standard deviation

$$\sigma_x = x_i - x_0 = \sqrt{2 \cdot D_p \cdot t_i} \quad (4a)$$

c) Time and spatial function of the particle concentration gradient $\text{grad } c_p \approx \frac{\delta c_p}{\delta x}$

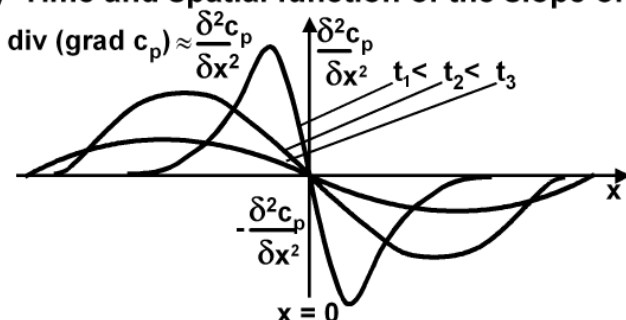


$$\frac{\delta c_p}{\delta x} = \frac{c_{p,0} - c_{p,1}}{\sqrt{4\pi D_p \cdot t}} \exp\left(-\frac{x^2}{4 \cdot D_p \cdot t}\right) \quad (3)$$

$$D_p = \frac{(c_{p,0} - c_{p,1})^2}{4\pi t \cdot (\delta c_p / \delta x)_{\max}^2} \quad (3a)$$

$$\frac{d(m_p / M_p)}{dt} = -D_p \cdot A \cdot \frac{\delta c_p}{\delta x} \quad (1)$$

d) Time and spatial function of the slope of particle concentration gradient

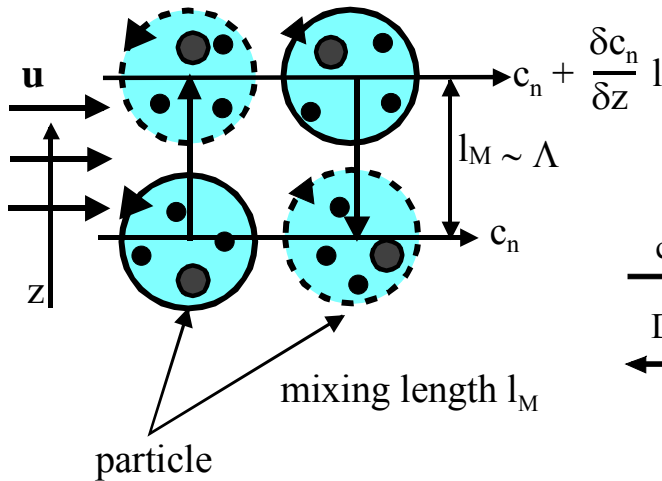


$$\frac{\delta c_p}{\delta t} = D_p \cdot \frac{\delta^2 c_p}{\delta x^2} \quad (2)$$

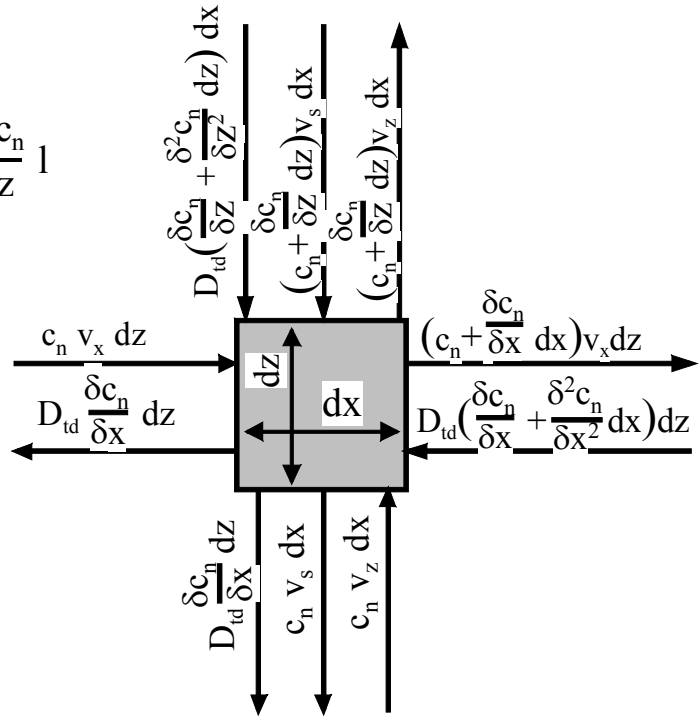
Figure 4.21

Particle Transport in Turbulent Fluid Flow

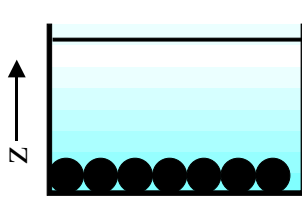
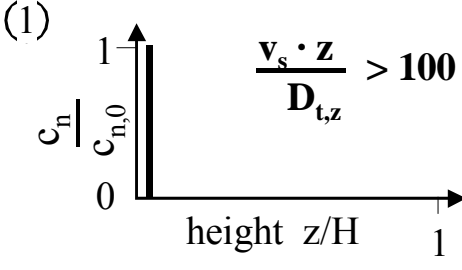
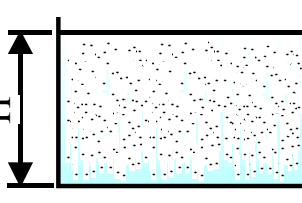
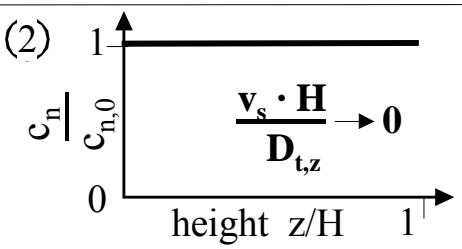
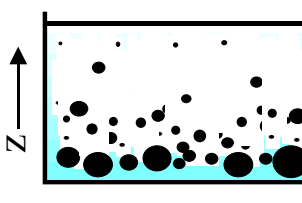
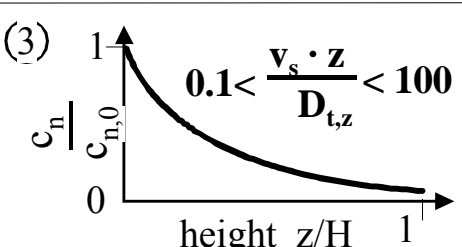
a) Schematic graph of turbulent transport by eddies



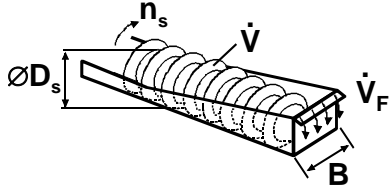
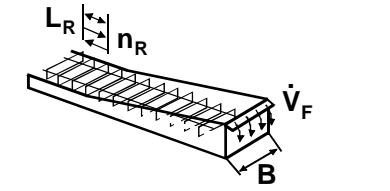
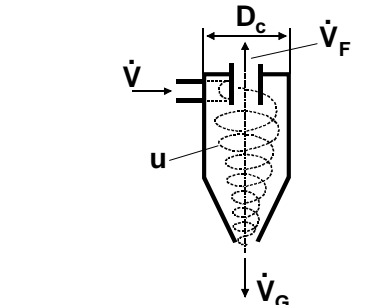
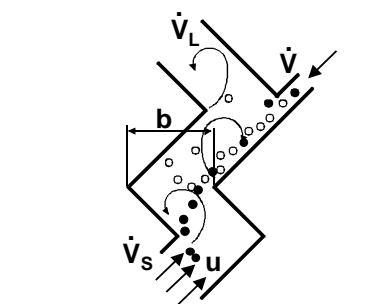
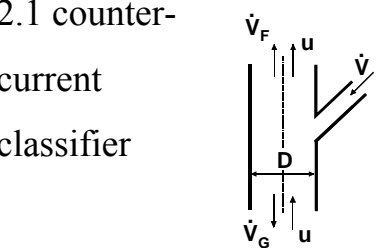
b) To derive the transport equation of particles (2-dimensional plane flow)



c) Particle concentration in a homogeneous turbulence field

characteristic equilibrium state	concentration distribution	$\frac{c_n}{c_{n,0}} = \exp[-z v_s / D_{t,z}]$
	(1)  $\frac{v_s \cdot z}{D_{t,z}} > 100$	1. Sedimentation in non-turbulent suspension $D_{t,z} = 0, v_s > 0$ 2. Sedimentation of coarse or heavy particles in turbulent suspension $D_{t,z} > 0, v_s \gg 0$
	(2)  $\frac{v_s \cdot H}{D_{t,z}} \rightarrow 0$	1. $v_s = 0$, if $\rho_s = \rho_f$ 2. $v_s \rightarrow 0$, if $d \rightarrow 0$ 3. high turbulence intensity
	(3)  $0.1 < \frac{v_s \cdot z}{D_{t,z}} < 100$	1. Moderate turbulence intensity $D_{t,z} > 0$ 2. wide distribution of particle settling velocity $v_s > 0$ 3. Exponential height distribution of particles

Turbulent Particle Separation Apparatuses

1. Cross flow separation apparatus	REYNOLDS number $Re = u \cdot D / \nu$	degree of turbulence $Tu = \sqrt{u'^2} / u$	turb. diffusion coefficient in $(\text{cm})^2/\text{s}$ $D_t = \Lambda \cdot \sqrt{u'^2}$	BODENSTEIN number $Bo = \nu \cdot L / D_{t,s}$
1.1 screw classifier 	$\frac{n_s \cdot D_s^2}{\nu}$ $Re_{crit} \approx 10^4$ $10^4 - 5 \cdot 10^5$	0.05 – 0.15	$0.014 \cdot n_s \cdot D_s^2 + \frac{0.48 \cdot \dot{V}_F}{B}$ $5 - 50$ $\approx (2)^2 - (7)^2$	$\frac{n_s \cdot D_s^2}{D_t} \approx 100$
1.2 rake classifier 	$\frac{n_R \cdot L_R^2}{\nu}$ $10^4 - 5 \cdot 10^4$	-	$0.31 \cdot n_R \cdot L_R^2 + \frac{0.48 \cdot \dot{V}_F}{B}$ $30 - 100$ $\approx (5.5)^2 - (10)^2$	$\frac{n_R \cdot L_R^2}{D_t} \approx 1.5 - 3$
1.3 cyclones 	$\frac{u \cdot D_c}{\nu}$ $Re_{crit} \approx 10^3$ $10^5 - 10^6$	0.01 - 0.05 ≈ 0.1 at input	water: $8 \cdot 10^{-4} \cdot u \cdot D_c$ air: $0.0035 \cdot u \cdot D_c$ $1 - 20$ $\approx (1)^2 - (4.5)^2$	$\frac{u \cdot D_c}{D_t} \approx 10^3$
1.4 zigzag apparatus* 	$\frac{u \cdot b}{\nu}$ $10^4 - 6 \cdot 10^5$	$Tu \approx \frac{D_t}{u \cdot b} \approx$ 0.11 - 0.13	$(0.11 - 0.13) \cdot u \cdot b$ 2000 - 4000 $\approx (45)^2 - (63)^2$	$\frac{u \cdot b}{D_t} \approx 1 - 15$
2. counter-current separation apparatus				
2.1 counter-current classifier 	$\frac{u \cdot D}{\nu}$ $10^3 - 10^6$	-	$0.02 \cdot u \cdot D$ $200 - 2000$ $\approx (14)^2 - (45)^2$	0.5 - 50

in Schubert, H.: Aufbereitung fester mineralischer Rohstoffe, Verlag für Grundstoffindustrie Leipzig 1989
 * Back-calculated from separation tests

Selected Flow Separation Models

	Separation Function $T(d) =$	Cut Size $d_{50} = d_T(T = 0,5) =$	Separation Efficiency $\kappa = d_{25}/d_{75} = \text{or } T' =$	Rem.
KAISER 1963	$\frac{1}{1 + (1/T_z - 1)^z}$	-	$\kappa_{ges} \approx \kappa_z^{1/z}$	CCS z
MOLERUS 1967/69	$\frac{1}{1 + \frac{u}{v_s(d)} \cdot \exp\left[-\frac{(v_s(d) - u) \cdot H}{D_{ax}}\right]}$	$\sqrt{\frac{18 \cdot \eta}{k_\phi \cdot (\rho_s - \rho_f) \cdot a}} \cdot u$	$\frac{dT}{d(d/d_T)} = \frac{1 + u \cdot H/D_{ax}}{4}$	CCS
NEESSE SCHUBERT 1969/73 splitting	$\frac{1 - \exp\left(-\frac{v_s(d) \cdot H_G}{D_t}\right)}{1 - \exp\left(-\frac{v_s(d) \cdot H}{D_t}\right)}$	$\sqrt{\frac{18 \cdot \eta}{(\rho_s - \rho_f) \cdot a} \cdot \frac{D_t}{H} \cdot F\left(\frac{\dot{V}_F}{\dot{V}_G}\right)}$	-	CFS
SCHUBERT, NEESSE 1973 tapping	$\frac{1}{1 + \frac{\dot{V}_F}{\dot{V}_G} \cdot \exp\left(-\frac{v_s(d) \cdot H}{D_t}\right)}$	$\sqrt{\frac{18 \cdot \eta}{(\rho_s - \rho_f) \cdot a} \cdot \frac{D_t}{H} \cdot \ln\left(\frac{\dot{V}_F}{\dot{V}_G}\right)}$ $Bo = \frac{u \cdot H}{D_t} \equiv \ln\left(\frac{\dot{V}_F}{\dot{V}_G}\right)$	$\left[\frac{\ln(\dot{V}_F / \dot{V}_G) - \ln 3}{\ln(\dot{V}_F / \dot{V}_G) + \ln 3}\right]^{1/\alpha}$	CFS
SENDEN 1979	$T_{L,0} = \frac{1 - p_A + K}{\frac{1}{p_{S(0,0)}} \cdot \left(\frac{p_L}{1 - p_S}\right)^A + \left(\frac{1 - p_L}{1 - p_S}\right) \cdot \left(\frac{1 - \left(\frac{p_L}{1 - p_S}\right)^A}{1 - \left(\frac{p_L}{1 - p_S}\right)}\right) + K}$ $K = \frac{1}{p_S} + \left(\frac{1}{p_L(Z,Z)} + \frac{(1 - p_L) \cdot p_S}{1 - p_S}\right) \cdot \left(\frac{1 - p_S}{p_L}\right)^{Z-A-1} + \frac{p_S \cdot (2 - p_L - p_S)}{p_L} \cdot \frac{1 - \left(\frac{1 - p_S}{p_L}\right)^{Z-A-2}}{1 - \left(\frac{1 - p_S}{p_L}\right)}$	-	-	MP z
BÖHME 1986	$\frac{1}{1 + \frac{\left(\frac{u - v_s}{k_G \cdot u} + 1\right) \cdot \exp\left(-\frac{(u - v_s) \cdot H_G}{D_t}\right) - 1}{1 + \left(\frac{u - v_s}{k_F \cdot u} - 1\right) \cdot \exp\left(-\frac{(u - v_s) \cdot H_F}{D_t}\right)}}$	-	$T' = \frac{\alpha}{4} \cdot \frac{u \cdot H}{D_t} \left(1 + \frac{1}{1 + k \frac{u \cdot H}{D_t}}\right)$	CCS
HUSEMANN 1990	$\frac{1}{1 + \frac{\left(\frac{\dot{m}_0 \cdot (u - v_s)}{k \cdot v_s \cdot \dot{m}_A} + 1\right) \cdot \exp\left(-\frac{(u - v_s) \cdot R_G \cdot (R_S - R_G)}{(u + v_u) \cdot R_S \cdot (s_{SS} + a_{SS})}\right) - 1}{\frac{A_{Q,S}}{A_{M,S}} + \left(\frac{u - v_s}{u} - \frac{A_{Q,S}}{A_{M,S}}\right) \cdot \exp\left(-\frac{(u - v_s) \cdot (R_S - R_F)}{(u + v_u) \cdot R_F}\right)}}$	-	-	CCS a

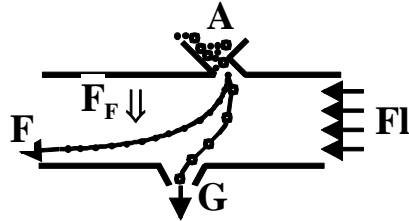
CFS cross flow separation; z number of separation stages; CCS counter-current separation; MP MARKOFF process; a acceleration; $\alpha = 2$ STOKES; $\alpha = 0,5$ NEWTON

Particle Flow Separation

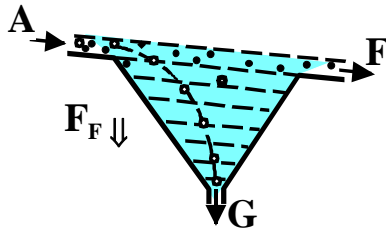
Operation Principles and Separation Models

1. Operation principles of particle flow classification

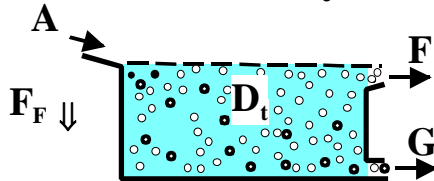
a) Cross-flow air classification (horizontal flow separator)



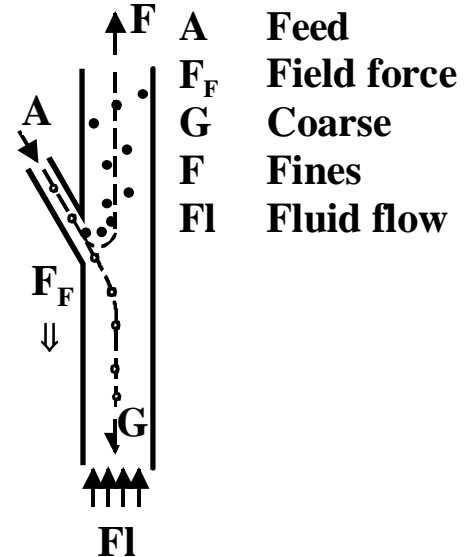
b) Laminar cross-flow hydroclassification



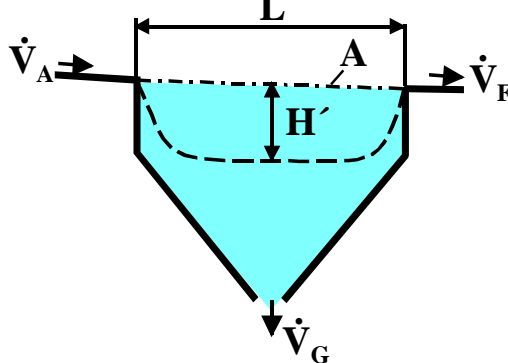
c) Turbulent cross-flow hydroclassification



d) Counter-current classification

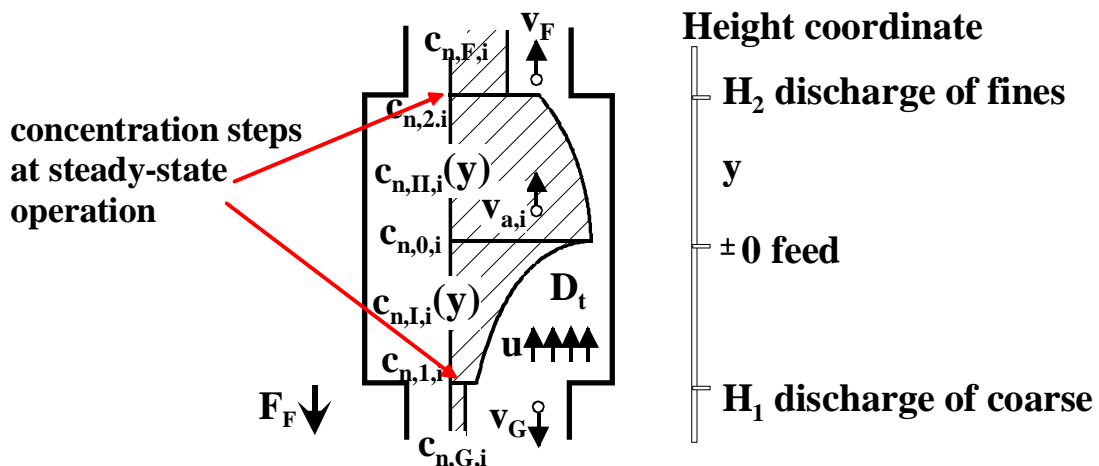


2. Separation model of laminar cross-flow hydroclassification



$$d_T = \sqrt{\frac{1}{k_\psi k_\phi} \cdot \frac{18 \cdot \eta}{(\rho_s - \rho_f)} \cdot \frac{\dot{V}_F}{A a}}$$

3. Particle number concentration $c_{n,i}$ of size fraction i versus apparatus height H at counter-current classification



Prerequisites for Turbulent Cross Flow Separation Model

- (1) **Particle hold-up probability distribution** (concentration per number $c_{n,i,j}$) versus height y independent each other, i.e., for every particle size fraction i as well as density fraction j the FOKKER-PLANCK Eq. is valid:

$$\frac{\partial c_{n,i,j}}{\partial t} = -(-v_{s,i,j}) \cdot \frac{1}{1!} \cdot \frac{\partial c_{n,i,j}}{\partial y} + D_{t,s} \cdot \frac{1}{2!} \cdot \frac{\partial^2 c_{n,i,j}}{\partial y^2} - \dots + \dots \quad (1)$$

- (2) For a homogeneous field of turbulence in the process chamber turbulent diffusion coefficient $D_t \approx D_{t,s}$ particle diffusion coefficient, i.e. **turbulence intensification by free turbulent particle flow pattern** > turbulence damping by particle concentration

$$\Lambda \cdot \sqrt{u_x'^2} \approx \text{const.} = D_t \quad (2)$$

- (3) Macro dimension of turbulence (diameter of **largest eddies** $d_{W,\max} = \Lambda/2$), \equiv characteristic dimension of a turbulence generating tool, here **channel width $b \approx 0.2$ m**,

$$\Lambda \propto b \quad (3)$$

- (4) The root mean square (RMS) of turbulent flow rate fluctuations across principal flow direction \propto eddy circumferential speed $u_\varphi \equiv$ charact. flow rate, **channel flow rate averaged u**

$$\sqrt{u_x'^2} \propto u_\varphi \propto \bar{u} \quad (4)$$

- (5) Particle size small compared with macro dimension of turbulence, i.e. channel width $d < 0.1 \cdot \Lambda < b$

- (6) Particle size small compared with micro dimension of turbulence ($d_{W,\min}$ diameter of **smallest eddies** with circular laminar flow), here not valid

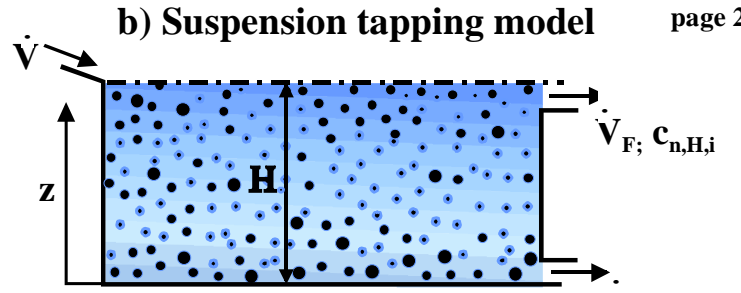
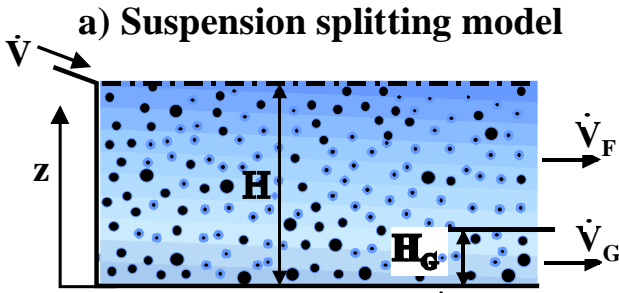
$$d < d_{W,\min} \approx 10 \cdot l_D \approx 0.3 \text{ mm} \quad (6)$$

KOLMOGOROV dimension $l_D = (v^3 / \varepsilon)^{1/4} = (15^3 \cdot 10^{-18} / 4W / g)^{1/4} \approx 30 \mu\text{m}$

- (7) For steady-state condition $\partial c_{n,i,j} / \partial t = 0$ (at bottom $y = 0$, $c_{n,i,j} = c_{n,0,i,j}$) an exponential particle concentration distribution versus height h is valid

$$\frac{c_{n,i,j}}{c_{n,0,i,j}} = \exp\left(-\frac{v_{s,i,j}}{D_{t,s}} \cdot h\right) \quad (7)$$

4. Separation models of turbulent cross-flow hydroclassification (Neeße/Schubert)



$$\dot{V} = \dot{V}_F + \dot{V}_G; H_G = H \frac{\dot{V}_G}{\dot{V}}$$

$$\dot{V} = \dot{V}_F + \dot{V}_G$$

$$T_i = \frac{c_{n,G,i} \cdot H_G}{c_{n,A,i} \cdot H} = \frac{1 - \exp\left(-\frac{v_{s,i}}{D_{td}} H_G\right)}{1 - \exp\left(-\frac{v_{s,i}}{D_{td}} H\right)}$$

$$T_i = \frac{c_{n,0,i} \dot{V}_G}{c_{n,0,i} \dot{V}_G + c_{n,H,i} \dot{V}_F} = \frac{1}{1 + \frac{\dot{V}_F}{\dot{V}_G} \exp\left(-\frac{v_{s,i}}{D_{td}} H\right)}$$

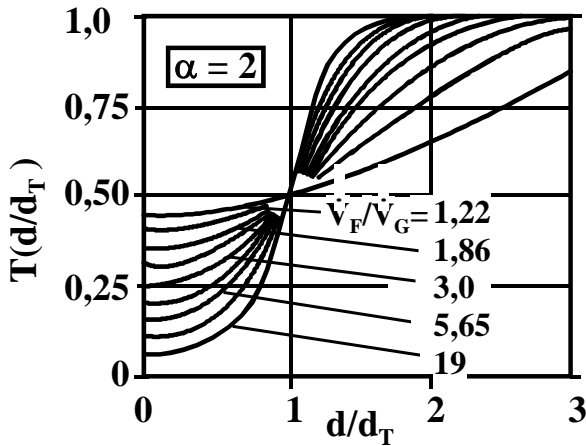
$$d_T = \sqrt{\frac{1}{k_\psi k_\phi} \frac{18\eta}{(\rho_s - \rho_f) a} \frac{D_{td}}{H} \ln \frac{\dot{V}_F}{\dot{V}_G}}$$

$\dot{V}, \dot{V}_G, \dot{V}_F$ suspension volume flow rate of feed, coarse and fine particles

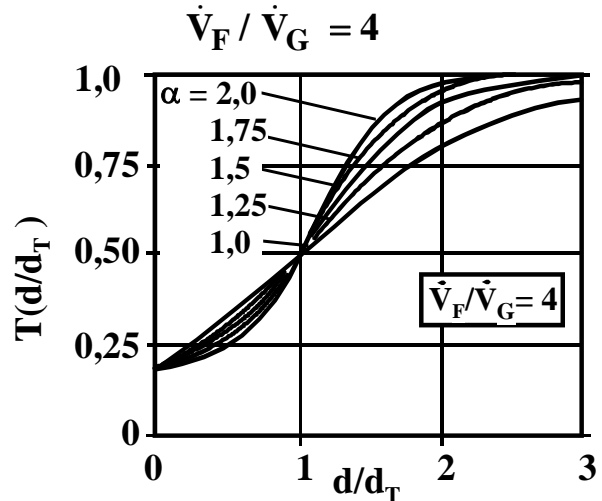
$$\kappa = \frac{d_{25}}{d_{75}} = \left[\frac{\ln(\dot{V}_F / \dot{V}_G) - \ln 3}{\ln(\dot{V}_F / \dot{V}_G) + \ln 3} \right]^{0,5}$$

5. Normalized separation function $T(d/d_T) = \frac{1}{1 + (\dot{V}_F / \dot{V}_G)^{1-(d/d_T)^\alpha}}$

a) for $\alpha = 2$ (Stokes range) and different ratios of volume flow rate



b) for different α -values at $\dot{V}_F / \dot{V}_G = 4$



6. Particle segregation of dilute and dense flow at cross-flow hydroclassification:

a) dilute flow segr.

b) dense flow segr.

c) combined dilute/dense flow

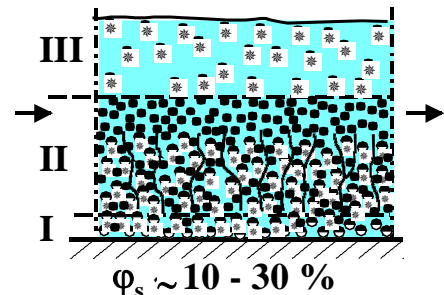
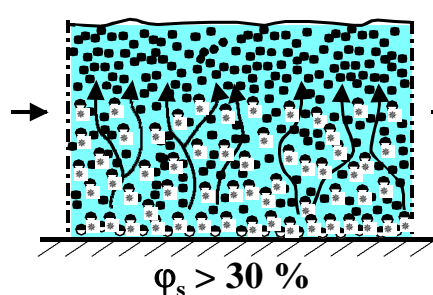
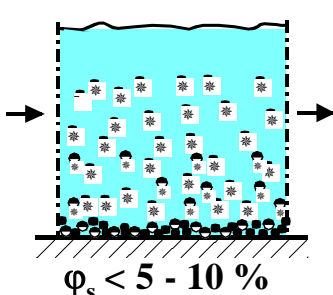
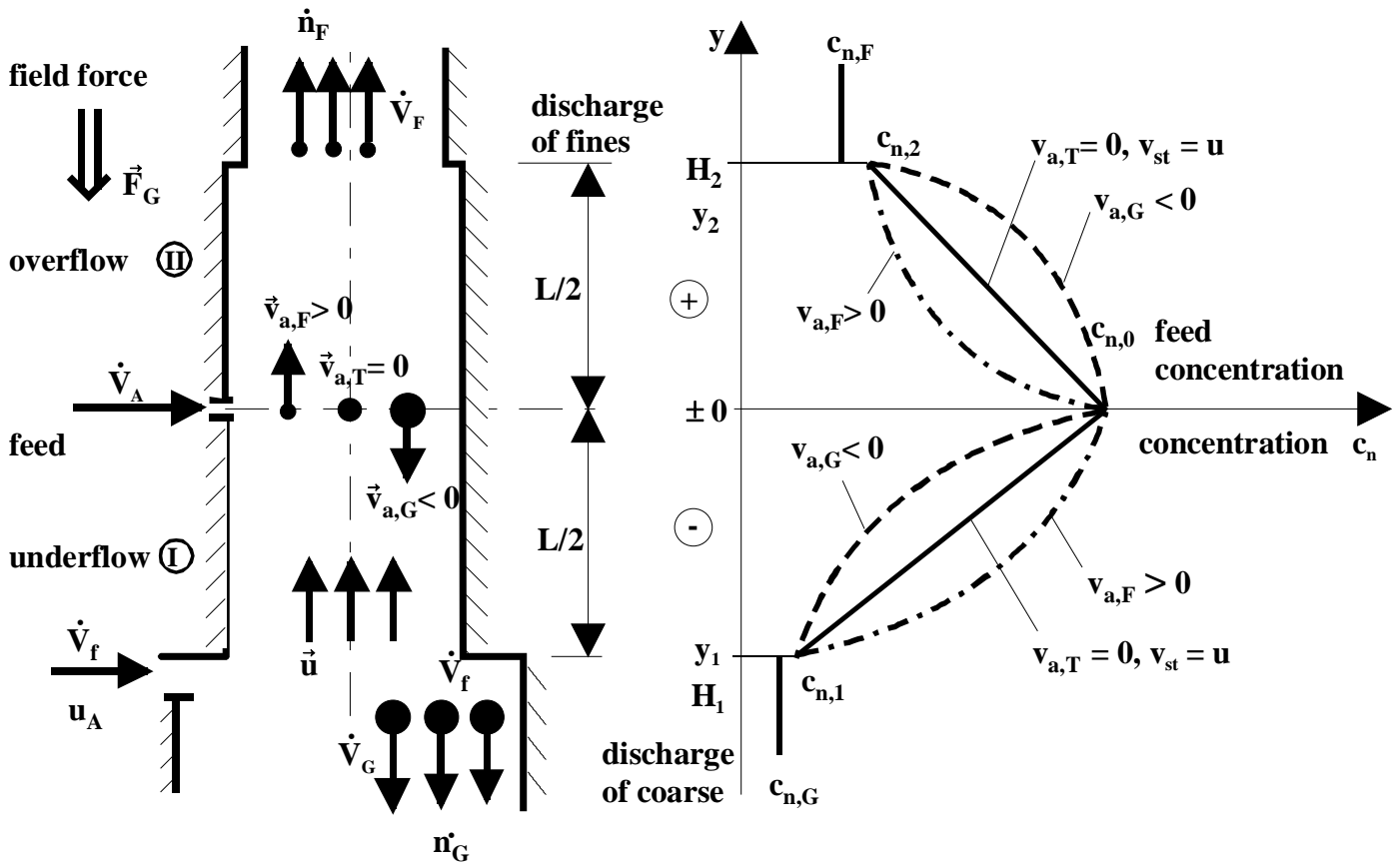


Figure 4.27

Model of Counter-current Particle Separation

Particle number concentration profile in the process chamber:



	Coarse (G)	Equilibrium particle	Fines (F)
Particle absolute velocity	$v_s > u$ $v_{a,G} < 0$	$v_{s,T} = u$ $v_{a,T} = 0$	$v_s < u$ $v_{a,F} > 0$
0. Feed $y = 0$	$c_{n,0} = c_{n,1} \left[1 + \frac{k_1 \cdot u_G}{D_{ts}} \cdot y_1 \right]$		$c_{n,0} = c_{n,2} \left[1 + \frac{k_2 \cdot u}{D_{ts}} \cdot y_2 \right]$
I. Underflow $y_1 < y < 0$	$c_{n,I} = \frac{c_{n,1}}{v_a} \cdot \left\{ -k_1 \cdot u_G + (v_a + k_1 \cdot u_G) \cdot \exp \left[\frac{v_a}{D_{ts}} \cdot (y + y_1) \right] \right\}$	$c_n = c_{n,1} \left[1 + \frac{k_1 \cdot u_G}{D_{ts}} \cdot (y + y_1) \right]$	$c_{n,I} = \frac{c_{n,1}}{v_a} \cdot \left\{ -k_1 \cdot u_G + (v_a + k_1 \cdot u_G) \cdot \exp \left[\frac{v_a}{D_{ts}} \cdot (y + y_1) \right] \right\}$
II. Overflow $0 < y < y_2$	$c_{n,II} = \frac{c_{n,2}}{v_a} \cdot \left\{ -k_2 \cdot u + (v_a - k_2 \cdot u) \cdot \exp \left[\frac{v_a}{D_{ts}} \cdot (y_2 - y) \right] \right\}$	$c_n = c_{n,2} \left[1 + \frac{k_2 \cdot u}{D_{ts}} \cdot (y_2 - y) \right]$	$c_{n,II} = \frac{c_{n,2}}{v_a} \cdot \left\{ -k_2 \cdot u + (v_a - k_2 \cdot u) \cdot \exp \left[\frac{v_a}{D_{ts}} \cdot (y_2 - y) \right] \right\}$
Discharge	$y = y_1: \dot{n}_G = k_1 \cdot u_G \cdot c_{n,1}$		$y = y_2: \dot{n}_F = k_2 \cdot u \cdot c_{n,2}$

Turbulent Counter-current Separation Model

(1) Particle absolute velocity $v_a(d)$ in locally fixed coordinates of the apparatus:

$$\vec{v}_a(d) = \vec{u} - \vec{v}_s(d) \quad (1)$$

(2) Separation function: $T_i = \frac{\dot{n}_{G,i}}{\dot{n}_{A,i}} = \frac{1}{1 + \dot{n}_{F,i} / \dot{n}_{G,i}}$

$$T(v_a(d)) = \frac{1}{-1 + \left(1 + \frac{v_{a,I}}{k_1 \cdot u_G}\right) \cdot \exp\left[\frac{v_{a,I}}{D_{t,s}} \cdot y_1\right] + \frac{1}{1 + \left(\frac{v_{a,II}}{k_2 \cdot u} - 1\right) \cdot \exp\left[-\frac{v_{a,II}}{D_{t,s}} \cdot y_2\right]}} \quad (2)$$

(3) Mean residence time: $\tau_m = \frac{1}{\dot{n}_A} \cdot \int_{-y_1}^{y_2} c_n(y) dy$

$$\tau_m = \frac{1}{v_a} \cdot \left[T \cdot \left(y_1 - \frac{D_{t,s}}{k_1 \cdot u_G} \right) + (1 - T) \cdot \left(y_2 + \frac{D_{t,s}}{k_2 \cdot u} \right) \right] \quad (3)$$

(4) Incremental separation sharpness (slope for $d \rightarrow d_T$) instead using κ :

$$\left. \frac{d[T(d/d_T)]}{d(d/d_T)} \right|_{d \rightarrow d_T} = \frac{\alpha}{4} \cdot \frac{u \cdot H}{D_{t,s}} \cdot \left(1 + \frac{1}{1 + k \cdot \frac{u \cdot H}{D_{t,s}}} \right) \quad (4)$$

for large BODENSTEIN numbers (mainly convective transport):

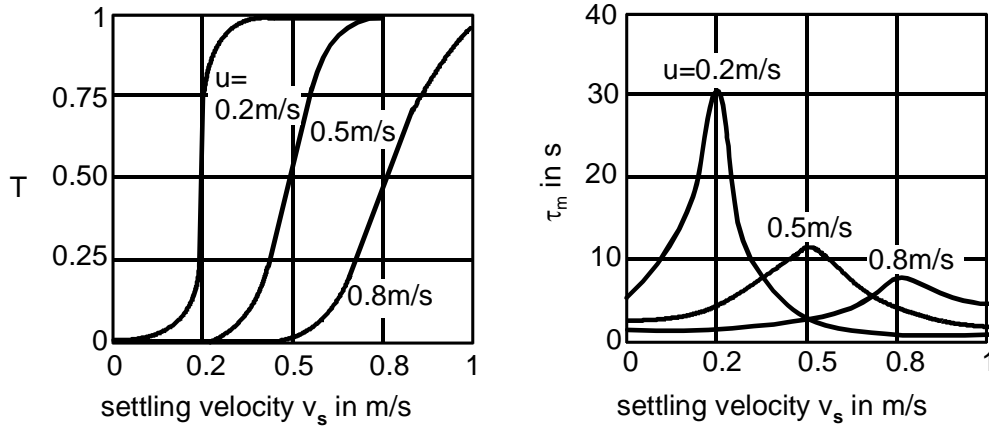
$$Bo = \frac{u \cdot H}{D_{t,s}} \gg 1 \quad (5)$$

$$\frac{d[T(d/d_T)]}{d(d/d_T)} = \frac{\alpha}{4} \cdot Bo \cdot \left(1 + \frac{1}{1 + k \cdot Bo} \right) \approx \frac{\alpha}{4} \cdot Bo \quad (6)$$

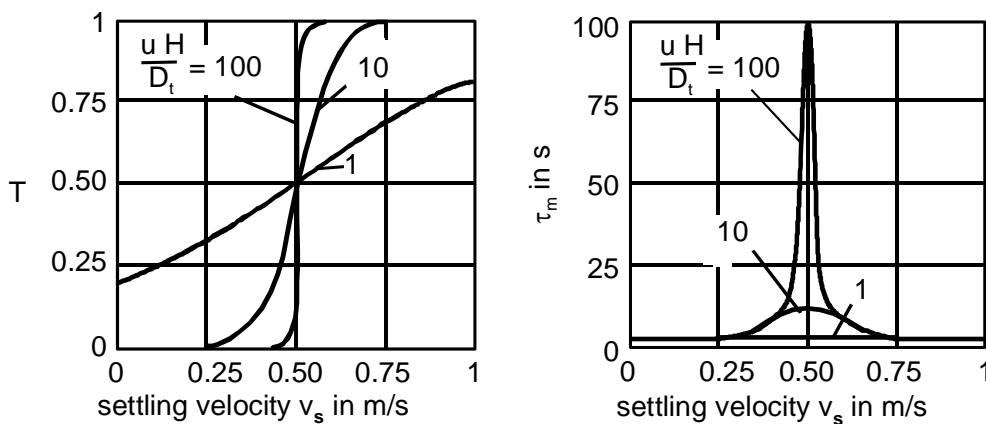
Evaluation of Turbulent Counter-current Hydroclassification

1. Separation function $T(v_s(d))$ and medium residence time $\tau_m(v_s(d))$ versus stationary settling velocity $v_s(d)$ for $k_1 = k_2 = 1$; $H_1 = H_2 = 1$ m

a) Different counter-flow rates u for BODENSTEIN-number $Bo = u H/D_t = 10$

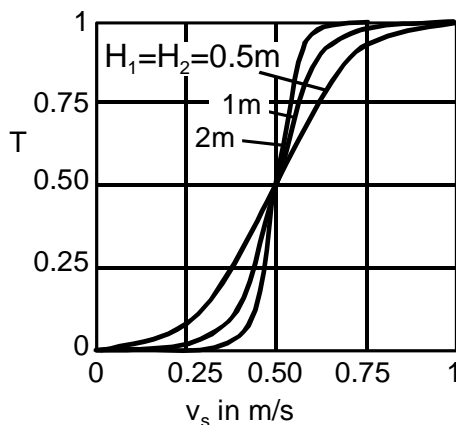


b) Different BODENSTEIN-numbers $Bo = u H/D_t$ for $u = 0.5$ m/s and $H = 1$ m

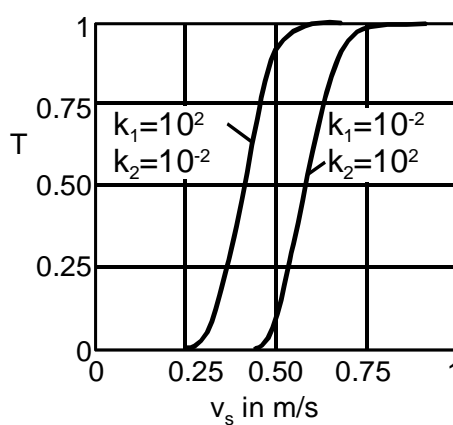


2. Separation function $T(v_s(d))$ versus stationary settling velocity $v_s(d)$ for $u = 0.5$ m/s; $H = 1$ m; $\Rightarrow Bo = 10$

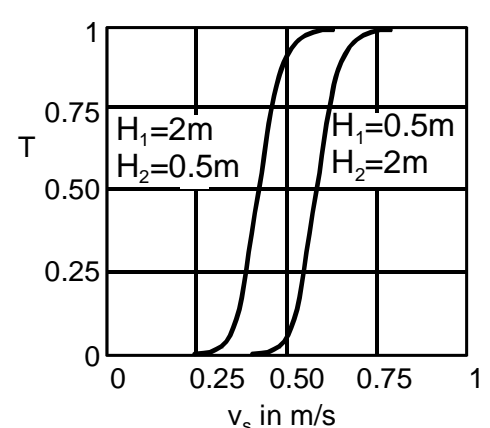
a) Different heights of separation chamber for $k_1 = k_2 = 1$



b) Different discharge coefficients for $H_1 = H_2 = 1$ m



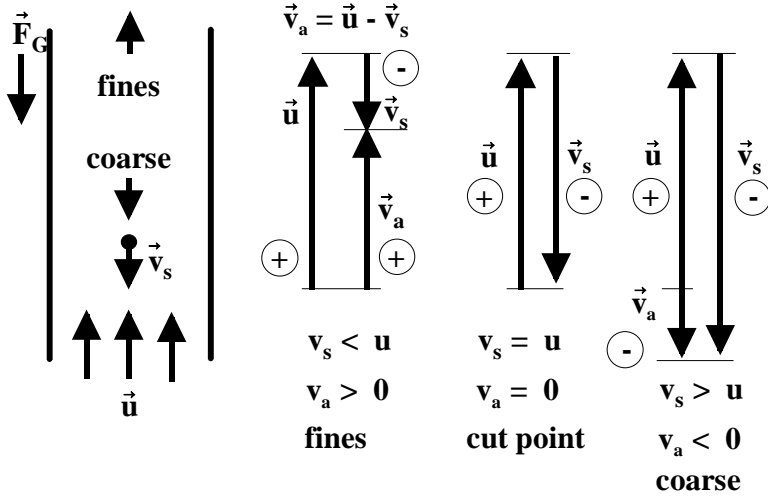
c) Different height ratios H_1/H_2 of separation sub-chambers for $H_1 + H_2 = 2.5$ m and $k_1 = k_2 = 1$



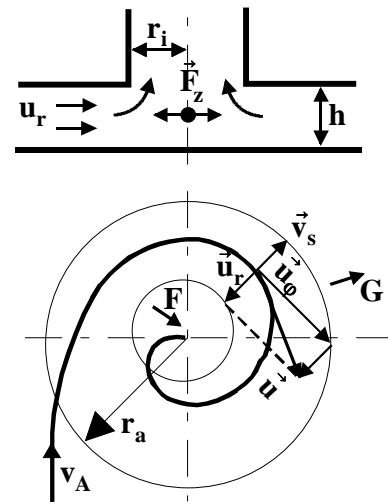
Principles of Particle Separation in an Air Stream

1. Counter-current separation

a) in a gravity field

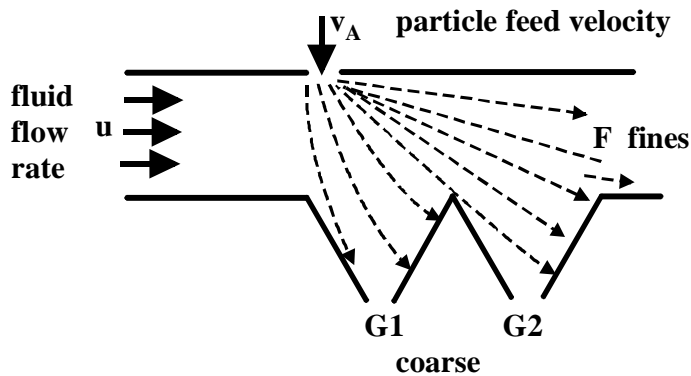


b) in a centrifugal force field

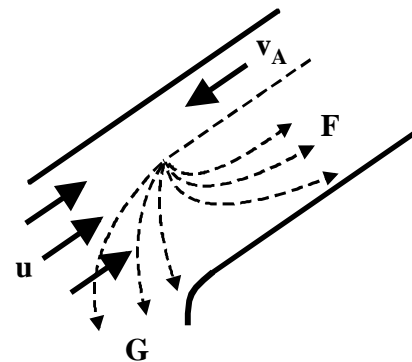


2. Cross flow separation (force of gravity and force of inertia)

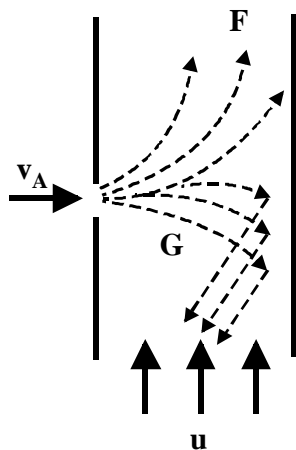
a) horizontal cross flow separator



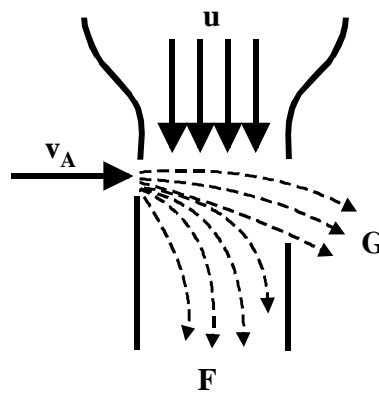
b) cross flow u-turn separator



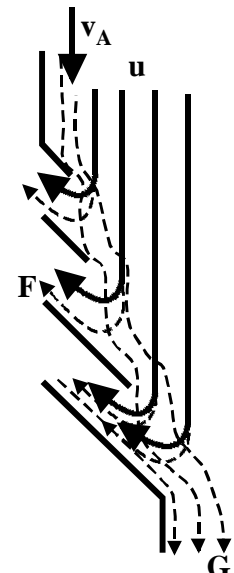
c) vertical cross flow separator



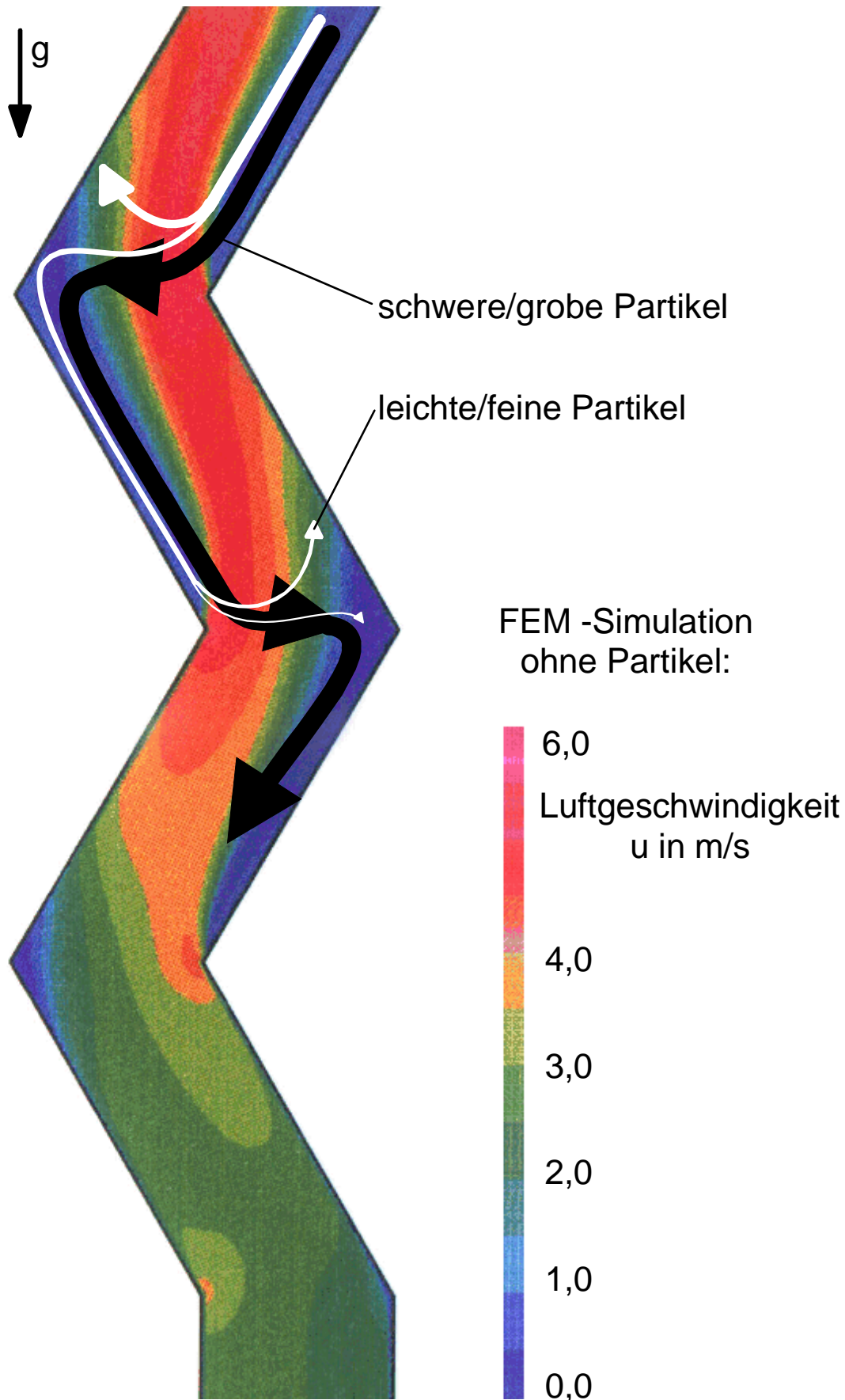
d) cross flow jet separator



e) blind u-turn separator



Mehrstufige Querstrom-Partikel-trennung in einem Zick-Zack-Kanal



Derivation of the Multistage Separation Function

With 3 stages:

$$T_{ges,j} = \frac{\dot{m}_{S,j}}{\dot{m}_{A,j}}$$

$$T_{1,j} = \frac{\dot{m}_{S1,j}}{\dot{m}_{A,j} + \dot{m}_{S2,j} + \dot{m}_{L3,j}}$$

$$T_{2,j} = \frac{\dot{m}_{S2,j}}{\dot{m}_{L1,j}} \quad \text{or} \quad \dot{m}_{S2,j} = T_{2,j} \cdot \dot{m}_{L1,j}$$

$$T_{3,j} = \frac{\dot{m}_{S3,j}}{\dot{m}_{S1,j}} \quad \text{or} \quad \dot{m}_{S3,j} = T_{3,j} \cdot \dot{m}_{S1,j}$$

$$\dot{m}_{L2,j} = \dot{m}_{L1,j} - \dot{m}_{S2,j} = \dot{m}_{L1,j} - T_{2,j} \cdot \dot{m}_{L1,j} = \dot{m}_{L1,j} \cdot (1 - T_{2,j})$$

$$T_{ges,j} = \frac{\dot{m}_{S,j}}{\dot{m}_{A,j}} = \frac{1}{1 + \frac{\dot{m}_{L2,j}}{\dot{m}_{S3,j}}} = \frac{1}{1 + \frac{\dot{m}_{L2,j}}{T_{3,j} \cdot \dot{m}_{S1,j}}} = \frac{1}{1 + \frac{\dot{m}_{L1,j} \cdot (1 - T_{2,j})}{T_{3,j} \cdot \dot{m}_{S1,j}}}$$

$$\dot{m}_{L1,j} = \dot{m}_{A,j} + \dot{m}_{S2,j} + \dot{m}_{L3,j} - \dot{m}_{S1,j} = (\dot{m}_{A,j} + \dot{m}_{S2,j} + \dot{m}_{L3,j}) \cdot (1 - T_{1,j})$$

$$T_{ges,j} = \frac{1}{1 + \frac{(\dot{m}_{A,j} + \dot{m}_{S2,j} + \dot{m}_{L3,j}) \cdot (1 - T_{1,j}) \cdot (1 - T_{2,j})}{T_{3,j} \cdot (\dot{m}_{A,j} + \dot{m}_{S2,j} + \dot{m}_{L3,j}) \cdot T_{1,j}}}$$

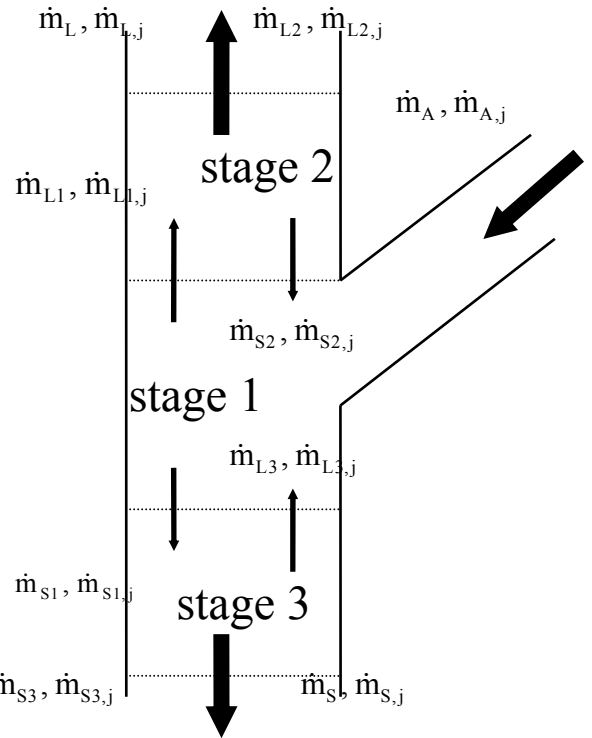
$$T_{ges,j} = \frac{1}{1 + \frac{(1 - T_{1,j}) \cdot (1 - T_{2,j})}{T_{1,j} \cdot T_{3,j}}} \quad (1)$$

with 5 stages:

$$T_{ges,j} = \frac{1}{1 + \frac{(1 - T_{1,j}) \cdot (1 - T_{2,j}) \cdot (1 - T_{4,j})}{T_{1,j} \cdot T_{3,j} \cdot T_{5,j}}} \quad (2)$$

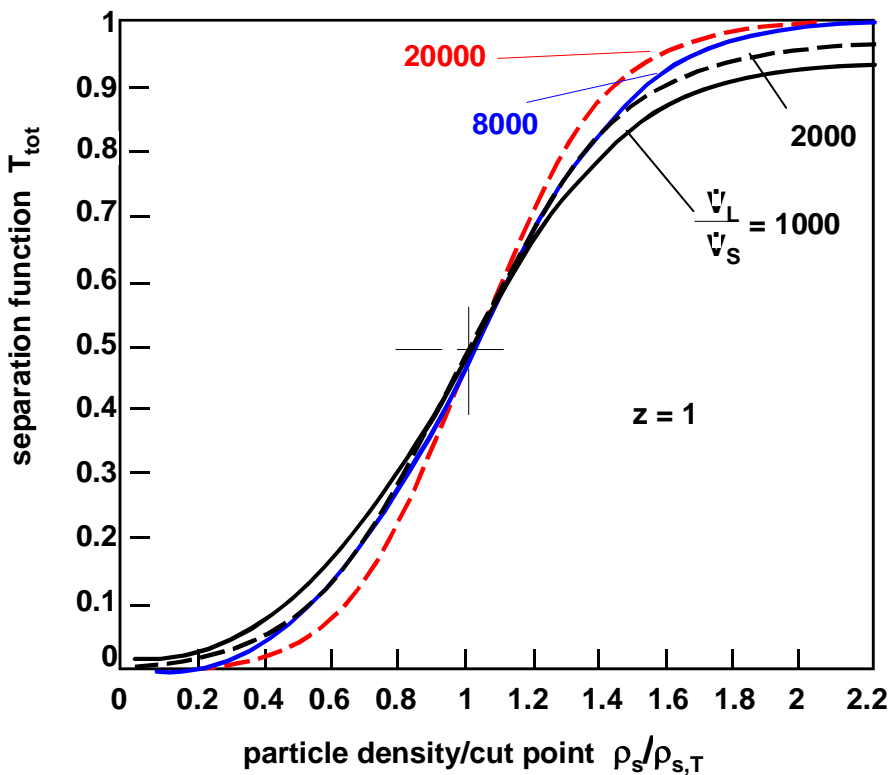
generally:

$$T_{ges,j} = \frac{1}{1 + \frac{\prod_{k_L=1}^{z_L} (1 - T_{k_L,j})}{\prod_{k_S=1}^{z_S} T_{k_S,j}}} \approx \frac{1}{1 + \frac{(1 - T_{z_L,j})^{z_L}}{T_{z_S,j}^{z_S}}} \quad (3)$$



Model of Multistage Turbulent Cross Flow Aeroseparation

1. Volume flow rate impact on separation function



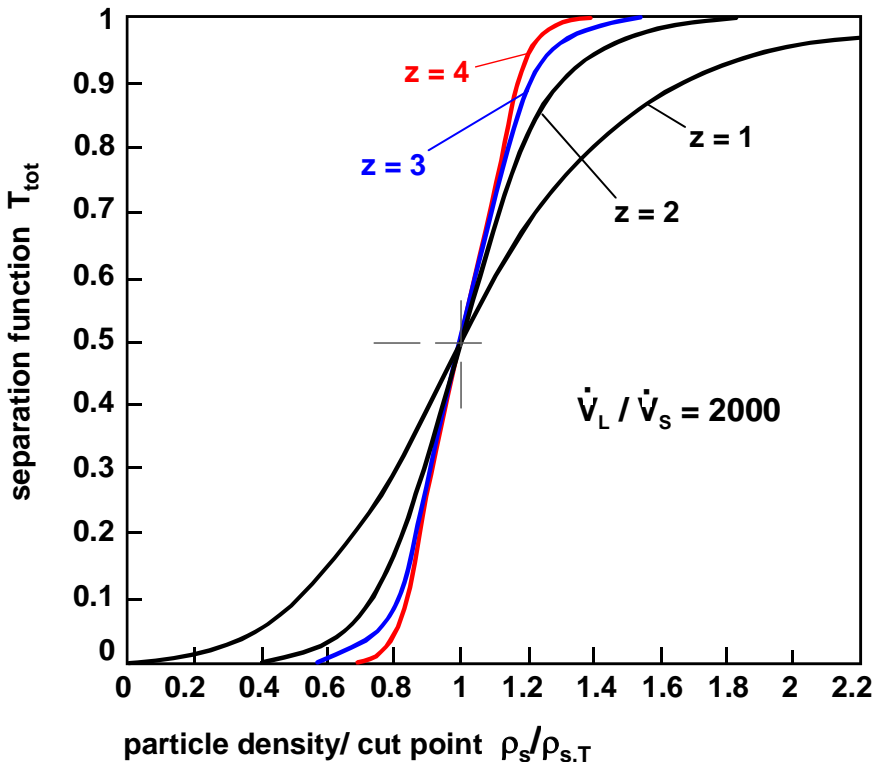
separation function of
 · overflow (light material) z_L or
 · underflow (heavy material) z_s

$$T_{z_L, z_S} \left(\frac{v_{s,j}}{v_{sT}} \right) = \frac{1}{1 + \left[\frac{\rho_{s,j}}{\rho_{s,j+1}} \cdot \frac{\dot{V}_L}{\dot{V}_S} \right]^{1 - \frac{v_{s,j}}{v_{sT}}}}$$

$$T_{z_L, z_S} = \frac{1}{1 + \left[\frac{\dot{V}_L}{\dot{V}_S} \right]^{1 - \left(\frac{\rho_{s,j} - \rho_g}{\rho_{s,T} - \rho_g} \right)^{0.5}}}$$

$$T_{tot,j} = \frac{1}{1 + \frac{(1 - T_{z_L,j})^{z_L}}{T_{z_S,j}^{z_S}}}$$

2. Stage number z impact on separation function = f(particle density/cut point)



total separation sharpness:

$$\kappa_{tot} = \left[\frac{z \cdot \ln(\dot{V}_L/\dot{V}_S) - \ln 3}{z \cdot \ln(\dot{V}_L/\dot{V}_S) + \ln 3} \right]^2$$

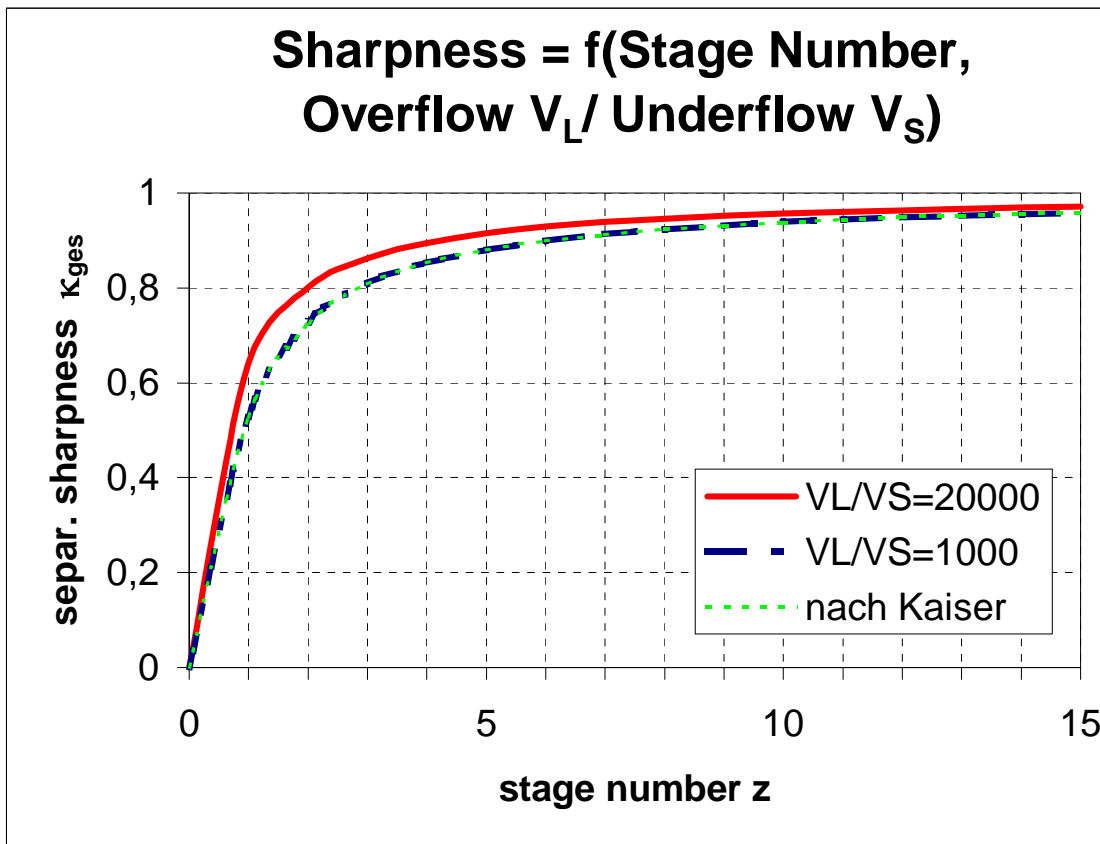
effective number of stages:

$$z_e = \frac{(1 + \sqrt{\kappa_{tot,mes}}) \cdot \ln 3}{(1 - \sqrt{\kappa_{tot,mes}}) \cdot \ln(\dot{V}_L/\dot{V}_S)}$$

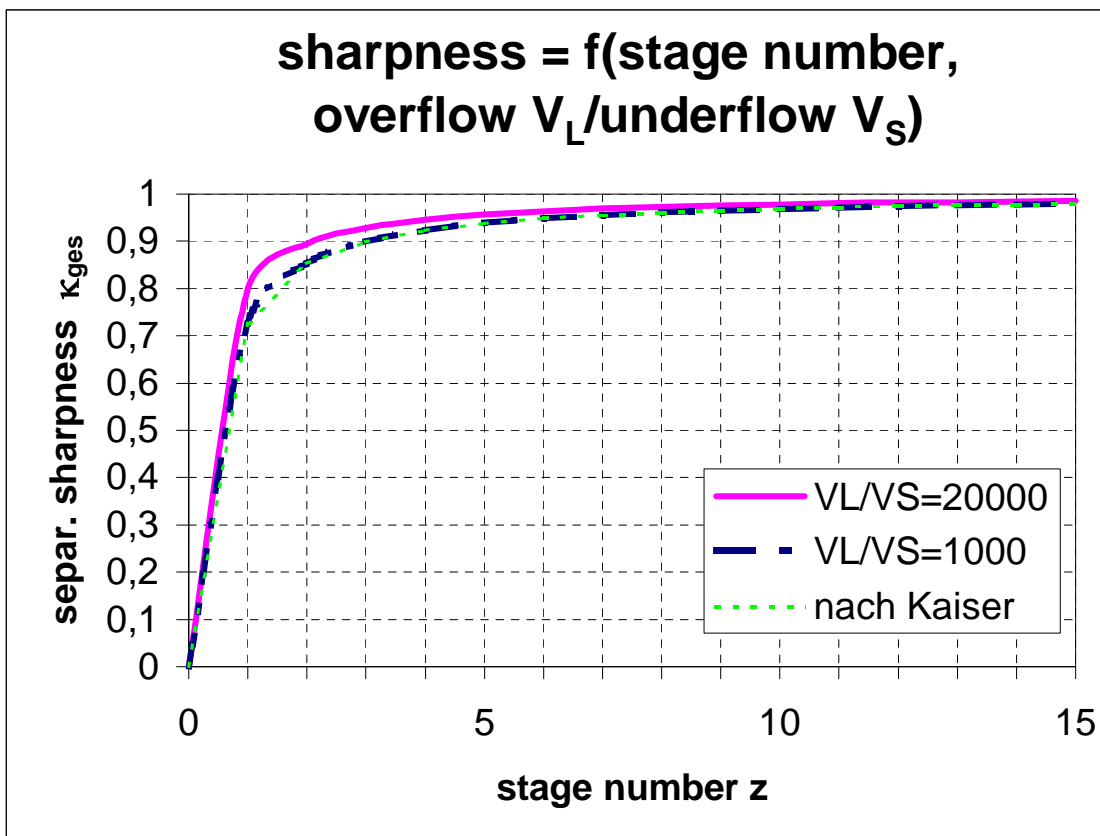
separation stage utilization:

$$\eta_{Tr} = \frac{2 \cdot z_e - 1}{n_{apparatus}}$$

Separation Sharpness versus Stage Number and Volume Flow Rate Ratios



turbulent particle flow pattern
 $\alpha = 0.5$



laminar particle flow pattern
 $\alpha = 2$



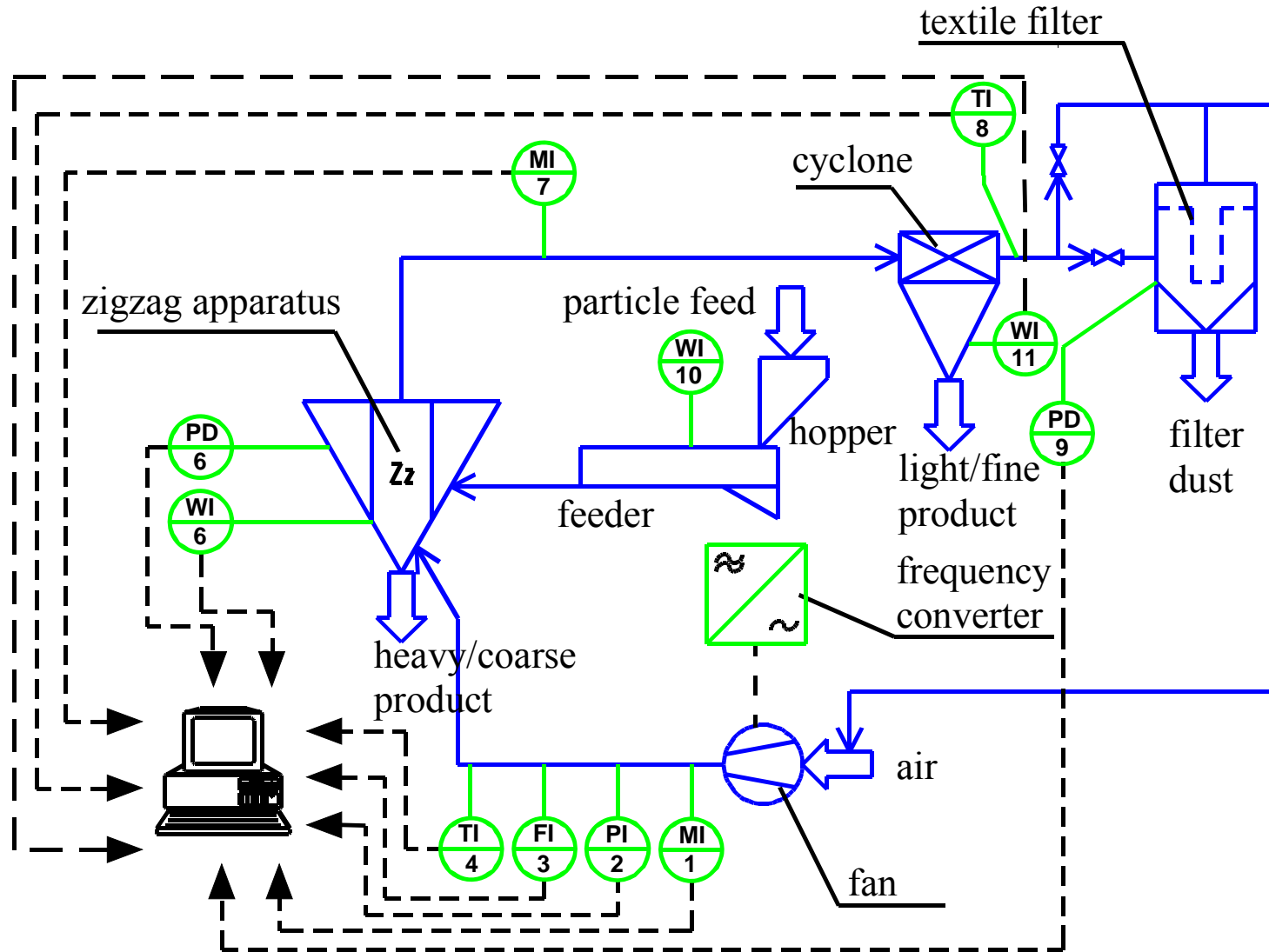
Assessment characteristics for multistage cross-flow separation in a symmetrical apparatus with $z_o = z_u = z$ number of separation stages

process goal	Separation function	Cut characteristic	Separation sharpness
	$T_{\text{tot}}(\xi/\xi_T) =$	$\xi_T = \xi_{50}(T_{\text{tot}} = 0.5) =$	$\kappa_{\text{tot}} = \xi_{25}/\xi_{75} =$
Fluid flow separation $\xi = v_s$	$\frac{1}{1 + \left(\frac{\dot{V}_o}{\dot{V}_u}\right)^{\left[1 - \frac{v_s(d, \rho_s)}{v_{sT}(d_T, \rho_{sT})}\right] \cdot z}}$	$v_{sT} = \sqrt{\frac{2 \cdot (\rho_{sT} - \rho_f) \cdot V_{P,T} \cdot g}{c_{W,T} \cdot \rho_f \cdot A_{P,T}}}$	$\frac{z \cdot \ln(\dot{V}_o / \dot{V}_u) - \ln 3}{z \cdot \ln(\dot{V}_o / \dot{V}_u) + \ln 3}$
Classification $\xi = d$ $\rho_s = \text{const.}$	$\frac{1}{1 + \left(\frac{\dot{V}_F}{\dot{V}_G}\right)^{\left[1 - \left(\frac{d}{d_T}\right)^\alpha\right] \cdot z}}$	$d_T \approx \frac{\rho_f}{3 \cdot \rho_s \cdot g} \left[\frac{D_{t,s}}{h} \cdot \ln\left(\frac{\dot{V}_F}{\dot{V}_G}\right) \right]^2$ for spheres $c_W = 0.44$	$\left[\frac{z \cdot \ln(\dot{V}_F / \dot{V}_G) - \ln 3}{z \cdot \ln(\dot{V}_F / \dot{V}_G) + \ln 3} \right]^{\frac{1}{\alpha}}$
Gravity separation $\xi = \rho_s$ $d = \text{const.}$	$\frac{1}{1 + \left(\frac{\dot{V}_L}{\dot{V}_S}\right)^{\left[1 - \left(\frac{\rho_{s,j} - \rho_f}{\rho_{s,T} - \rho_f}\right)^{\frac{\alpha+1}{3}}\right] \cdot z}}$	$\rho_{sT} \approx \frac{\rho_f}{3 \cdot d \cdot g} \left[\frac{D_{t,s}}{h} \cdot \ln\left(\frac{\dot{V}_L}{\dot{V}_S}\right) \right]^2$ for spheres $c_W = 0.44$	$\left[\frac{z \cdot \ln(\dot{V}_L / \dot{V}_S) - \ln 3}{z \cdot \ln(\dot{V}_L / \dot{V}_S) + \ln 3} \right]^{\frac{3}{\alpha+1}}$

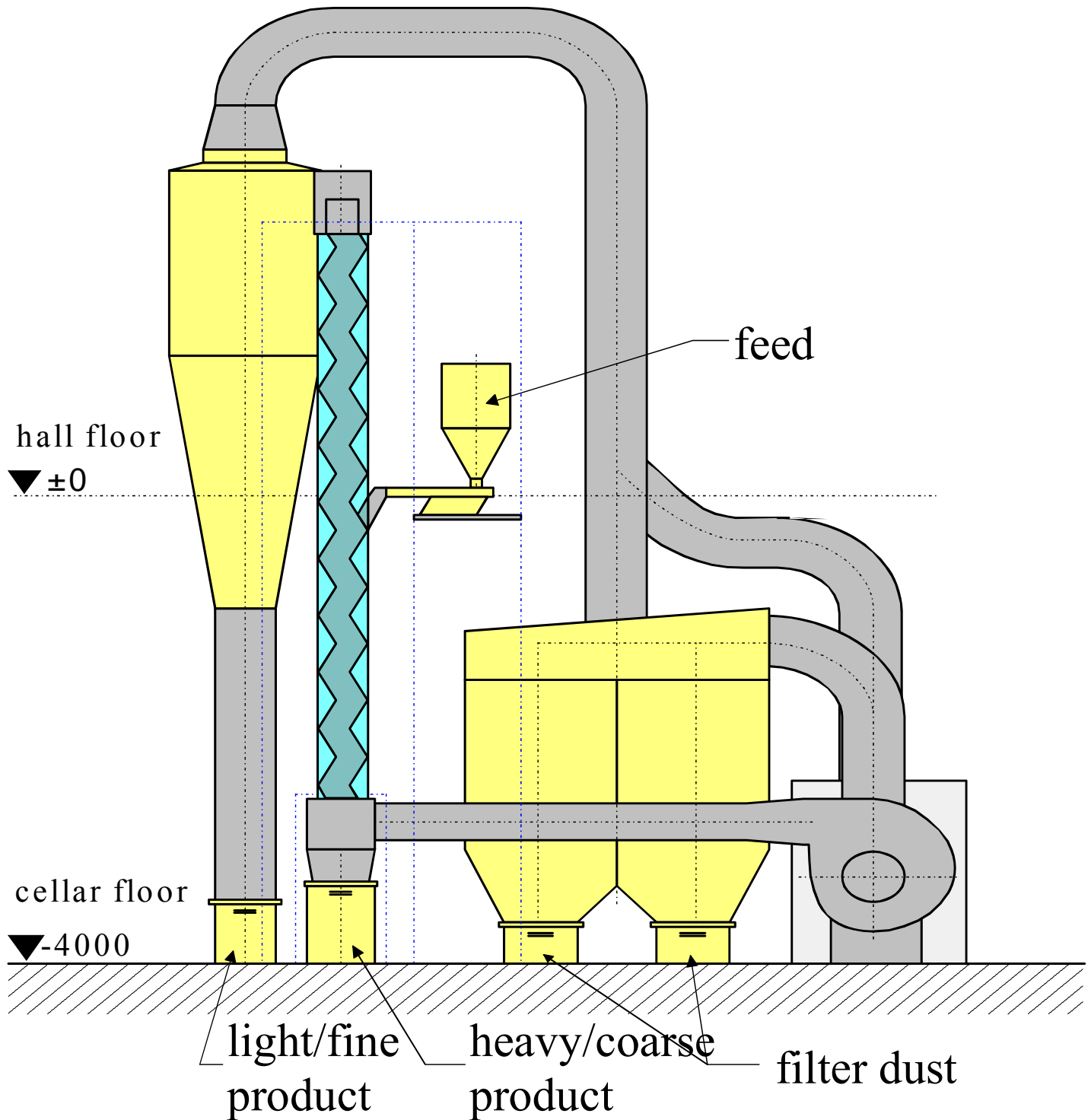
$\dot{V}_o, \dot{V}_F, \dot{V}_L$ overflow, fine or lightweight particle suspension volume flow rates, $\dot{V}_u, \dot{V}_G, \dot{V}_S$ underflow, coarse or heavy particle volume flow rates
 $\alpha = 2$ laminar (Stokes), $\alpha = 0.5$ turbulent (Newton) flow pattern acc. to $v_s \propto d^\alpha$



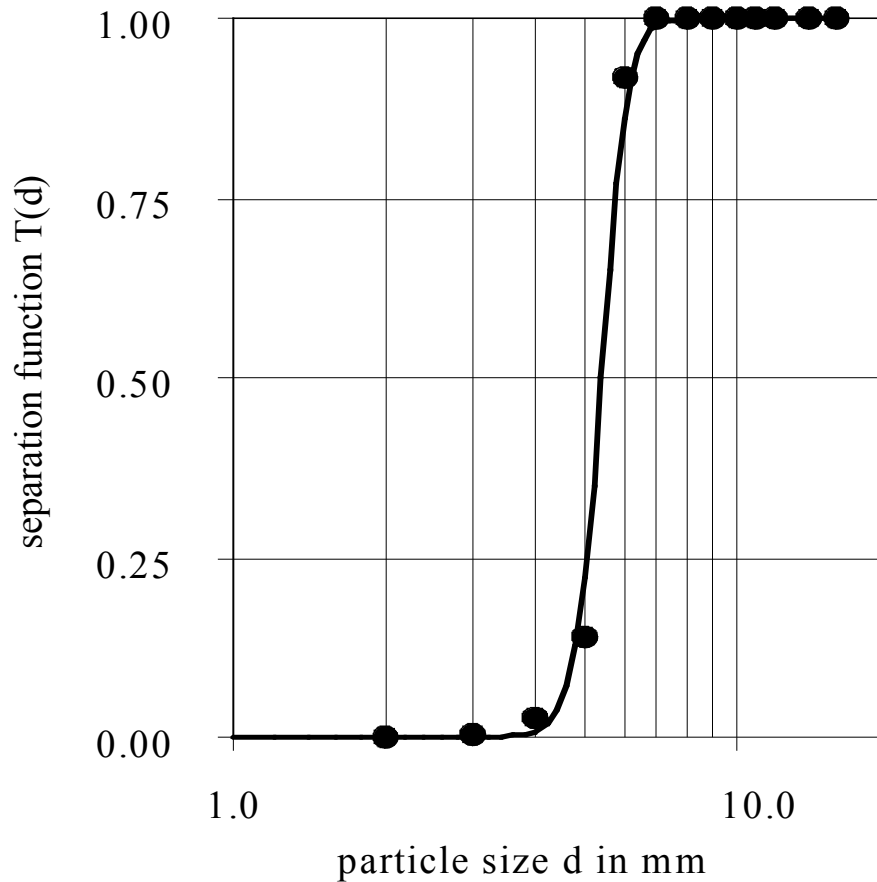
PI-Flow Chart of the Test Rig "Aeroseparation"



Installation Plan of Zigzag Aeroseparator

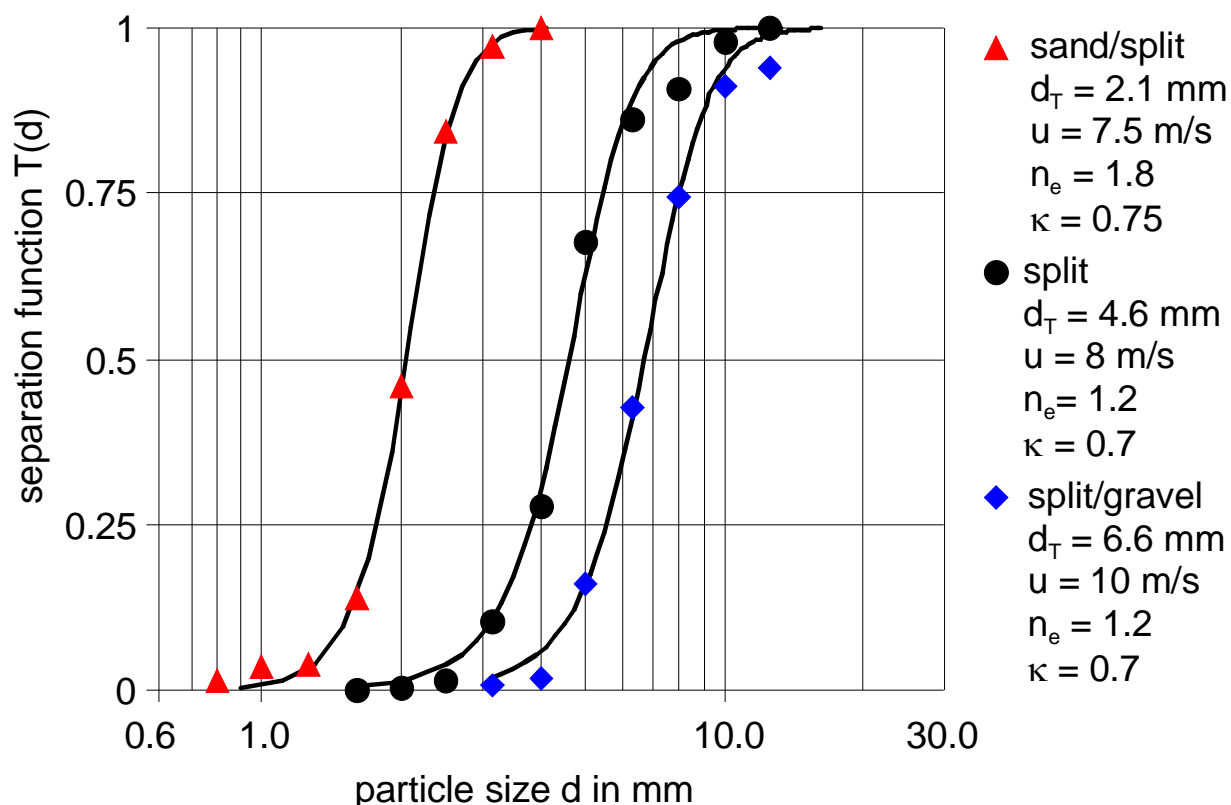


Classification of Log. Normal Distributed Glas Beads



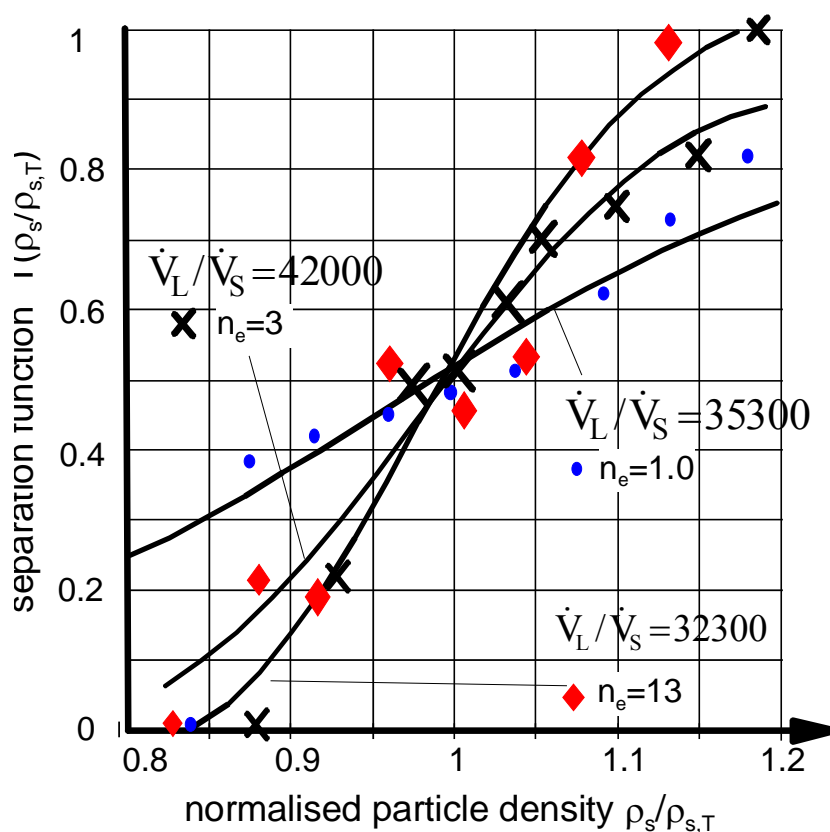
particle fraction $d_{u,i} - d_{o,i}$ in mm	2 - 16
channel velocity u in m/s	13
particle settling velocity $v_{sT}(d_{u,i})$ in m/s	18.2
mass flow rate \dot{m}_s in t/h	0.12
specific mass flow rate $\dot{m}_{s,A}$ in $t/(m^2 \cdot h)$	3.0
particle concentration $\mu_{s,g}$ in g/kg	82
cut size d_T in mm	5.4
separation sharpness κ	0.89
$n = 7$, effective separation stages n_e	5.8
utilisation of separation stages η_{Tr} in %	83
pressure drop Δp_{ZZ} in Pa	440
specific energy consumption $W_{m,ZZ}$ in kWh/t	1.25

Classification of Sand, Split and Gravel



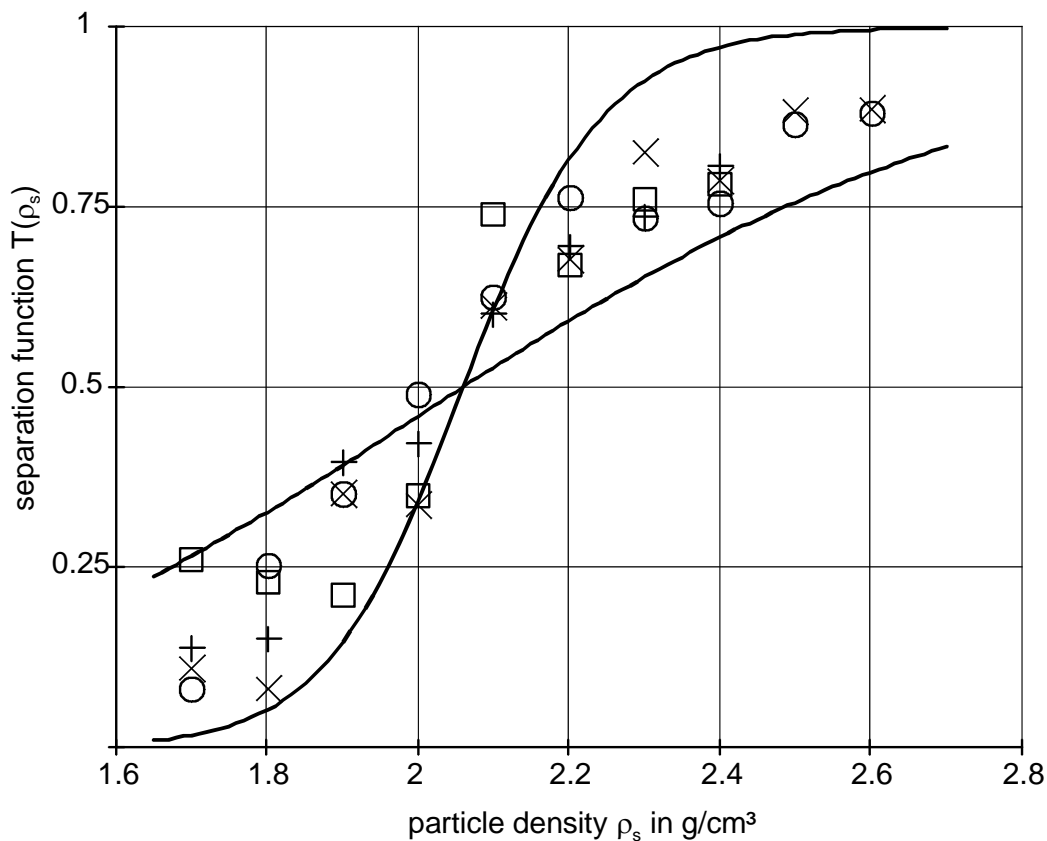
	▲	●	◆
channel velocity u in m/s	7.5	8	10
particle settling velocity $v_{sT}(d_T)$ in m/s	11.5	15.6	18.7
mass flow rate \dot{m}_s in t/h	0.34	0.12	0.16
specific mass flow rate $\dot{m}_{s,A}$ in t/(m ² ·h)	8.5	3	4
particle concentration $\mu_{s,g}$ in g/kg	262	82	94
cut size d_T in mm	2.1	4.6	6.6
separation sharpness κ	0.75	0.7	0.7
$n = 7$, effective separation stages n_e	1.8	1.2	1.2
utilisation of separation stages η_{Tr} in %	26	17	17
pressure drop Δp_{ZZ} in Pa	440	440	700
specific energy consumption $W_{m,ZZ}$ in kWh/t	0.39	1.25	1.72

Gravity Separation of Partially Liberated Aggregate Fragments of a B 35 Concrete



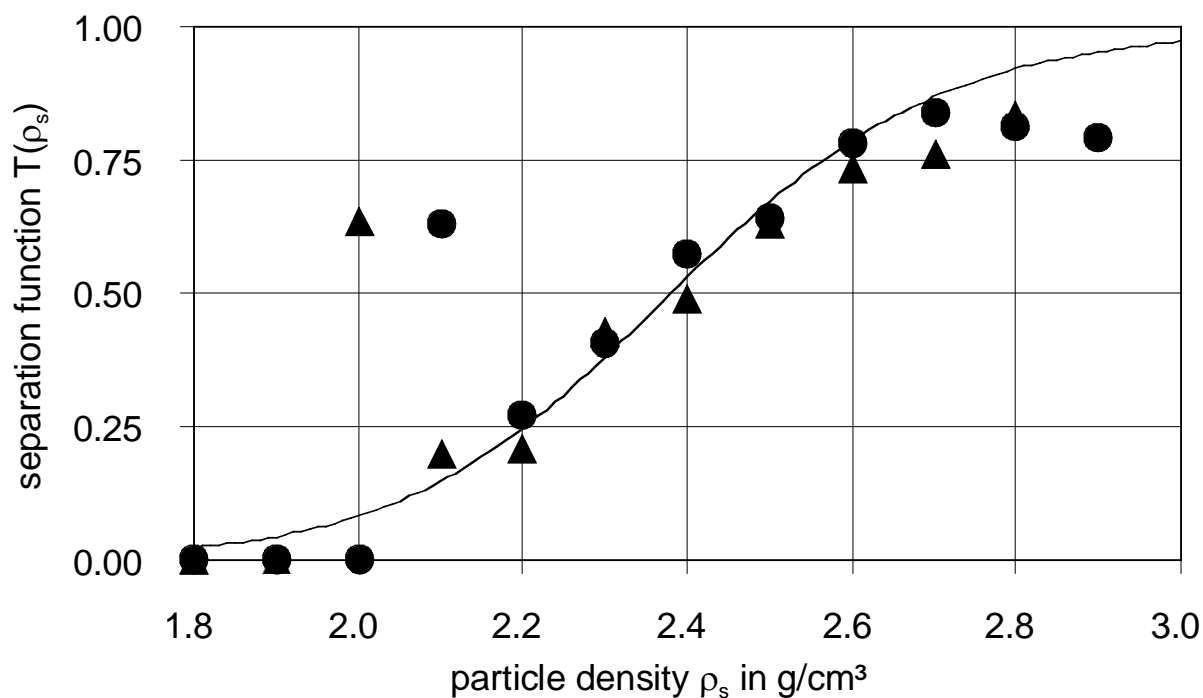
particle fraction $d_{u,i} - d_{o,i}$ in mm	● 6.3 - 8	◆ 8 - 10	× 10 - 12
channel velocity u in m/s	13.6	15.5	16.5
particle settling velocity $v_{sT}(d_{u,i})$ in m/s	18.2	21.1	23.0
particle flow rate \dot{m}_s in t/h	0.12	0.17	0.13
specific particle flow rate $\dot{m}_{s,A}$ in t/(m ² ·h)	3.1	4.2	3.3
particle concentration $\mu_{s,g}$ in g/kg	52	62	45
cut density $\rho_{s,T}$ in g/cm ³	2.2	2.4	2.3
separation sharpness κ	0.66	0.94	0.84
$n = 15$, effective separation stages n_e	1	13	3
utilisation of separation stages η_{Tr} in %	7	87	20
misplaced product $\mu_{LS}(\rho_s < 2.3 \text{ g/cm}^3)$	0.19	0.27	0.11
pressure drop Δp_{ZZ} in Pa	1500	1600	1900
spec. energy consumption $W_{m,ZZ}$ kWh/t	6.9	5.5	9.5

Gravity Separation of a Concrete-Brick-Mixture



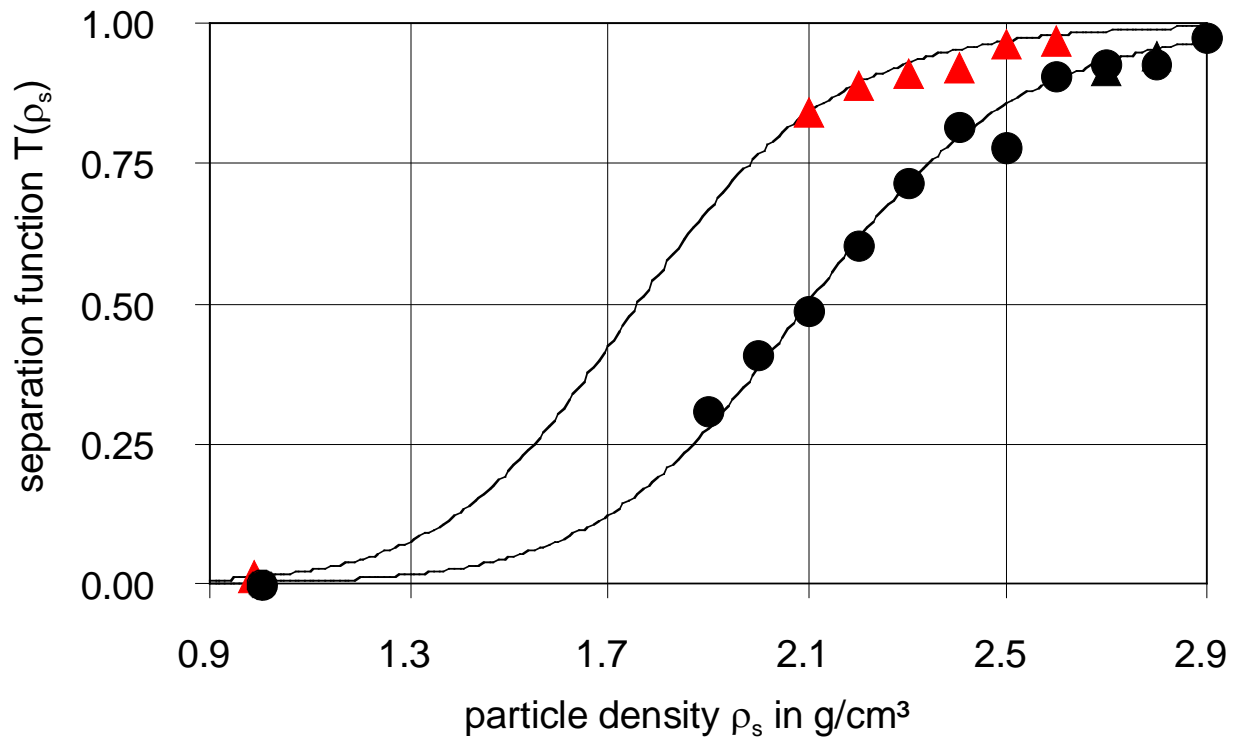
particle fraction $d_{u,i} - d_{o,i}$ in mm	8 - 12
channel velocity u in m/s	14
particle settling velocity $v_{sT}(d_{u,i})$ in m/s	20.3
mass flow rate \dot{m}_s in t/h	0.12
specific mass flow rate $\dot{m}_{s,A}$ in $\text{t}/(\text{m}^2 \cdot \text{h})$	3.0
particle concentration $\mu_{s,g}$ in g/kg	50
cut density $\rho_{s,T}$ in g/cm^3	2.1
separation sharpness κ	0.7 - 0.9
$n = 15$, effective separation stages n_e	1 - 7
utilisation of separation stages η_{Tr} in %	7 - 47
pressure drop Δp_{ZZ} in Pa	1600
specific energy consumption $W_{m,ZZ}$ in kWh/t	8.0

Gravity Separation of a Concrete-Brick-Mixture



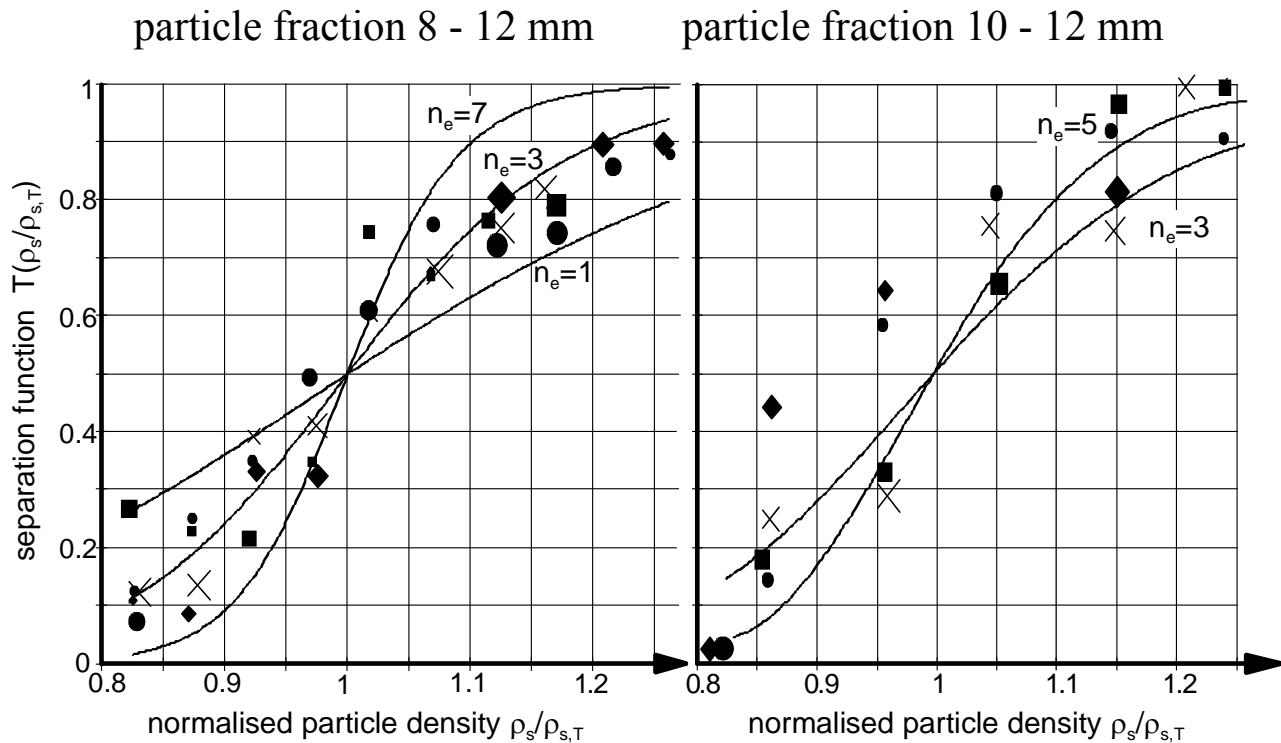
particle fraction $d_{u,i} - d_{o,i}$ in mm	8 - 10
channel velocity u in m/s	12.5
particle settling velocity $v_{sT}(d_{u,i})$ in m/s	21.7
mass flow rate \dot{m}_s in t/h	0.15
specific mass flow rate $\dot{m}_{s,A}$ in t/(m ² ·h)	3.7
particle concentration $\mu_{s,g}$ in g/kg	68
cut density $\rho_{s,T}$ in g/cm ³	2.4
separation sharpness κ	0.86
$n = 7$, effective separation stages n_e	3.8
utilisation of separation stages η_{Tr} in %	54
pressure drop Δp_{ZZ} in Pa	815
specific energy consumption $W_{m,ZZ}$ in kWh/t	2.75

Gravity Separation of a Concrete-Brick-Rubber-Mixture



particle fraction $d_{u,i} - d_{o,i}$ in mm	● 4 - 5	▲ 5 - 6.3
channel velocity u in m/s	8.5	8.5
particle settling velocity $v_{sT}(d_{u,i})$ in m/s	14.3	14.9
mass flow rate \dot{m}_s in t/h	0.15	0.63
specific mass flow rate $\dot{m}_{s,A}$ in t/(m ² ·h)	3.7	15.8
particle concentration $\mu_{s,g}$ in g/kg	98	417
cut density $\rho_{s,T}$ in g/cm ³	2.1	1.8
separation sharpness κ	0.80	0.78
$n = 7$, effective separation stages n_e	3	3.4
utilisation of separation stages η_{Tr} in %	43	49
pressure drop Δp_{ZZ} in Pa	350	350
specific energy consumption $W_{m,ZZ}$ in kWh/t	0.83	0.19

Gravity Separation of a Concrete-Brick-Mixture



separation process characteristics	concrete brick mixture	
particle fraction $d_{u,i} - d_{o,i}$ in mm	8 - 12	10 - 12
channel velocity u in m/s	14.0	14.0
particle settling velocity $v_{sT}(d_{u,i})$ in m/s	19.9	22.3
particle flow rate \dot{m}_s in t/h	0.12	0.12
specific particle flow rate $\dot{m}_{s,A}$ in t/(m ² ·h)	3.0	3.0
particle concentration $\mu_{s,g}$ in g/kg	50	50
cut density $\rho_{s,T}$ in g/cm ³	2.1	2.1
separation sharpness κ	0.7 - 0.8	0.82
$n = 15$, effective separation stages n_e	1 - 5	3 - 5
utilisation of separation stages η_{Tr} in %	7 - 33	20 - 33
misplaced product $\mu_{LS}(\rho_s < 2.3 \text{ g/cm}^3)$	0.30	0.22
pressure drop Δp_{ZZ} in Pa	1600	1700
specific energy consumption $W_{m,ZZ}$ in kWh/t	8.0	8.0



Assessment characteristics for multistage cross-flow separation in a symmetrical apparatus with $z_o = z_u = z$ number of separation stages

process goal	Separation function	Cut characteristic	Separation sharpness
	$T_{\text{tot}}(\xi/\xi_T) =$	$\xi_T = \xi_{50}(T_{\text{tot}} = 0.5) =$	$\kappa_{\text{tot}} = \xi_{25}/\xi_{75} =$
Fluid flow separation $\xi = v_s$	$\frac{1}{1 + \left(\frac{\dot{V}_o}{\dot{V}_u} \right)^{\left[1 - \frac{v_s(d, \rho_s)}{v_{sT}(d_T, \rho_{sT})} \right] \cdot z}}$	$v_{sT} = \sqrt{\frac{2 \cdot (\rho_{sT} - \rho_f) \cdot V_{P,T} \cdot g}{c_{W,T} \cdot \rho_f \cdot A_{P,T}}}$	$\frac{z \cdot \ln(\dot{V}_o / \dot{V}_u) - \ln 3}{z \cdot \ln(\dot{V}_o / \dot{V}_u) + \ln 3}$
Classification $\xi = d$ $\rho_s = \text{const.}$	$\frac{1}{1 + \left(\frac{\dot{V}_F}{\dot{V}_G} \right)^{\left[1 - \left(\frac{d}{d_T} \right)^\alpha \right] \cdot z}}$	$d_T \approx \frac{\rho_f}{3 \cdot \rho_s \cdot g} \left[\frac{D_{t,s}}{h} \cdot \ln \left(\frac{\dot{V}_F}{\dot{V}_G} \right) \right]^2$ for spheres $c_W = 0.44$	$\left[\frac{z \cdot \ln(\dot{V}_F / \dot{V}_G) - \ln 3}{z \cdot \ln(\dot{V}_F / \dot{V}_G) + \ln 3} \right]^{\frac{1}{\alpha}}$
Gravity separation $\xi = \rho_s$ $d = \text{const.}$	$\frac{1}{1 + \left(\frac{\dot{V}_L}{\dot{V}_S} \right)^{\left[1 - \left(\frac{\rho_{s,j} - \rho_f}{\rho_{s,T} - \rho_f} \right)^{\frac{\alpha+1}{3}} \right] \cdot z}}$	$\rho_{sT} \approx \frac{\rho_f}{3 \cdot d \cdot g} \left[\frac{D_{t,s}}{h} \cdot \ln \left(\frac{\dot{V}_L}{\dot{V}_S} \right) \right]^2$ for spheres $c_W = 0.44$	$\left[\frac{z \cdot \ln(\dot{V}_L / \dot{V}_S) - \ln 3}{z \cdot \ln(\dot{V}_L / \dot{V}_S) + \ln 3} \right]^{\frac{3}{\alpha+1}}$

$\dot{V}_o, \dot{V}_F, \dot{V}_L$ overflow, fine or lightweight particle suspension volume flow rates, $\dot{V}_u, \dot{V}_G, \dot{V}_S$ underflow, coarse or heavy particle volume flow rates, $\alpha = 2$ laminar (Stokes), $\alpha = 0.5$ turbulent (Newton) flow pattern acc. to $v_s \propto d^\alpha$

Summary and Conclusions

- 1) The separation efficiency of multistage turbulent cross flow process principle of zigzag apparatus could be proved to be
 - good to very good separation sharpness $\kappa = \mathbf{0.67 - 0.9}$,
 - sufficient to good utilisation of separation stages $\eta_{Tr} = 17$ to 54% ,
 - small specific energy consumption down to $\mathbf{0.2\ kWh/t}$,
 - variability of apparatus geometry,for fragments with small density differences $\rho_{s,L}/\rho_{s,S} = 1.7/2.6 = 0.65$ or in terms of classification with a sharp particle cut size.
- 2) **Light weight material** $\rho_{s,L} \leq 1.2\ \text{g/cm}^3$ can be completely separated.
- 3) Suitable separation of **partially liberated aggregate fragments** $\kappa = \mathbf{0.74 - 0.94}$ with sufficient to good utilisation of separation stages 27 to 87 % after successful liberation in an impact crusher.
- 4) These practically essential results will be pointed out here by the adaptability of **multistage turbulent dispersion model** being suitable for **apparatus design** in order to develop a **full-scale recycling process**.

Particle Separation and Classification

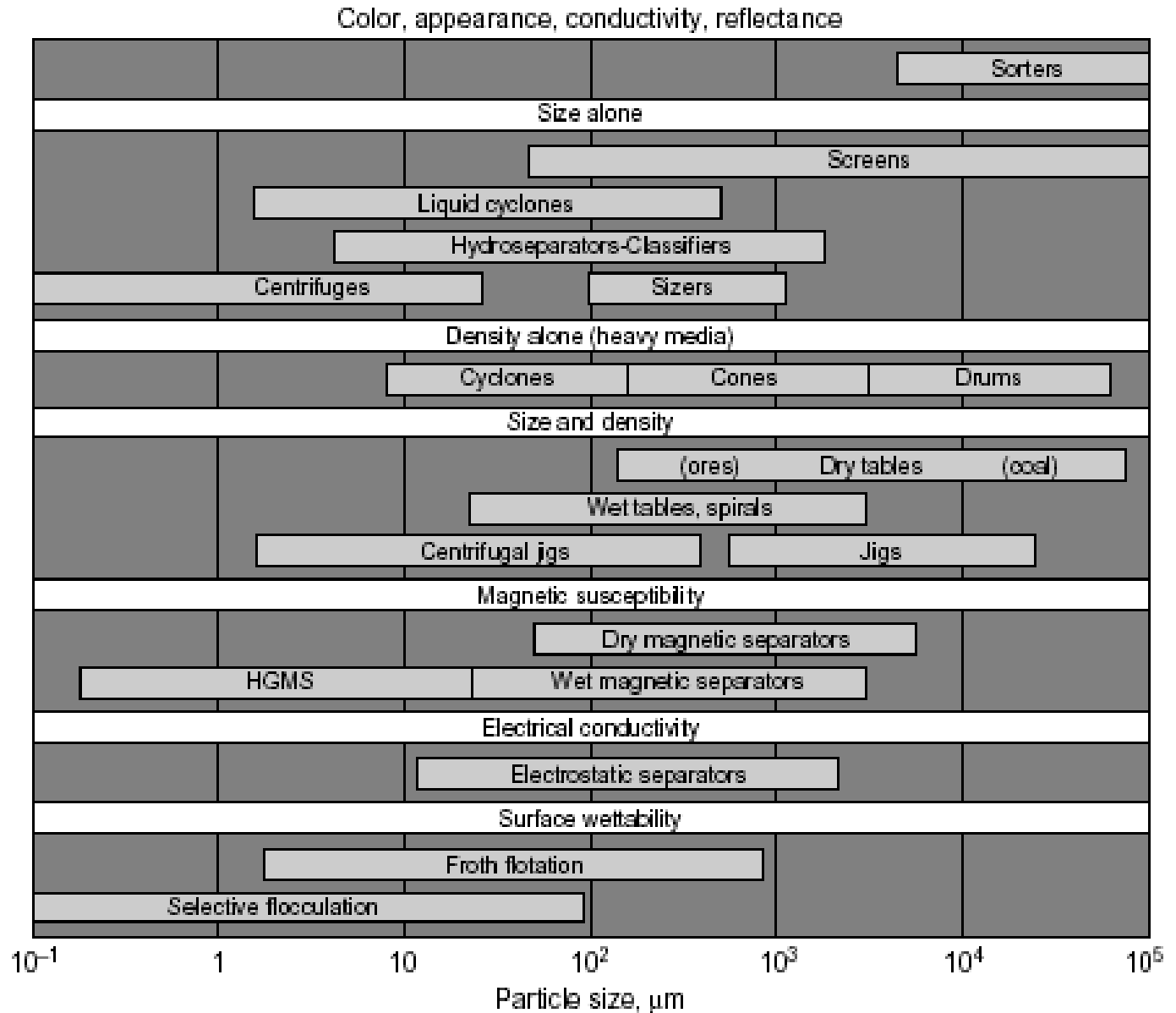







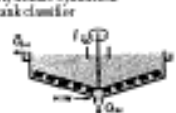




FIG. 19-1 Particle-size range as a guide to the range of applications of various solid-solid operations.

TABLE 19-8 The Major Types of Classifiers

Classifier	(Type ^a)	Description	Size (m) Width Diameter Max. length	Limiting size (max. feed size)	Feed rate (t/hr)	Vol. % solids Feed overflow underflow	Power (kW)	Stability and applications
 Sloping tank classifier (spiral, rake drag)	OM-S	Classification occurs near deep end of sloping, elongated pool. Spiral, rake or drag mechanism lifts sands from pool.	0.3 to 7.0 2.4 (spiral) 34	1 mm to 40 µm (20 mm)	3 to 800	Not critical 2 to 20 43 to 60	0.4 to 110	Used for closed circuit grinding, washing and dewatering, dewatering, particularly where clean dry underflow is important. (Drag classifier tends not to clean.) In closed circuit grinding discharge mechanism (spiral especially) may give enough lift to eliminate pump.
 Log washer	OM-S	Essentially aspiral classifier with paddles replacing the spiral.	0.6 to 2.0 0.6 to 1.1 4.6 to 11	(10 mm)	40 to 400		7.5 to 60	Used for rough separations such as removing trash, clay from sand. Also to remove or break down agglomerates.
 Bowl classifier	OM-S	Extension of sloping tank classifier, with seating occurring in large circular pool, which has rotating mechanism to scrape sand inward toward Bowl Divider to discharge into spiral.	0.5 to 0.9 1.2 to 1.5 32	100 µm to 40 µm (12 mm)	3 to 225	Not critical 0.4 to 5 20 to 60 (13 to 23 in Bowl Divider)	Best, 0.75 to 7.5 Also, 0.70 to 20	Used for closed circuit grinding (particularly spiral circuit) where clean dry underflow is necessary. Larger pool allows finer separation. Bowl Divider has large pools (and capacities). Relatively expensive.
 Hydraulic bowl classifier	OM-F	Basically a hydraulic bowl classifier. Vibrating plate replaces rotating mechanism in pool. Hydraulic water passes through perforations in plate and flushes sand.	-1.2 to 3.7 1.2 to 4.3 32	1 mm to 100 µm (12 mm)	3 to 225	Not critical 2 to 15 20 to 60	Vib. 2.2 to 7.0 Also, 3.7 to 15	Gives very clean sands and has relatively low hydraulic water requirements (0.5 to underflow). One of the most efficient single-stage classifiers available for closed circuit grinding and washing. Relatively expensive.
 Cylindrical tank classifier	OM-S	Effectively an overloaded thickener. Rotating rakes feed sands to central underflow.	— 3 to 45 —	100 µm to 43 µm (6 mm)	3 to 625	Not critical 0.4 to 5 33 to 23	0.70 to 11	Simple, but gives relatively inefficient separation. Used for primary dewatering where the separation involves large feed volumes, and underflow drainage is not critical.

^aM. Mechanical transport of sands to discharge
 N. Nonmechanical (gravity or pressure) discharge of underflow
 S. Sedimentation classifier
 F. Fluidized bed classifier
 From Kolay, E. G. and D. J. Spornwood, *Introduction to Mineral Processing*, John Wiley & Sons, New York, 1982, pp. 200-201, with permission.

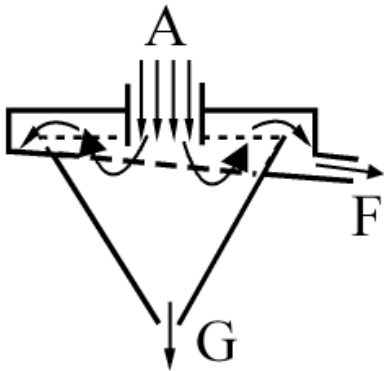
TABLE 19-8 The Major Types of Classifiers (Continued)

Classifier	(Type ^a)	Description	Size (m) Width Diameter Max. length	Limiting size (max. feed size)	Feed rate (t/hr)	Vol. % solids Feed overflow underflow	Power (kW)	Stability and applications
 Hydraulic cylindrical tank classifier	OM-F	Hydraulic form of overloaded thickener. Spiral-Sizer (S-F) uses rakes to discharge underflow instead of rotating rakes.	— 1.0 to 4.0 —	1.4 mm to 43 µm (20 mm)	1 to 100	Not critical 0.4 to 13 20 to 30	0.70 to 11	Two-product device giving very clean underflow. Gives relatively fine hydraulic water (2 to 30 µm). Used for washing, dewatering, and closed circuit grinding.
 Cone classifier	OM-S	Similar to cylindrical tank classifier in open tank is conical to eliminate need for rakes.	— 0.6 to 3.7 —	600 µm to 43 µm (6 mm)	2 to 100	Not critical 5 to 30 30 to 60	None	Low cost (simple enough to be made locally), and simplicity can justify relatively inefficient separation. Used for dewatering and primary dewatering. Solids buildup can be a problem.
 Hydraulic cone classifier	OM-F	Open cylindrical upper section with conical lower section containing slowly rotating mechanism.	— 0.6 to 1.6 —	400 µm to 100 µm (6 mm)	10 to 120	Not critical 2 to 15 30 to 50	3 to 7.5	Used primarily in closed circuit grinding to achieve hydro-cyclone underflow.
 Hydrocyclone	OM-S	Pumped pressure feed generates centrifugal action to give high separating forces, and discharge.	— 0.01 to 1.2 —	200 µm to 5 µm (1400 µm to 40 µm)	to 20 m ³ /min	4 to 25 2 to 15 30 to 50	25 to 400 kPa/m ² pressure head	Small cheap device, widely used for closed circuit grinding. Gives relatively efficient separation of fine particles in dilute suspensions.
 Air separator	OM-S	Similar shape to hydrocyclones, but higher included angle. Internal impeller or induces recirculation classifier.	— 0.5 to 7.5 —	2 mm to 39 µm	to 2000		4 to 300	Used where solids must be kept dry, such as cement grinding. Air classifiers may be integrated into grinding mill streams.

Flow Classification - Gravitational Force Hydroclassifier - Horizontal or Cross-Flow Classifiers

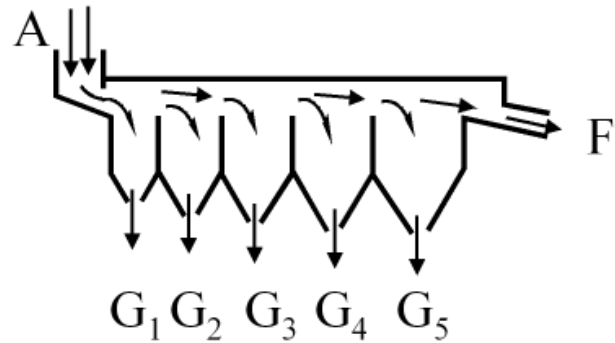
1. Horizontal or cross-flow classifier, schematic:

a) Cone classifier

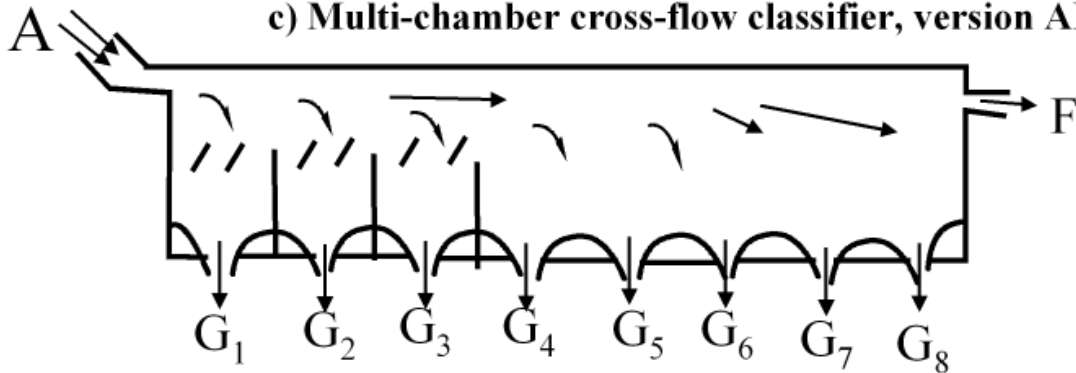


A Feed
 F Fines
 G Coarse

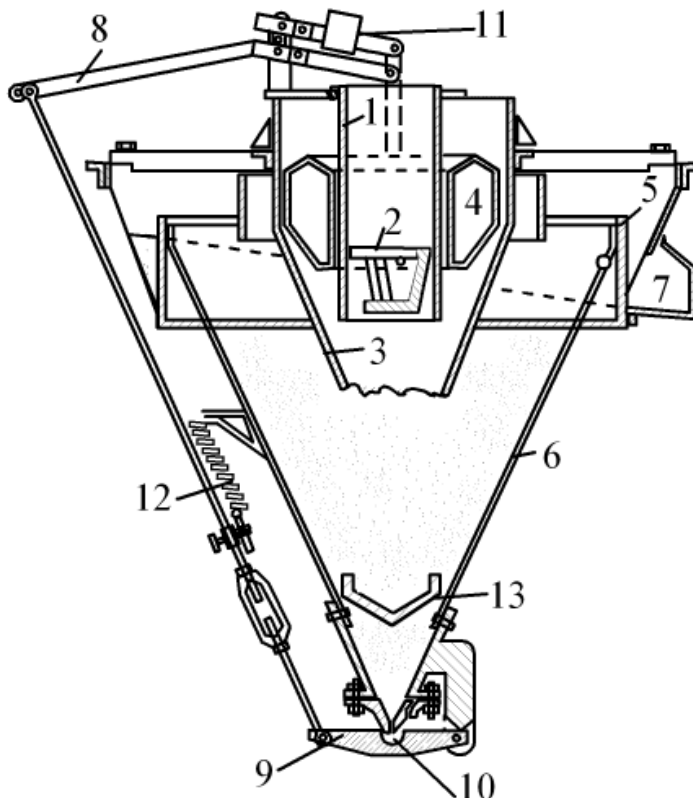
b) Multi-chamber cross-flow classifier



c) Multi-chamber cross-flow classifier, version AKW



2. Cone classifier with float discharge control

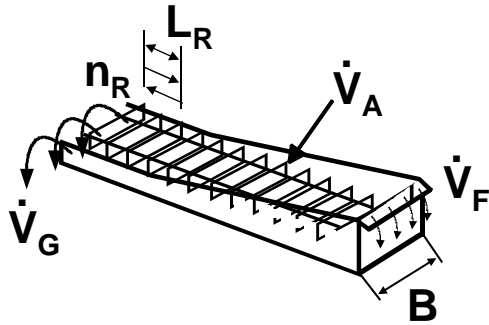


- 1 Feed pipe of suspension
- 2 Inserts (baffles) to calm the feed flow
- 3 Internal cone shell
- 4 Float
- 5 Overflow discharge sill of fine product
- 6 Basic cone
- 7 Discharge launder of fine product
- 8 Lever & rod mechanism
- 9 Ball support
- 10 Underflow ball valve for coarse product
- 11 Adjustable mass
- 12 Spring
- 13 Discharge obstacle (disk)

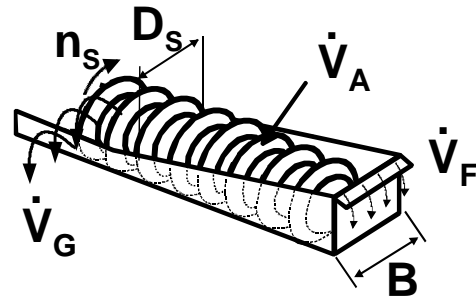
Flow Classification - Gravitational Force Hydroclassifier - Horizontal or Cross-Flow Classifiers

3. Cross-flow classifier with mechanical discharge device of coarse product (mechanical classifier), schematic:

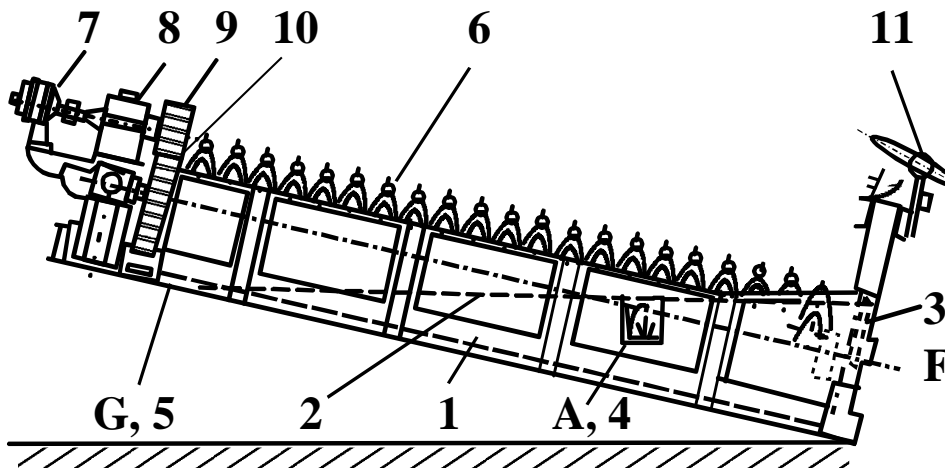
a) Rake classifier



b) Screw classifier



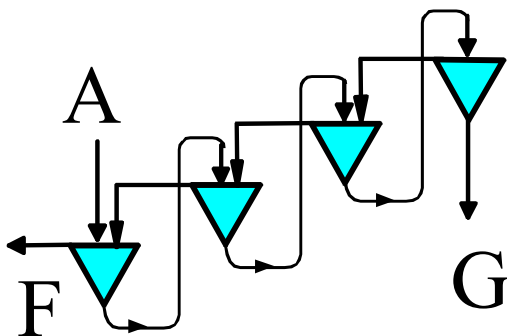
4. Screw classifier, version SKET



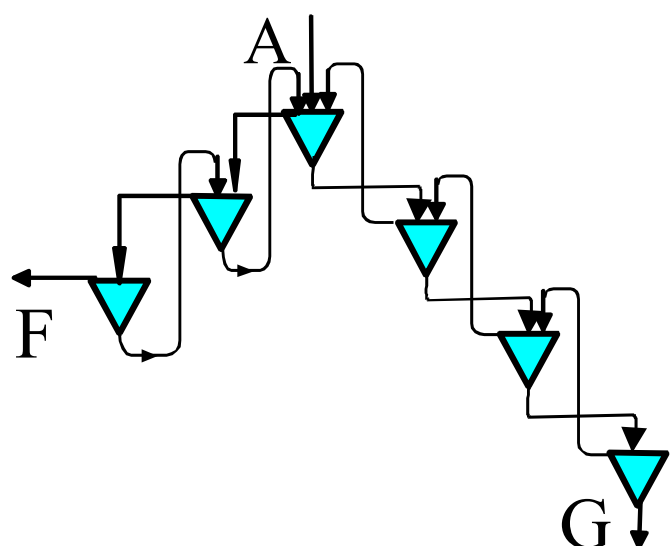
- 1 Sheet metal trough
- 2 Suspension level
- 3 Adjustable over-flow sill
- 4 Feed launder
- 5 Discharge of coarse
- 6 Screw conveyor
- 7 Drive motor
- 8 Gear
- 9 Drive pinion
- 10 Gear of discharge screw
- 11 Lift mechanism

5. Arrangement of horizontal or cross-flow classifiers, version Rheax

a) Counter-current arrangement



b) "Phalanx" arrangement



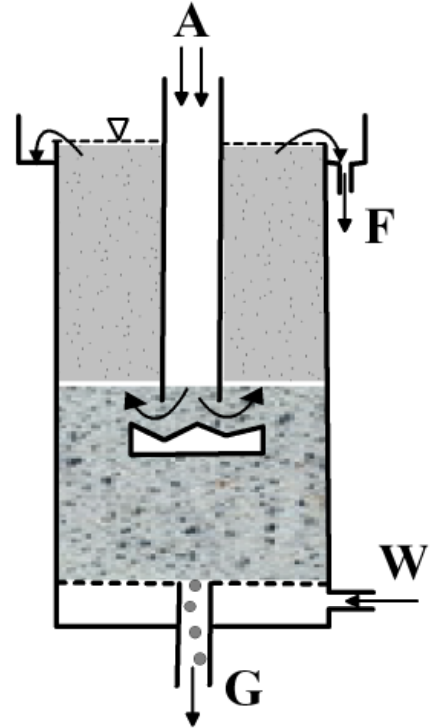
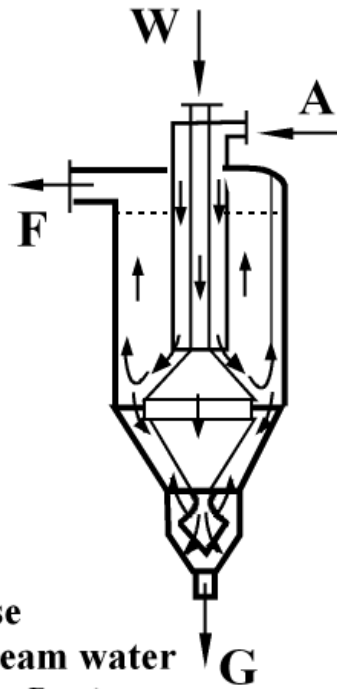
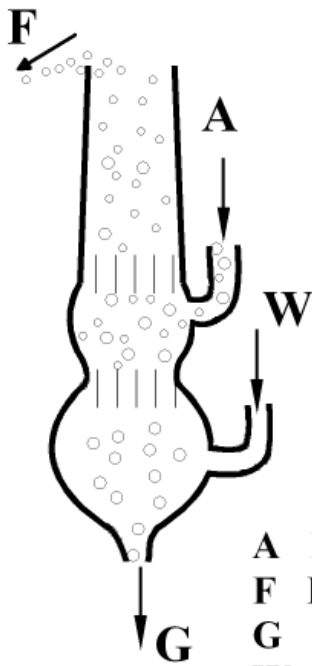
Flow Classification - Gravitational Force Hydroclassifier - Upstream or Counter-Current Classifiers

1. Upstream or counter-current classifiers (hydrosizers) of different versions:

a) Rheax

b) Sogreah (Lavoflux)

c) Hydrosort (with fluidized bed)

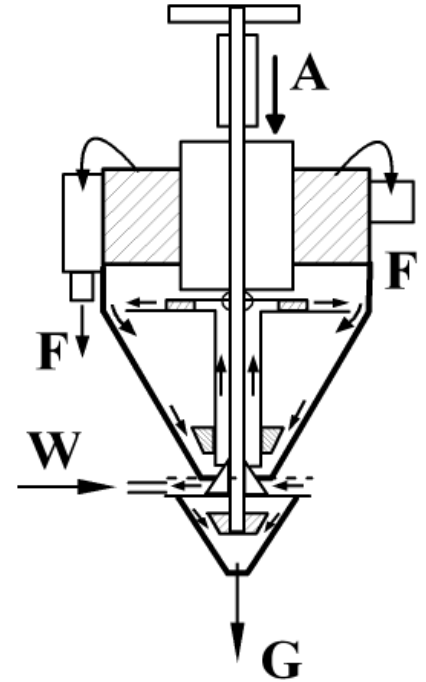
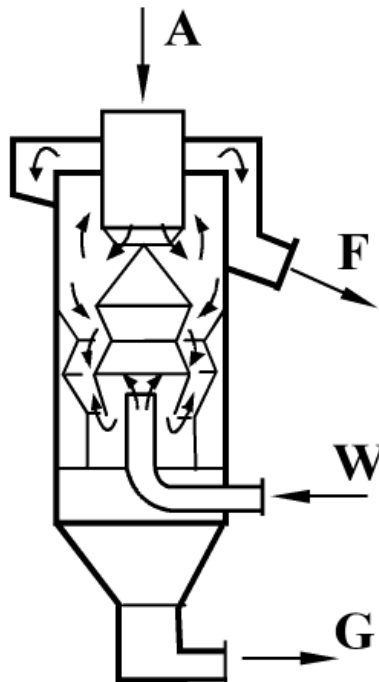
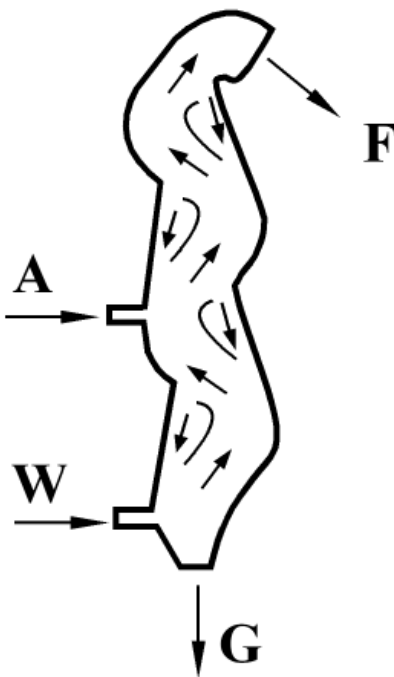


A Feed
 F Fines
 G Coarse
 W Upstream water
 (rising flow)

d) Rheax (zigzag classifier)

d) Hydrofors

e) Larox



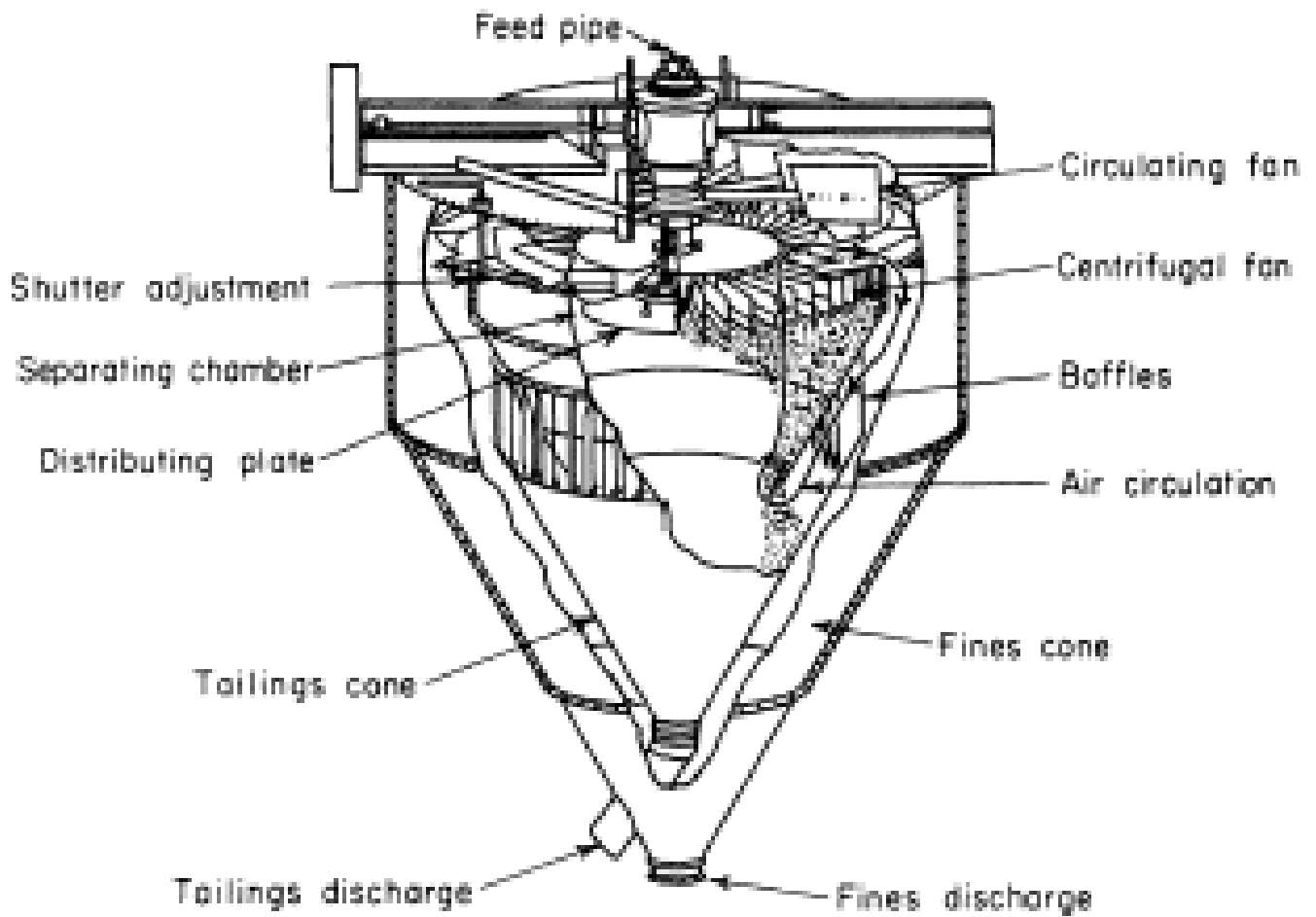
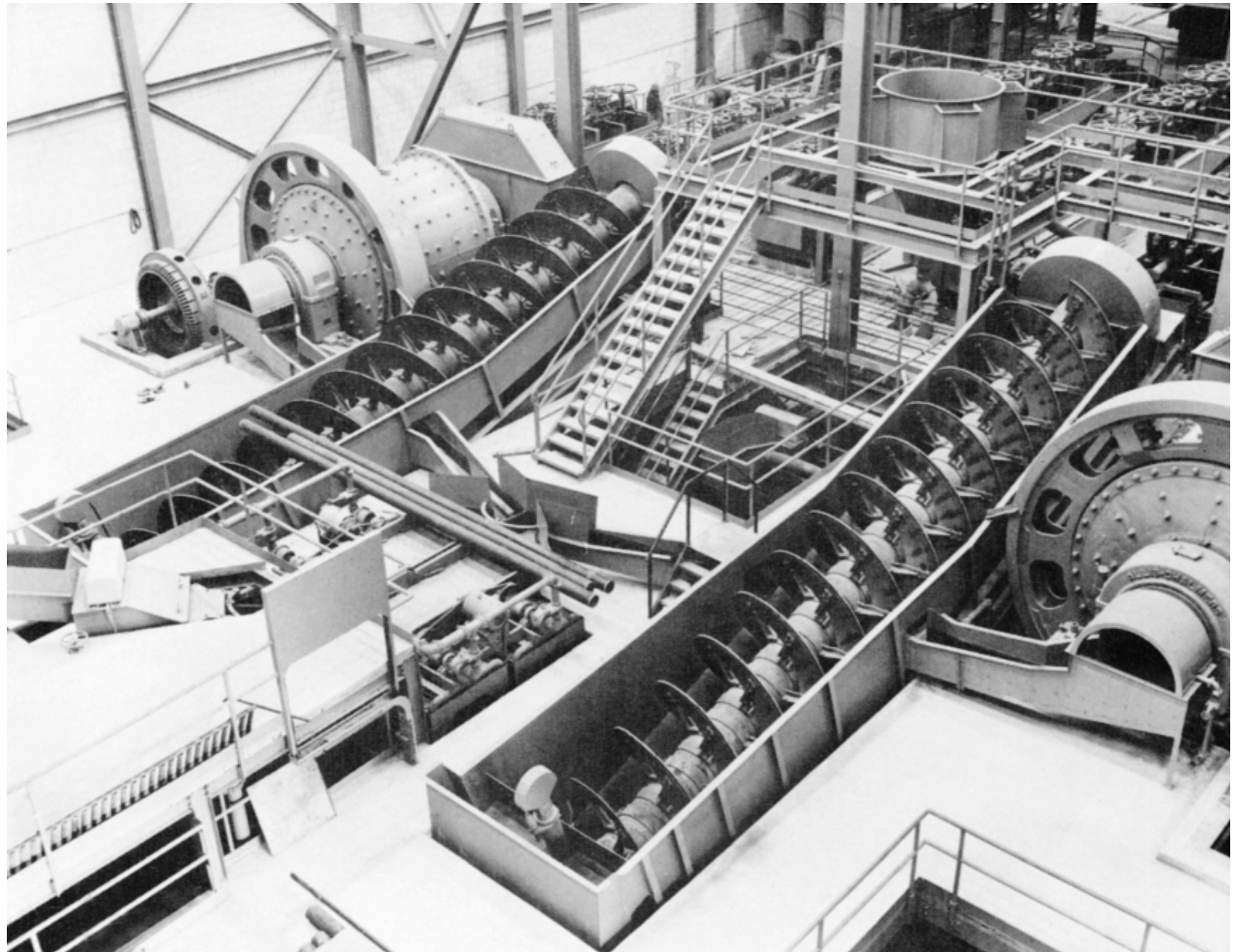


FIG. 20-41 Typical centrifugal separator.



Screw classifier

Version Wemco
S-H 78 in a
closed milling
circuit of
St. Joseph Lead
Co., Indian Creek
Plant



Counter-current classifier

Version TAK Amberger

Kaolinwerke

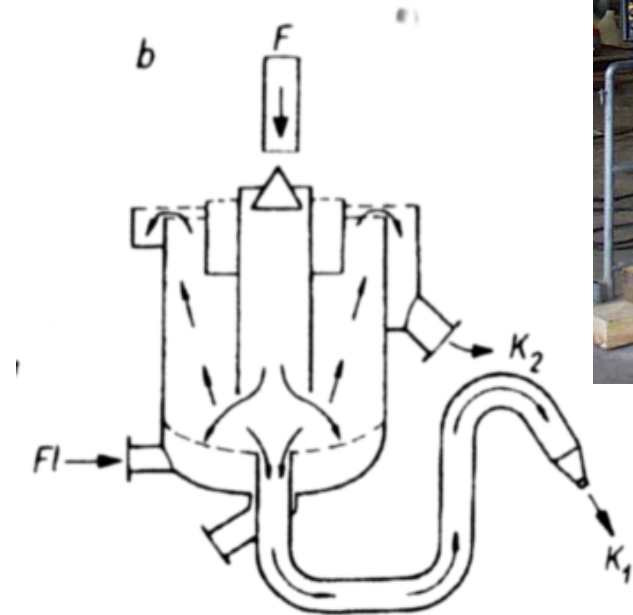
for sand, cut size:
above 200 - 500 μm

F feed

K_1 coarse product

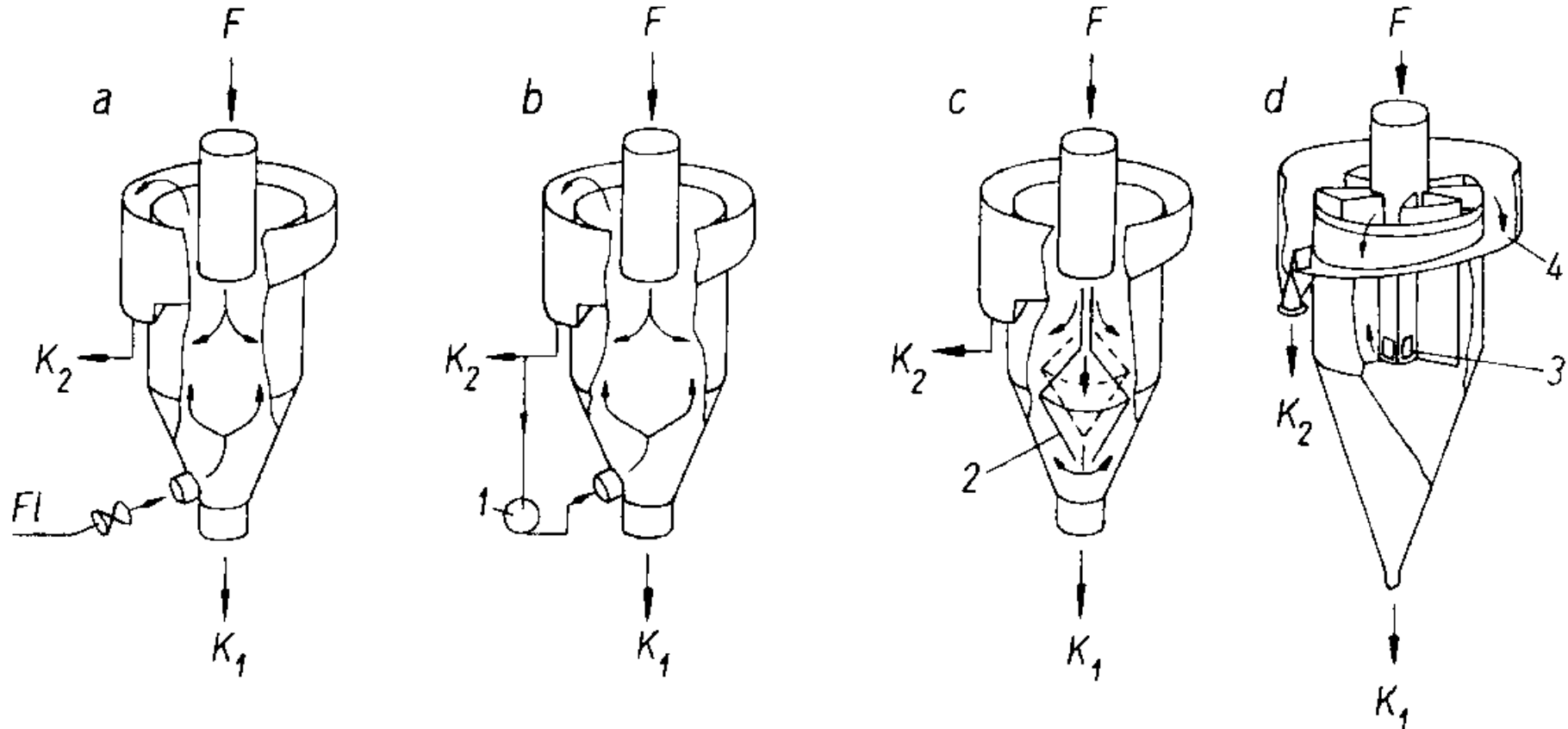
K_2 fine product

F1 fluid





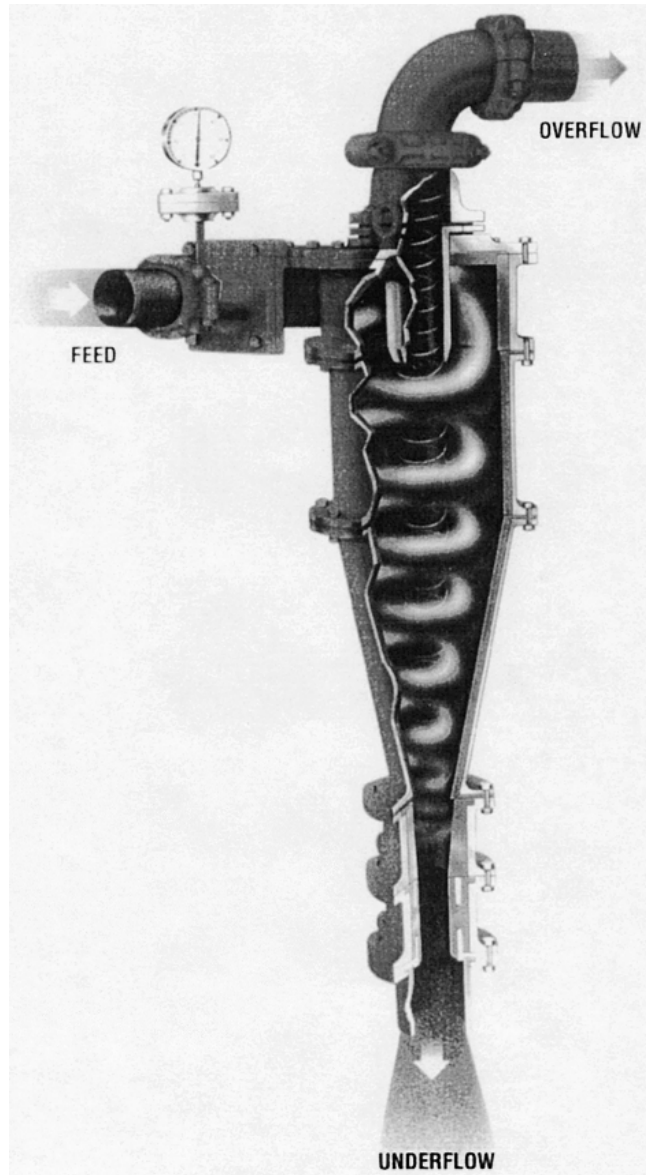
Counter-current Control in Counter-current Classifiers



F feed, K_1 coarse product,
 1 pump control by revolution number
 3 feed valve

K_2 fine product, F1 fluid
 2 height adjustable diving cone insert
 4 walls to separate segments

Particle Flow Separation by Hydrocyclone



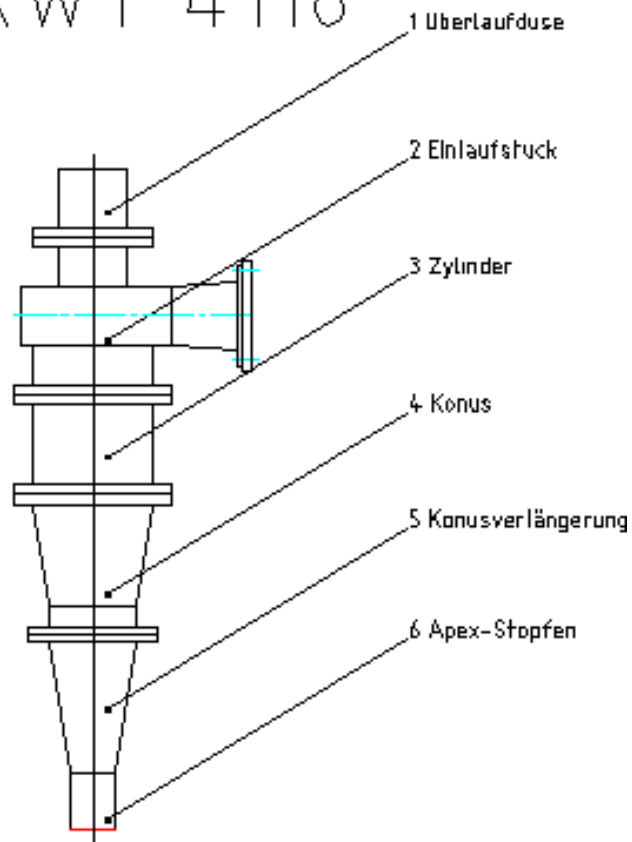
Schematic view of fluid flow Oblique or horizontal built-in is possible



Particle Flow Separation by Hydrocyclone

Version TAK Amberger Kaolinwerke

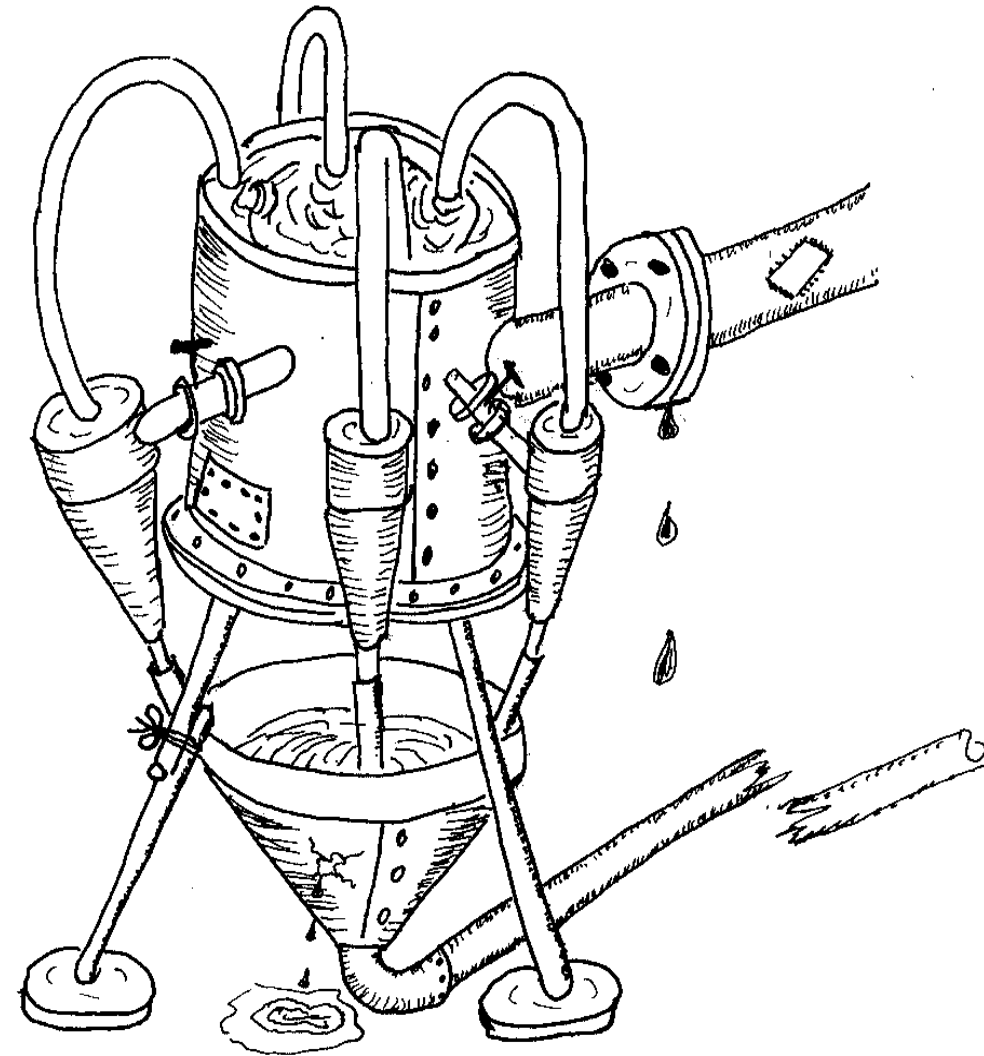
200 mm Zyklon
RWT 4118





Multi-cyclones, Cyclone Batteries

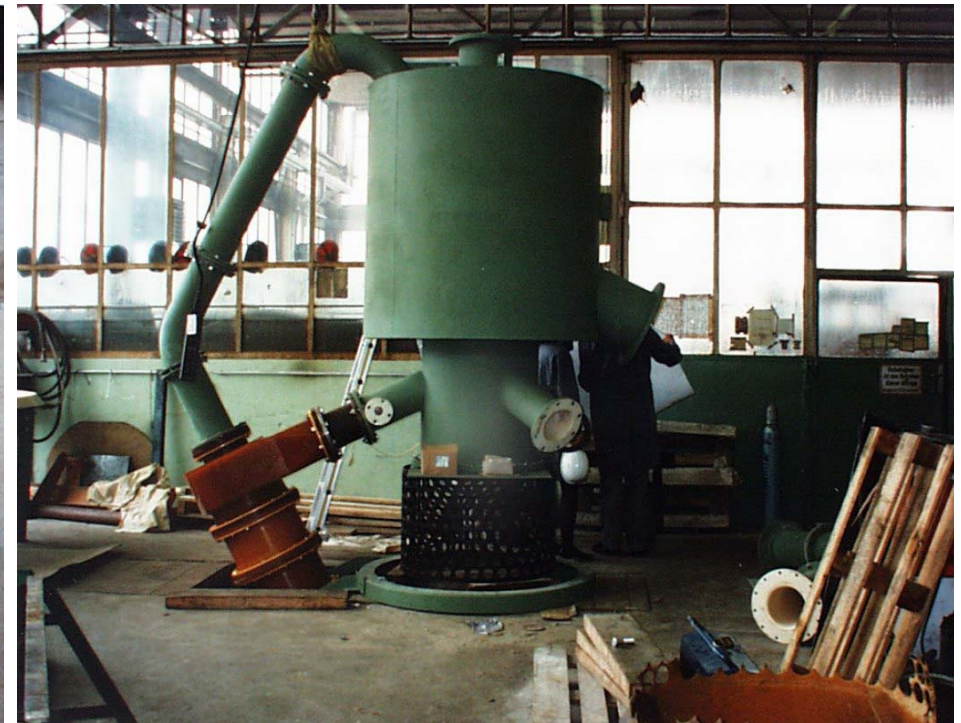
- pre-processing or replacement of thickeners
- separation of clay and solid, non-soluble constituents
- thickening/cleaning of suspensions
- multistage cyclone arrangements
- washing by cyclones



Multi-cyclones, Cyclone Batteries

Feed distribution vessel of cyclone battery
with wear-resistant lining by ceramics

Feed vessel during assembly



Dust Separation

Crude gas volume flow rates to vacuum for dust separation

Locations of vacuum	crude gas volume flow rate \dot{V} in m ³ /min
Transfer of belt conveyors	10 ... 40
Bucket elevators	10 ... 40
Bunkers	10 ... 30
Comminution machines	15 ... 150
Magnetic separators	30 ... 40

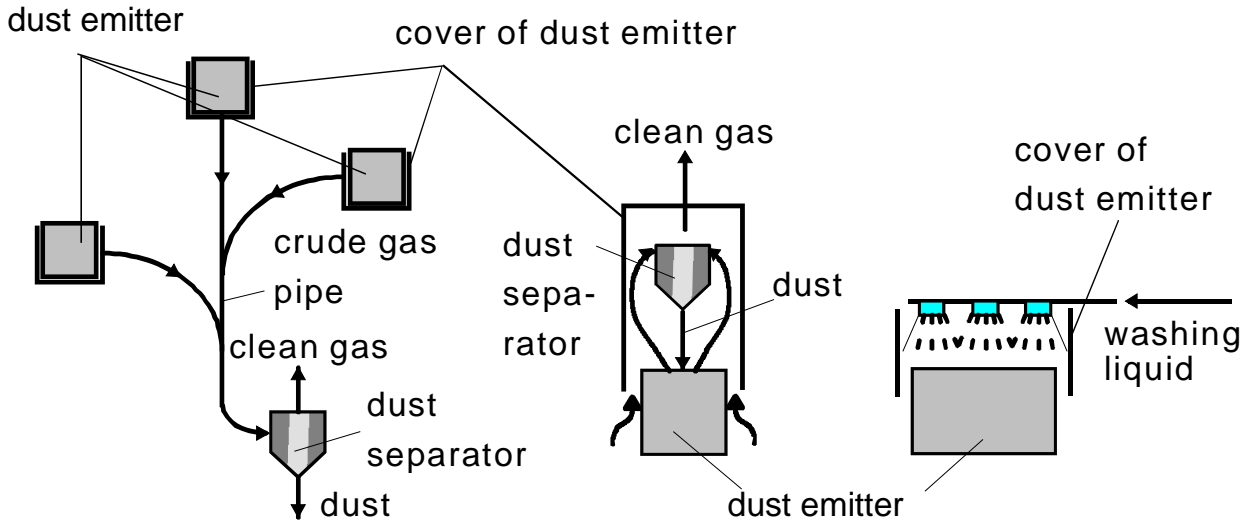
Process application data of dust separation

Process data	Centrifugal separation	Electrical separation	Filtration	Wet separation
High separation function (fraction separation efficiency) $T_i \rightarrow 1$ at particle sizes d_i in μm	> 10	> 1	> 0,5	> 0,1
Crude gas dust concentration $c_{s,g,roh}$ in g/m ³	< 1000	< 50	< 100	< 10
Achieved clean gas dust concentration $c_{s,g,rein}$ in mg/m ³	100 - 200	< 50	< 30	50 - 100
Pressure drop Δp in Pa	300 - 2500	50 - 150	500 - 1500	100 - 1000
max. gas temperature θ_g in °C	450	450 (1000)	140 (350)	300
Range of crude gas volume flow rate \dot{V} in m ³ /h	3000 - 200,000	10 000 - 300,000	1000 - 100,000	3000 - 100,000

Dust Separation

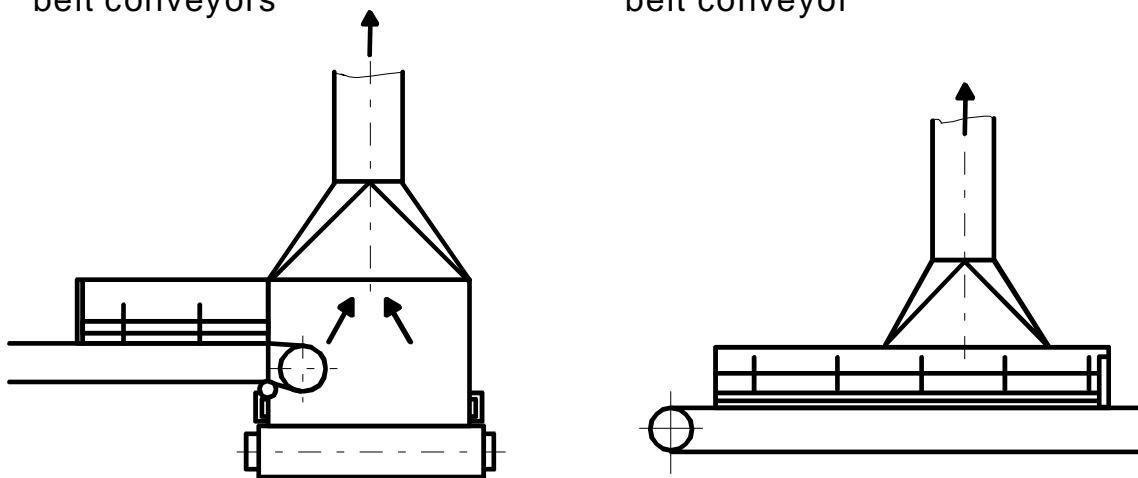
1. Spatial arrangement of dust separation units

- a) Central dust separation b) and c) decentral sparation directly located at dust emitter



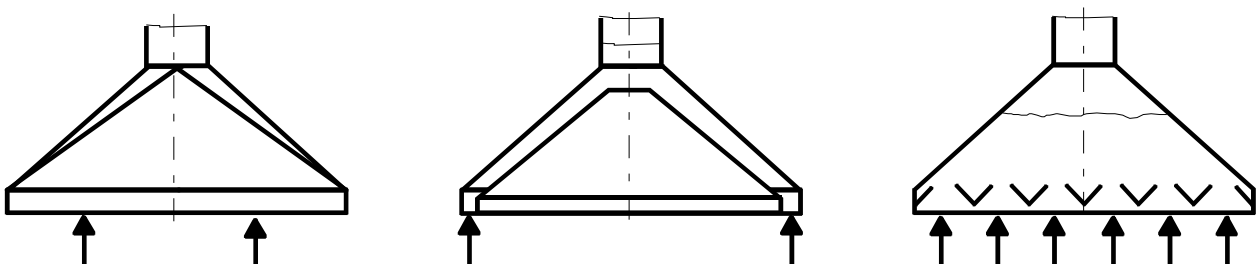
2. Cover to vacuum (collect) dust

- a) transfer between two belt conveyors b) Interface between transfer chute and belt conveyor



3. Dust vacuum covers (hoover)

- a) open rectangular vacuum cross-section b) periphere vacuum (comparatively small vacuum cross section) c) with obstacles (small cross-section)

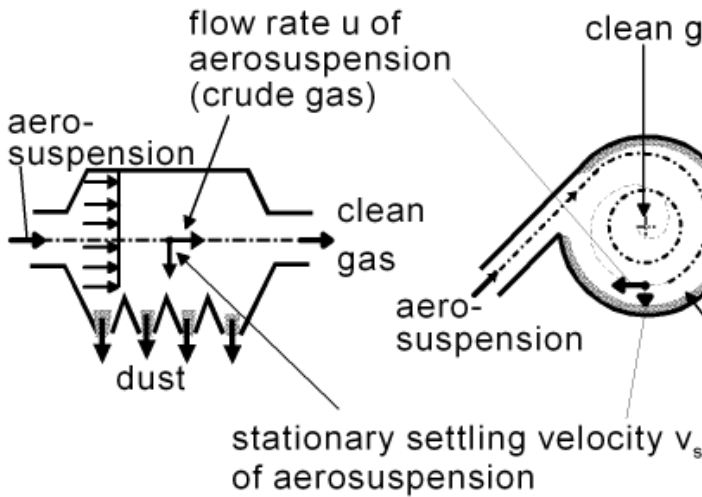


Dust Separation

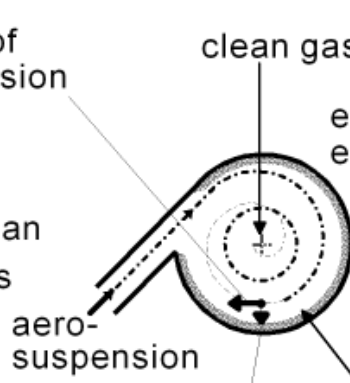
4. Processes of dust separation, operation principles

Cross-flow separations at

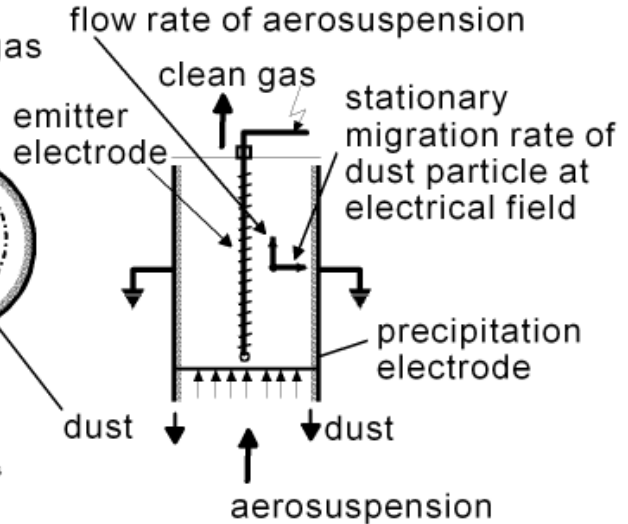
a) gravitational force field



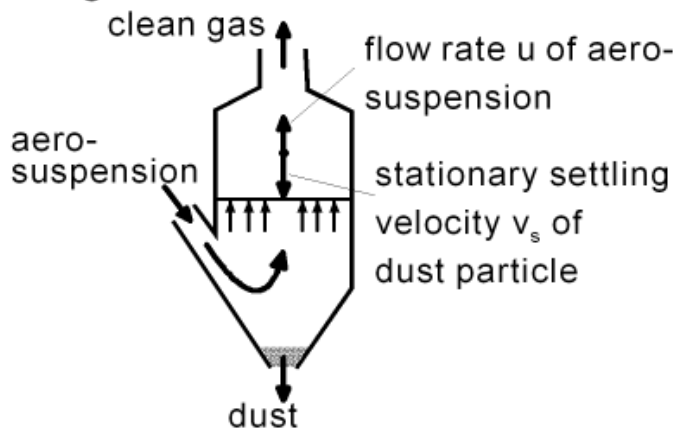
b) centrifugal field



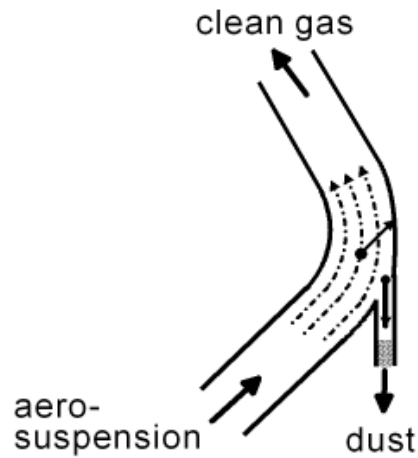
c) electrical field



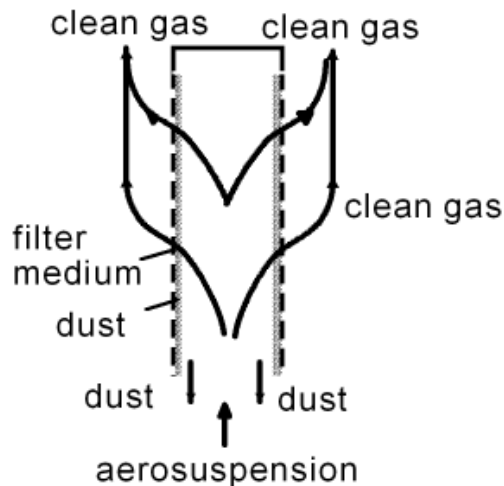
d) Counter-current separation at gravitational force field



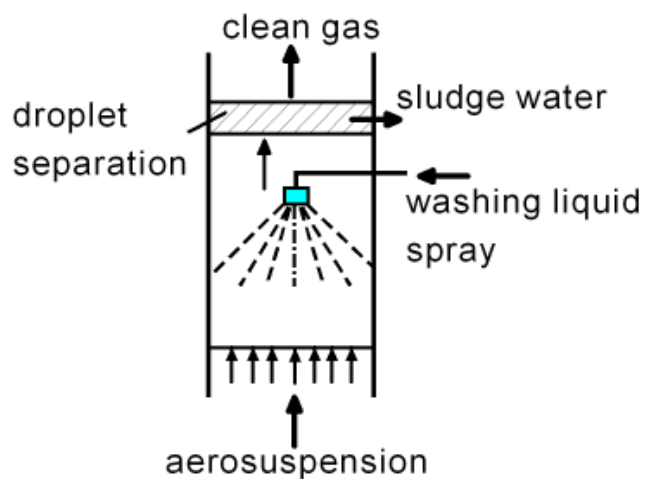
e) Cross-flow impact separation



f) Filtration

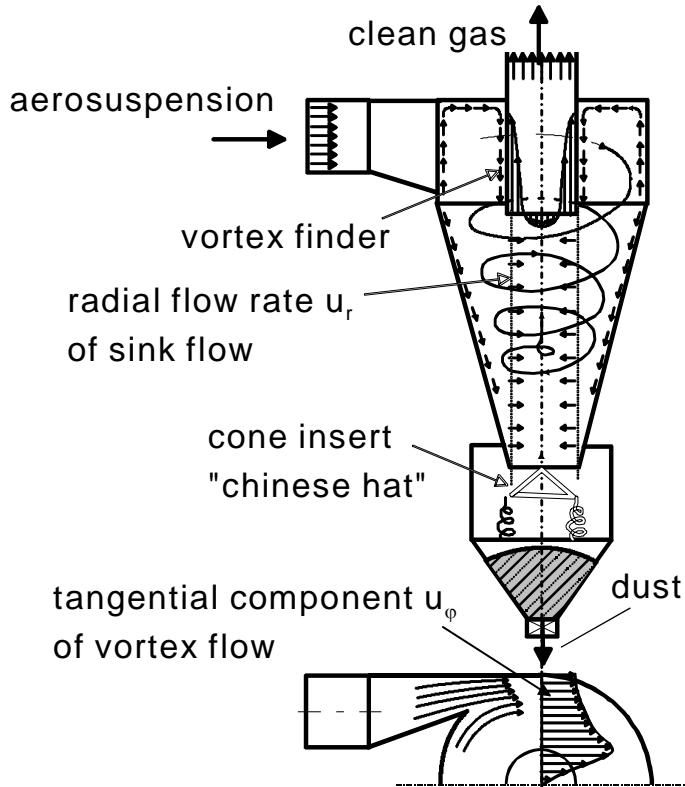


g) Heterocoagulation



Aerocyclones

5. Aerocyclone with characteristic flow rates



separation function:

$$T(d) = \left[1 + 2 \cdot \left(\frac{d}{1,3 \cdot d_T} \right)^{-3,564} \right]^{-1,235}$$

cut size:

$$d_T = 1,3 \cdot \sqrt{\frac{9 \cdot \eta}{\pi \cdot (\rho_s - \rho_g)} \cdot \frac{A_i^2}{H_o} \cdot \left(\frac{D_o}{D} \right)^{2n} \cdot \frac{1}{\dot{V}}}$$

dust concentration of clean gas:

$$\mu_{s,g, rein} = \mu_{s,g, roh} \cdot (1 - R_m) = \mu_{s,g, G} \cdot Q_3(1,3 \cdot d_T)$$

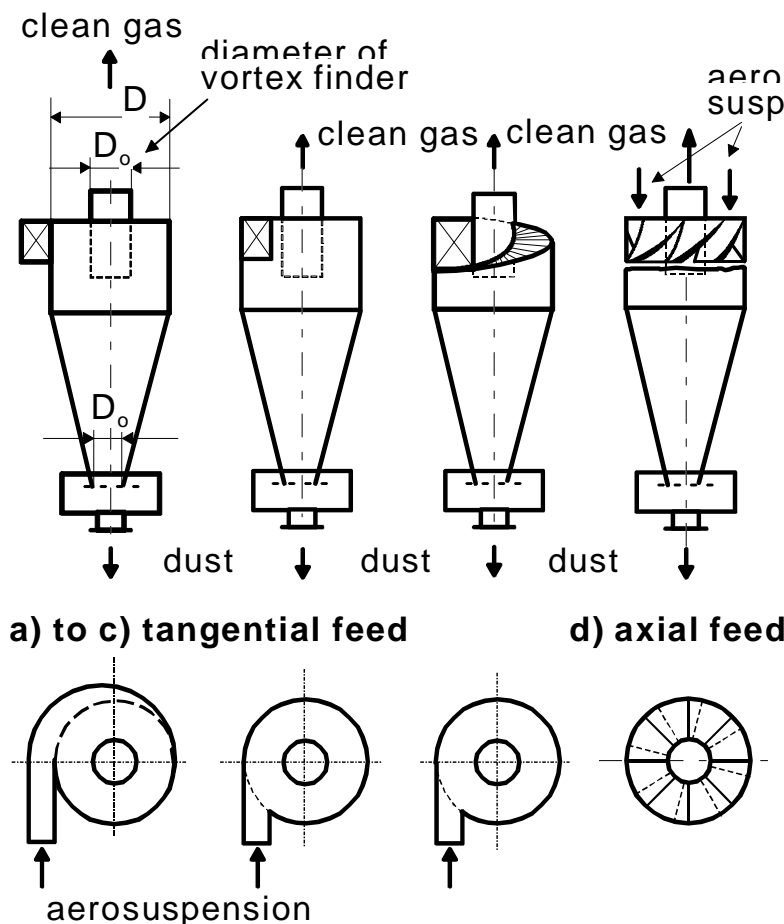
pressure drop:

$$\Delta p = \xi_{ges} \frac{\rho_g}{2} u_o^2 = 8 \xi_{ges} \rho_g \frac{\dot{V}^2}{\pi^2 D_o^4}$$

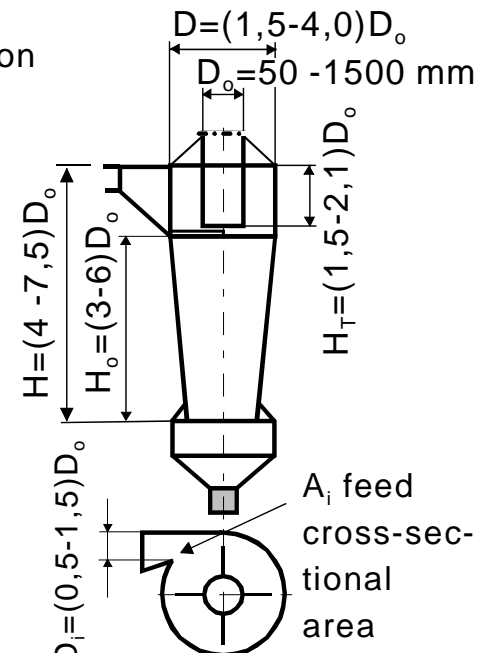
power consumption:

$$P = \Delta p \cdot \dot{V} = 8 \xi_{ges} \rho_g \frac{\dot{V}^3}{\pi^2 D_o^4}$$

6. Various designs of aerocyclones



7. Experiences to design tangential aerocyclones



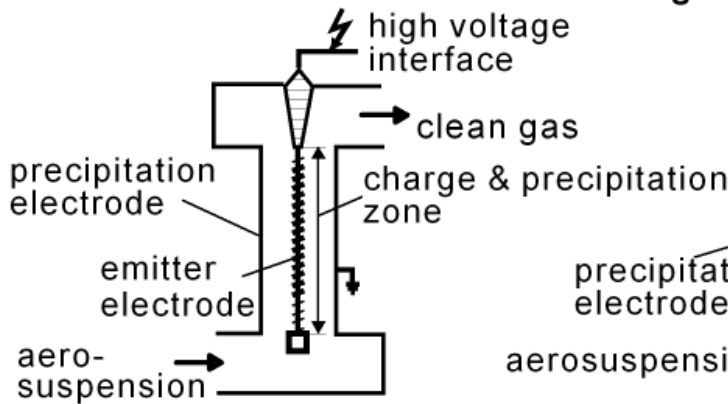
feed (input) flow rate $u_i = 7 - 17 \text{ m/s}$
 vortex flow rate $u_o = 5 - 20 \text{ m/s}$
 pressure drop $\Delta p = 0,4 - 2 \text{ kPa}$

d_T in μm	ρ_s in kg/m^3
6,0 - 14	1000
5,0 - 10	2000
3,5 - 7	4000

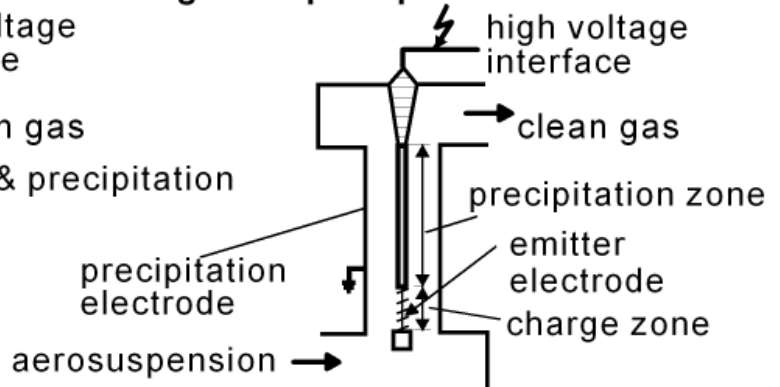
Dust Separation

8. Variants of electrical separators

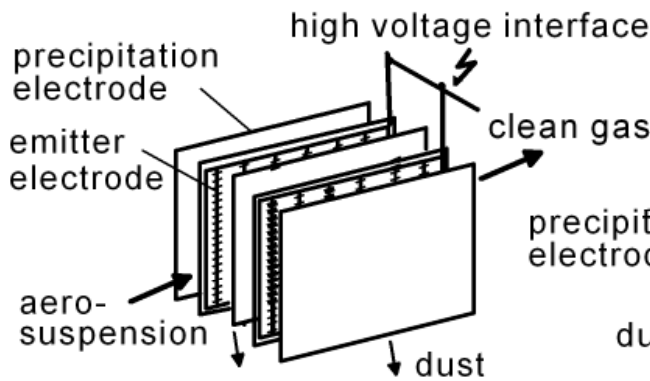
a) Tube separator



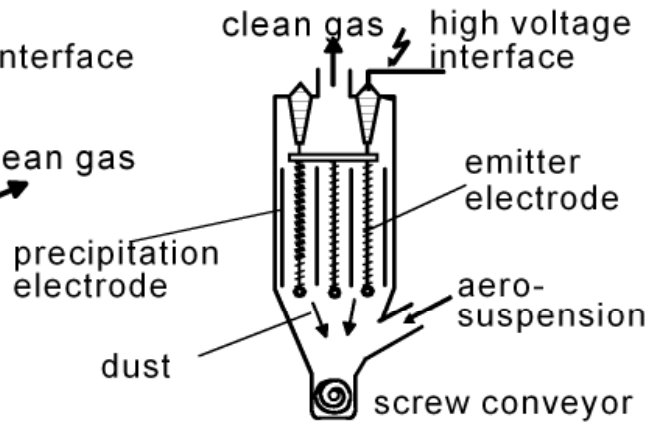
b) Tube apparatus with separate charge and precipitation zone



c) Cross-flow plate separator

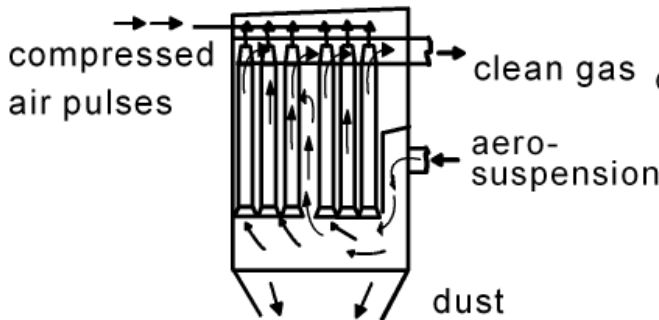


d) Counter-current plate separator

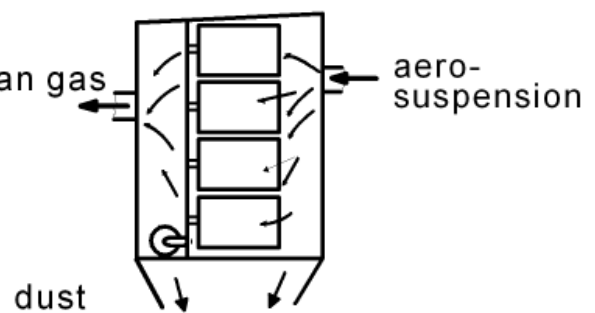


9. Filter

a) Hose, tube & candle filter

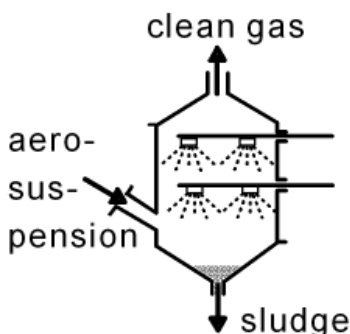


b) Bag filter

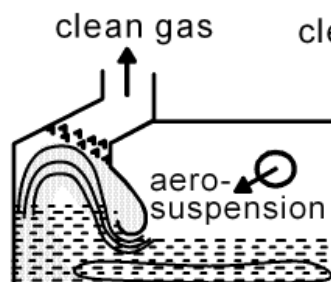


10. Wet precipitation, schematic

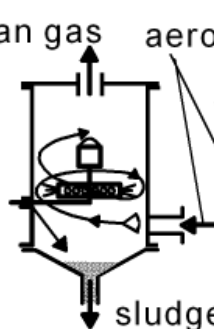
a) Spray washer



b) Vortex washer



c) Rotor washer



d) VENTURI washer

